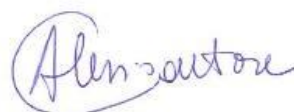


**UNIVERSITA' VITA-SALUTE SAN RAFFAELE**  
**CORSO DI DOTTORATO DI RICERCA INTERNAZIONALE**  
**IN MEDICINA MOLECOLARE**

**CURRICULUM IN FISIOPATOLOGIA CELLULARE E MOLECOLARE**

**INVESTIGATING LIVER TISSUE DYNAMICS**  
**TO IMPROVE IN VIVO GENE THERAPY**

DoS: Dr. Alessio Cantore



Second Supervisor: Prof. Ludovic Vallier

Tesi di DOTTORATO di RICERCA di Francesco Starinieri

matr. 014385

Ciclo di dottorato XXXIV

SSD BIO/11 BIO/13 BIO/17

Anno Accademico 2020/2021

## CONSULTAZIONE TESI DI DOTTORATO DI RICERCA

Il/la sottoscritto/I Francesco Starinieri  
Matricola / *registration* 014385  
*number*  
nato a/ *born at* Pescara  
il/on 15/03/1993

autore della tesi di Dottorato di ricerca dal titolo / *author of the PhD Thesis titled*  
Investigating Liver Tissue Dynamics To Improve In Vivo Gene Therapy

AUTORIZZA la Consultazione della tesi / *AUTHORIZES the public release of the thesis*

NON AUTORIZZA la Consultazione della tesi per 12 mesi / *DOES NOT AUTHORIZE the public release of the thesis for 12 months*

a partire dalla data di conseguimento del titolo e precisamente / *from the PhD thesis date, specifically*

Dal / *from* 17/12/2021 Al / *to* 17/12/2022

Poiché / *because*:

l'intera ricerca o parti di essa sono potenzialmente soggette a brevettabilità/ *The whole project or part of it might be subject to patentability;*

ci sono parti di tesi che sono già state sottoposte a un editore o sono in attesa di pubblicazione/ *Parts of the thesis have been or are being submitted to a publisher or are in press;*

la tesi è finanziata da enti esterni che vantano dei diritti su di esse e sulla loro pubblicazione/ *the thesis project is financed by external bodies that have rights over it and on its publication.*

E' fatto divieto di riprodurre, in tutto o in parte, quanto in essa contenuto / *Copyright the contents of the thesis in whole or in part is forbidden*

Data /Date 17/11/2021 Firma /Signature



## DECLARATION

This thesis has been composed by myself and has not been used in any previous application for a degree. Throughout the text I use both 'I' and 'We' interchangeably.

All the results presented here were obtained by myself, except for:

- 1) *3D imaging (Results, chapter 3.2.2, figure 6 C-F) was performed in collaboration with C. Covino, ALEMBIC facility, IRCCS San Raffaele Scientific Institute, Milan, Italy, who acquired the images, and Dr. F. Moalli and Gioia Ambrosi, IRCCS San Raffaele Scientific Institute, Milan, Italy, who analyzed the images.*
- 2) *FIX ELISA assay (Results, chapters 3.3.1, 3.3.2, 3.6, figures 8 A-B, 9 A, 15 D-E) was performed by Mauro Biffi, SR-TIGET, Milan, Italy.*
- 3) *Count of mono- and bi-nucleated hepatocytes (Results, chapter 3.3.2, figure 9B) was performed by Eugenia Cammarota, ALEMBIC facility, IRCCS San Raffaele Scientific Institute, Milan, Italy, who analyzed images.*
- 4) *IHC analysis (Results, chapter 3.4.1, figure 10 A-B) was performed by Amleto Focchi, IRCCS San Raffaele Scientific Institute, Milan, Italy, who prepared slides and performed staining and acquisition, and Chiara Simoni, SR-TIGET, Milan, Italy, who analyzed images.*
- 5) *Zonation analysis of IF images (Results, chapter 3.4.1, 3.4.2, 3.4.3, 3.5.1, 3.6, figure 10 D-F, 11B, 12 C-D, 13 D, 15 F-G) was performed by Cammarota, ALEMBIC facility, IRCCS San Raffaele Scientific Institute, Milan, Italy, who analyzed images.*
- 6) *Blood samples collection for ELISA assays was performed by Fabio Russo, SR-TIGET, Milan, Italy.*
- 7) *Statistical analysis was performed upon consulting with Chiara Brombin and Alessandro Nonis, San Raffaele University Center for Statistics in the Biomedical Sciences (CUSSB), Milan, Italy.*

All sources of information are acknowledged by means of reference.

## Abstract

The liver is a relevant target organ for *in vivo* gene therapy, being involved in several coagulation disorders and metabolic diseases. Adeno-associated viral (AAV) vectors have been extensively used for liver gene therapy, obtaining successful results in clinical trials. Despite AAV vector genomes remain mostly episomal, the transgene has been shown to be maintained for several years in the adult liver. However, active hepatocyte proliferation during liver growth currently challenges application of AAV-vector gene therapy to young individuals. We have previously developed lentiviral vectors (LV) that integrate their genome into host DNA and achieve stable transgene expression in adult mice, dogs, and non-human primates. Here we performed an in-depth analysis of maintenance of LV-transduced hepatocytes following post-natal liver growth and homeostasis and of the age-dependent impact on liver-directed LV gene therapy in mice. We observed a high hepatocyte proliferation rate in newborn mice that decreased over time, with only 25% of hepatocytes contributing to liver growth, generating the vast majority of the adult liver. No major differences have been observed between proliferation of LV-transduced and non-transduced hepatocytes. We then observed a higher hepatocyte transduction efficiency in young (newborn and juvenile) mice compared to adults, paralleled by a lower uptake of LV by non-parenchymal cells. By intravenously (i.v.) administering LV expressing a human coagulation factor IX (FIX) transgene we observed the highest FIX output in mice treated as juvenile, which substantially dropped when mice were treated from the 4<sup>th</sup> week of age. Newborn-treated mice showed an intermediate level of transgene output. Young mice also showed a higher percentage of multiple-transduced hepatocytes, which might contribute to the differences in transgene output. We then investigated the distribution of transduced hepatocytes in the liver lobule and observed a preferential transduction in the peri-central area in young-treated mice and in the peri-portal area in adult-treated mice. We observed that also Kupffer cells shift from the central to the portal area during growth, however their depletion did not reduce the peri-portal transduction bias in adult mice, indicating that they are not determining the LV transduction bias. Overall, our work showed that i.v. LV administration to young mice results in higher hepatocytes transduction and transgene output than in adult-treated mice, with maintenance of the transgene following cell proliferation during liver growth. These findings inform further development of liver-directed LV gene therapy towards application to pediatric patients and shed light on mechanisms of post-natal liver growth in mice, which are relevant also for genome editing strategies.

## Table of Contents

Acronyms and abbreviations .....	4
List of tables and figures.....	9
1. Introduction .....	10
1.1 Gene therapy .....	10
1.1.1 Half century of gene therapy .....	11
1.1.2. Results, concerns and future perspectives .....	16
1.2. Gene therapy vectors .....	19
1.2.1. Non-integrating viral vectors: Adenoviral and AAV vectors.....	20
1.2.2. Integrating viral vectors: retroviral vectors.....	22
1.2.3. Non-viral vectors.....	24
1.3. Lentiviral vectors .....	25
1.4. The liver: architecture, function and tissue dynamics.....	28
1.4.1. Hepatocytes metabolic functions .....	30
1.4.2 Tissue dynamics.....	34
1.4.3 Liver immunological functions .....	38
1.5. Liver gene therapy .....	39
1.5.1. Hemophilia gene therapy.....	40
1.5.2. Gene therapy for inborn errors of metabolism.....	42
1.5.3. Current challenges and limitations of in vivo liver gene therapy .....	43
1.5.4. LV-based liver gene therapy .....	45
1.5.5. In vivo genome editing .....	46
1.6. Liver gene therapy during liver growth.....	48
2. Aim of the work .....	50
3. Results .....	51
3.1 Hepatocytes proliferation during growth and homeostasis .....	51
3.1.1 A fraction of proliferating hepatocytes in newborn mice gives rise to most of the adult liver .....	52

3.1.2 Reduced proliferation rate of hepatocytes from the second week of age .....	54
3.2 Proliferation of LV-transduced and untransduced hepatocytes.....	57
3.2.1 LV-transduced and untransduced hepatocytes proliferate at a similar rate .....	57
3.2.2 3D analysis show local proliferation and expansion of transduced and untransduced hepatocytes .....	59
3.2.3. Reduction of proliferation rate of hepatocytes inside single-cell derived cluster .....	61
3.3. Age-dependent differences in liver-directed LV gene therapy.....	63
3.3.1. Administration of LV to newborn and juvenile mice improves hepatocyte transduction efficiency and transgene output .....	63
3.3.2. Mono- and bi-nucleated hepatocytes are transduced with the same efficiency at all ages.....	65
3.4. Analysis of the distribution of LV transduction in the liver lobule at different ages of treatment .....	67
3.4.1 The LV transduction preference switches from peri-central to peri- portal during growth .....	67
3.4.2 KC distribution in the liver lobule follows LV transduction bias.....	69
3.4.3. Peri-portal transduction bias in adult mice is independent from phagocytosis of LV by KC.....	71
3.5. Multiple transduction of hepatocytes.....	72
3.5.1 The frequency of multiple-transduction events is lower in adult-treated than young-treated mice .....	72
3.5.2. LV transduction does not induce a proliferative advantage in hepatocytes .....	75
3.6. Role of pseudotype, promoter and integration on gene therapy efficiency at different ages of treatment .....	76
3.7. LV transduce the same hepatocyte subset in newborn and 2-week-old mice .....	78
3.8. Physiological protein expression in the growing liver.....	81
4. Discussion .....	83

4.1 Hepatocyte proliferation rate during growth and homeostasis .....	83
4.2. Proliferation of transduced hepatocytes.....	84
4.3. Effect of age at treatment on liver transduction .....	86
4.4. Effect of age at treatment on transgene output.....	87
4.5. Role of KC on gene therapy efficiency .....	89
4.6. Limitations of the work .....	90
4.7. Future directions .....	91
4.8. Conclusions .....	92
5. Material and methods .....	94
5.1. Plasmid construction.....	94
5.2. Plasmid DNA preparation .....	94
5.3. Cell culture.....	94
5.4. LV production .....	95
5.5. LV titration .....	95
5.6. ddPCR for LV titration and VCN determination.....	96
5.7. Flow cytometry .....	96
5.8. Mice experiments .....	96
5.9. Sorting of liver cell subpopulations .....	97
5.10. Gene expression analysis .....	98
5.11. ELISA assays .....	98
5.12. Immunofluorescence imaging .....	99
5.13. Immunohistochemistry imaging .....	101
5.14. Liver clearing and 3D imaging .....	101
5.15. Western blot.....	102
6. References .....	103

## Acronyms and abbreviations

2D	2-dimensional
3D	3-dimensional
AAP	Assembly-activating protein
AAT	$\alpha$ 1 anti-trypsin
AAV	Adeno-associated virus
AAVS1	Adeno-Associated Virus Integration Site 1
ABC	ATP binding cassette
ABE	Adenine base editor
AcNPV	Autographa californica nuclear polyhedrosis virus
ADA	Adenosine deaminase deficiency
AdV	Adenovirus-derived vector
AIDS	Acquired immunodeficiency syndrome
Alb	Albumin
ALD	X-linked adrenoleukodystrophy
ALL	Acute lymphoblastic leukemia
ALT	Alanine aminotransferase
APC	Antigen presenting cell
ARSB	Arylsulfatase B
AST	Aspartate transaminase
BBB	Blood-brain barrier
BDD	B-domain-deleted
BEC	Biliary epithelial cells
BMP	Bone morphogenetic protein
BSA	Bovine serum albumin
CALD	Cerebral adrenoleukodystrophy
CAR	Chimeric antigen receptor
Cas9	CRISPR associated protein 9
CBE	Cytosine base editor
cFIX	Canine FIX
CK7	Cytokeratin-7
CMV	Cytomegalovirus
CNS	Central nervous system
cPPT	Central polypurine tract
CRISPR	Clustered regularly interspaced short palindromic repeats
CTS	Central termination site



dCas9	Dead Cas9
ddPCR	Digital droplet PCR
DLBCL	Large B-cell lymphoma
DRG	Dorsal root ganglion
EdU	5-ethynyl-2'-deoxyuridine
EMA	European medicines agency
ERT	Enzyme replacement therapy
ET	Enhanced transthyretin
FACS	Fluorescence-activated cell sorting
FBS	Fetal bovine serum
FDA	Food and drug administration
FGF	Fibroblast growth factor
FISH	Fluorescence in situ hybridization
FIX	Coagulation factor IX
FVIII	Coagulation factor VIII
Fz	Frizzle
GAA	Acid $\alpha$ -glucosidase
GAG	Glycosaminoglycan
GBM	Glioblastoma multiforme
gDNA	Genomic DNA
GFP	Green fluorescent protein
GP64	Major envelope glycoprotein
gRNA	Guide RNA
GS	Glutamine synthetase
GSD1a	Glycogen storage disease type Ia
hAAT	Human AAT
HBSS	Hank's balanced salt solution
HCC	Hepatocellular carcinoma
HCR	Hepatocyte control region
HDR	Homology directed repair
HEK	Human embryo kidney
hFIX	Human FIX
HIF	Hypoxia-inducible factor
HIV	Human immunodeficiency virus
HNF4a	hepatocyte nuclear factor 4a
HSC	Hematopoietic stem cells
HybHP	Hybrid hepatocytes

IDLV	Integrase-defective lentiviral vector
IF	Immunofluorescence
IFN	Interferon
IgG	Immunoglobulin G
IgM	Immunoglobulin M
IHC	Immunohistochemistry
IL	Interleukin
IL2R	IL-2 receptor
IMDM	Iscove's modified Dulbecco's medium
i.p.	Intraperitoneally
IRES	Internal ribosome entry site
IS	Integration site
ITR	Inverted terminal repeat
IU	International units
kb	Kilobases
KC	Kupffer cell
kDa	kilo-Dalton
LB	Luria-Bertan medium
LDL-R	Low density lipoprotein receptor
LNP	Lipid nanoparticle
LPC	Liver progenitor cells
LPL	Lipoprotein lipase
LPLD	LPL deficiency
LPS	Lipopolysaccharides
LRP	LDL-R related proteins
LSD	Lysosomal storage diseases
LSECs	Liver sinusoid endothelial cells
LTR	Long terminal repeat
LV	Lentiviral vector
M6P	Mannose-6-phosphate
MAAP	Membrane-associated accessory protein
MHC	Major histocompatibility complex
miRNA	micro-RNA
MLD	Metachromatic leukodystrophy
MM	Multiple myeloma
MMLV	Moloney murine leukemia virus
MOI	Multiplicity of infection

MPS	Mucopolysaccharidosis
Mtz	1-(2-hydroxyethyl)- 2-methyl-5-nitroimidazo
NAB	Neutralizing antibodies
NHEJ	Non-homologous end joining
NHP	Non-human primates
NIH	National Institutes of Health
nt	Nucleotides
NTR	Nitroreductase
OCT	Optimal cutting temperature
ORF	Open reading frames
OTC	Ornithine transcarbamylase
PAM	Protospacer adjacent motif
PBS	Phosphate saline buffer
PC	Peri-central
PCSK9	Proprotein convertase subtilisin/kexin type 9
pDC	Plasmacytoid dendritic cells
PEG	Poly-ethylene glycol
PFA	Paraformaldehyde
PolyA	Polyadenylation
PP	Peri-portal
PRR	Pattern recognition receptor
PSCs	portal-to-systemic collaterals
qPCR	Quantitative polymerase chain reaction
rAAV	Recombinant AAV
RFP	Red fluorescent protein
RPE65	Retinal pigment epithelium-specific 65 kDa protein
RRE	Rev responsive element
RSPO	R-spondin
SA	Splice acceptor
s.c.	Subcutaneously
scAAV	Self-complementary AAV
scFV	Single-chain variable fragment
SCID	Severe combined immunodeficiency
SCID-X1	X-linked SCID
scRNAseq	Single-cell RNA sequencing
SD	Splice donor
SD	Standard deviation

SEM	Standard error of the mean
SIN	Self-inactivating
siRNA	Small interfering RNA
SIRP $\alpha$	Signal Regulatory Protein $\alpha$
SMA	Spinal muscular atrophy
ssDNA	Single stranded DNA
TALEN	Transcription activator-like effector nucleases
TetO	Tetracycline operator
TNF	Tumor necrosis factor
TTR	Transthyretin
TU	Transducing units
UGT1A1	UDP-glucuronosyltransferases
VCN	Vector copy number
vg	vector genomes
VSV.G	Vesicular stomatitis virus G protein
WAS	Wiskott-Aldrich syndrome
WHV	Woodchuck Hepatitis Virus
WPRE	WHV Posttranscriptional Regulatory Element
wt	Wild-type
X-CGD	X-linked chronic granulomatous disease
YFP	Yellow fluorescent protein
ZFN	Zinc-finger nuclease
$\beta$ 2M	$\beta$ 2-microglobulin

## List of tables and figures

Figure I.....	26
Figure II.....	30
Table I.....	36
Figure III.....	48
Figure 1.....	51
Figure 2.....	53
Figure 3.....	55
Figure 4.....	56
Figure 5.....	57
Figure 6.....	60
Figure 7.....	62
Figure 8.....	64
Figure 9.....	66
Figure 10.....	68
Figure 11.....	70
Figure 12.....	71
Figure 13.....	73
Figure 14.....	75
Figure 15.....	77
Figure 16.....	79
Figure 17.....	81

# 1. Introduction

## 1.1 Gene therapy

Genetic mutations are a rather common event occurring spontaneously or induced by external factors during cell replication, and the resulting genetic variations deriving from these errors represent the motor of evolution, thanks to the appearance of new characteristics that could confer a survival or reproductive advantage to the organism in a constantly changing environment. Despite the utility of this mechanism from an evolutionary perspective, genetic mutations may also be deleterious. Indeed, the accumulation of mutations in somatic cells during life are not significant for the transmission of new characteristics to descendants, and although are often silent, they can potentially induce a malignant transformation of cells that leads to development of tumors. On the other hand, heritable genetic mutations occurring in germline cells can be responsible of the appearance of genetic diseases. The modification even of a single nucleotide in a gene could induce an aminoacidic change that impair the normal function of the protein coded, or the appearance of a premature stop codon that blocks the translation of mRNA into protein, or an alteration in the regulation of the expression of the protein. This single mutation can be responsible of a serious reduction of quality or expectancy of life of the affected person. For a long time, medicine has tried to tackle genetic diseases by treating symptoms and/or supplying the absent or altered protein to the organism (enzyme replacement therapy, ERT), but this approach presents several limitations. The protein administered intravenously is often recognized as "non-self" by the organism, because of the lack of an active immune tolerance for that antigen that is normally established during development for all the endogenous proteins. The production of anti-drug-antibodies strongly affects the efficacy of the therapy (Banugaria *et al*, 2011). Moreover, this approach showed good results only in the case of the administration of circulating proteins, such as coagulation factors in the case of hemophilia (Orlova *et al*, 2012), or proteins that could be internalized by the target cells, such as in lysosomal storage diseases (LSD) (Li, 2018), thus reducing its applicability. But even for those diseases for which ERT has been effective, variation of protein level over time and constant need for drug re-administration significantly impact patients' quality of life. Conversely to the treatment approach comprising ERT, that intervenes on symptoms instead of causes, in the last 50 years there has been a growing interest into gene therapy, a curative approach that tackles the disease at its root and that is based on substitution or modification of the gene causing the

disease. The major advantage of gene therapy, if successful, is the achievement of the complete rescue of the normal phenotype by a single administration of the drug product. The most common approach used in gene therapy is called gene addition (or gene replacement), that consist in the introduction into the cell of genetic material containing a correct version of the gene, which, when mutated causes the disease. Gene addition is based on the introduction into the patient cells of genetic material to allow expression of a functional form of the protein involved in the disease. The most obvious way to deliver the curative genetic material would be the administration of naked DNA or RNA into the patients or cells, but this method is very inefficient (Yin *et al*, 2014), therefore many kinds of vectors have been developed over time, and the most efficient and widely used are based on viruses.

In recent years, other gene therapy strategies have been developed beside gene addition. In particular, the availability of engineered sequence-specific DNA endonucleases opened the possibility to introduce precise edits in the genome, which is referred to as genome editing. Genome editing has the potential to obtain correction of the mutated gene directly in the locus (gene correction), or its knockout through the induction of a DNA damage (gene suppression), or to target integration of genetic material into a specific genomic site (targeted integration). Nuclease proteins can induce a double-strand DNA break in a genomic locus by recognition of a specific sequence. The cell can correct the damage in 2 ways: non-homologous end joining (NHEJ) or homology-driven repair (HDR) (O'Driscoll & Jeggo, 2006). NHEJ is an error-prone mechanism by which DNA ends are attached, but often with small insertions or deletions, that if occurs in a coding region can alter or stop the expression of the protein, and therefore can be used for gene suppression strategies. Conversely, cells can try to repair DNA through HDR, exploiting another DNA sequence with homology to the nuclease target site, that can be copied to restore a functional version of the gene. HDR can be exploited to correct mutations and is therefore considered a gene correction strategy. Gene suppression can be obtained also through the insertion of small non-coding RNAs that can suppress the expression of a protein by pairing with RNA and inducing its degradation.

### **1.1.1 Half century of gene therapy**

The idea of gene addition therapies lay its foundations on the finding of Tatum in the 1960s that viruses can transfer their genetic material into infected cells, and they are inherited through cells division because of chromosomal insertion of the viral genome (Temin, 1961; Sambrook *et al*, 1968; Tatum, 1966). The first gene replacement therapy ever attempted dates back to 1974, when unmodified Shope

papilloma virus was administered intravenously into 3 patients affected by hyperargininemia, caused by lack of the arginase I enzyme, resulting into high concentration of arginine in circulation. The idea was that Shope papilloma virus carries a functional version of arginase I enzyme and could thus reduce arginine bloodstream levels. Unfortunately, no beneficial effect was observed in treated patients (Terheggen *et al*, 1975) because, as was later found out, Shope papilloma virus genome did not code for arginase I enzyme. The arrival of genetic engineering techniques in the 70s and 80s paved the way for modern gene therapy, thanks to the opportunity to generate recombinant viral genomes. In particular, genetic engineering has been used to introduce a therapeutic gene into the viral genome, to be carried inside the patient cells, but also to change part of the viral genome that are responsible for their infectivity, to make them replication defective and safer. As a consequence, in the 80s and 90s there has been an increasing interest into gene therapy, and a first wave of clinical trials were carried out in USA and Europe. In this phase 2 branches of gene therapy were carried on: on one side, thanks to the advancement of hematopoietic stem cells (HSC) transplantation,  $\gamma$ -retroviral vectors were used for *ex vivo* gene therapy; on the other side adenovirus-derived vectors (AdV) and adeno-associated virus (AAV)-derived vectors were directly injected into the patient for *in vivo* gene therapy. *Ex vivo* gene therapy is based on the collection of autologous cells from the patient, which are then corrected *in vitro* by the introduction of the therapeutic transgene and then infused again in the organism. Thanks to their accessibility for explant and the ease in reinfusion, hematopoietic cells are the most common target of *ex vivo* gene therapy, and in particular HSC and T lymphocytes. The first *ex vivo* gene therapy trial was approved in 1990 by US Food and Drug Administration (FDA) for the treatment of patients affected by adenosine deaminase deficiency (ADA), a form of severe combined immunodeficiency (SCID), by infusion of autologous T cells transduced with  $\gamma$ -retroviral vector containing ADA transgene (Blaese *et al*, 1995). Short after, another clinical trial in ADA-SCID patients obtained promising results by targeting bone marrow HSC (Bordignon *et al*, 1995), paving the way for the approval of the first *ex vivo* gene therapy product by the European Medicines Agency (EMA) in 2016, commercialized with the name Strimvelis and administered to more than 50 patients so far (Ferrua & Aiuti, 2017). Simultaneously, AAV vectors were developed for *in vivo* gene therapy, leading to a pioneering clinical trial for hemophilia B targeting hepatocytes. In this trial, expression of therapeutic levels of coagulation factor IX (FIX), the protein missing in hemophilia B, was obtained, however, unfortunately, it lasted for only a few weeks because of an immune reaction directed against transduced liver cells (Manno *et al*,



2006). Despite this phase of expansion and enthusiasm for gene therapy provided the first promising results, it was also characterized by unfortunate events. Integration of vector genome into host cells resulted in 5 cases of leukemia out of 20 patients in 2 clinical trials for X-linked SCID (SCID-X1) based on correction of bone marrow HSC by transduction with  $\gamma$ -retroviral vector carrying IL-2 receptor (IL2R) gene (Hacein-Bey-Abina *et al*, 2008; Howe *et al*, 2008). Moreover, the use of retroviral vectors resulted in genotoxicity also in a clinical trial to treat Wiskott-Aldrich syndrome (WAS), in which 7 out of 10 patients developed acute leukemia (Braun *et al*, 2014). 2 cases of myelodysplasia have been detected also in patients affected by X-linked chronic granulomatous disease (X-CGD) in a clinical trial exploiting  $\gamma$ -retroviral vector (Stein *et al*, 2010). Another event that represented a turning point for gene therapy was the death of Jesse Gelsinger, that could be attributed directly to the administration of the vector. Jesse was affected by ornithine transcarbamylase (OTC) deficiency, a metabolic disease affecting aminoacidic metabolism, and at 18 years of age was enrolled in a clinical trial based on the intra-hepatic administration of AdV. He started to experience severe complications short after the treatment and died 2 days later of multiple organ system failure caused by a massive immune response induced in response to systemic vector administration (Raper *et al*, 2003). These adverse events pushed scientist to go back from bedside to bench to deepen the understanding of vector biology and safety and their interactions with the host genome and the immune system. One of the major subsequent advances was the development of human immunodeficiency virus (HIV)-derived lentiviral vectors (LV), which are integrating vector like  $\gamma$ -retroviral vectors but with a higher safety profile and have the advantage to integrate their genome into non-dividing cells (Reiser *et al*, 1996). LV progressively replaced  $\gamma$ -retroviral vectors for transduction of hematopoietic cells (Akkina *et al*, 1996), but showed to be efficient also for *in vivo* applications (Naldini *et al*, 1996). Over time, LV found multiple applications besides *ex vivo* gene therapy for immunological syndromes. It turned out that hematopoietic cells can be used as a cargo to carry therapeutic molecules, expressed by the transgene, into specific site, such as the central nervous system (CNS). Promising results have been achieved for X-linked adrenoleukodystrophy (ALD) (Cartier *et al*, 2009), a fatal demyelinating disease, and metachromatic leukodystrophy (MLD) (Biffi *et al*, 2013), a neurodegenerative LSD. Gene therapy for MLD has recently obtained market authorization by EMA and will be commercialized with the name Libmeldy (Fumagalli *et al*, 2020; Jensen *et al*, 2021). Market authorization has been accorded in 2021 also for treatment of cerebral adrenoleukodystrophy (CALD), a severe form of ALD (Skysona; (Eichler *et al*, 2017). LV-based *ex vivo* gene therapy has been

widely explored also to treat hematological disorders such as hemoglobinopathies. Promising results have been achieved for sickle-cell disease and  $\beta$ -thalassemia (Cavazzana & Mavilio, 2018), and for the latter Zynteglo, a drug based on HSC transduced with LV encoding a  $\beta$ -globin gene, received EMA authorization in 2019 (Thompson *et al*, 2018). In the last twenty years *ex vivo* gene therapy has been also explored to fight cancer, and now it represents its most common application. The first attempts were based on the idea of introducing cytotoxic or suicide genes in the tumor (Oldfield *et al*, 1993), but their efficacy was limited to the primary solid tumor and not on metastasis, therefore the attention shifted again to hematopoietic cells, that can be used to carry molecules that redirect immune system to attack cancer cells. This has been attempted with expression of cytokines, such as interferon- $\alpha$  (IFN $\alpha$ ), that can be narrowed to tumor-infiltrating macrophages, with the purpose of inverting the immunosuppressive tumor microenvironment and stimulate an immune response in the tumor (Escobar *et al*, 2018), and promising preclinical results have been achieved for different types of solid and liquid tumors (Escobar *et al*, 2018; de Palma *et al*, 2008). Currently this strategy is under evaluation in 2 clinical trials in patients with glioblastoma multiforme (GBM) (NCT03866109) and multiple myeloma (MM) (NCT03875495). A different strategy for cancer gene therapy consists in the genetic modification of autologous T-cells to express a chimeric antigen receptor (CAR) that is able to recognize a tumor antigen. This is obtained through the fusion of the single-chain variable fragment (scFV) from an antibody specific for the antigen of interest, with the intracellular activation domain from CD3 zeta chain (CD3 $\zeta$ ) and a costimulatory domain (CD28, 4-1BB or both) (June *et al*, 2018). CAR-T have already obtained market authorization for B-cell acute lymphoblastic leukemia (ALL, Kymriah) and large B-cell lymphoma (DLBCL, Kymriah and Yescarta), in both cases with targeting of CD19 antigen (Locke *et al*, 2019; Schuster *et al*, 2019; Maude *et al*, 2018).

From the 90s also AdV progressively left the stage to AAV vectors, which became the most used non-integrating vector, and found applications for *in vivo* gene therapy in liver, eye, muscle and CNS (Mingozzi & High, 2011), which are considered post-mitotic organs, and therefore the low or absent proliferation of parenchymal cells reduces the risk of dilution of the episomal vector genome. Among the first approved gene therapy product was Glybera, an AAV1 delivering lipoprotein lipase (LPL) gene through multiple intramuscular injection in patients affected by lipoprotein lipase deficiency (LPLD), a defect in triglycerides metabolism (Scott, 2015). The product was administered to 31 patients in total before being retracted from the market due to the high cost and low number of patients available, therefore has been judged

unprofitable by the developer (Shukla *et al*, 2019). Subretinal administration of AAV vector carrying RPE65 gene, coding for retinal pigment epithelium-specific 65 kDa protein, improved visual function in patients affected by a genetic form of retinal degeneration (Leber congenital amaurosis) in multiple clinical trials, one of which (NCT01208389) showed sustained expression over time, with also injection in the contralateral eye (Bennett *et al*, 2016), and led to the approval of Luxturna by FDA in 2017, the first gene therapy approved in the USA. AAV vectors versatility has been improved through the exploration of different serotypes, either by using the ones available in nature or by designing new ones. This led also to the creation of a tool that can overcome one of the major obstacles for the treatment of diseases affecting CNS, which is the crossing of the blood-brain barrier (BBB). Indeed, AAV9 has been found to be able to naturally cross BBB (Foust *et al*, 2008), and therefore has been exploited for brain-directed gene therapy. In particular, it has been studied in the context of spinal muscular atrophy (SMA), a disease caused by a mutation in SMN1 gene that results in the loss of motor neurons. A clinical trial on 15 patients less than 1 year old obtained a remarkable improvement in survival and motor function score (Mendell *et al*, 2017), and led to the approval of the therapy by FDA in 2019 with the commercial name Zolgensma.

In parallel to gene addition, gene correction strategies have been developed in the last twenty years. The first genome editing attempts exploited zinc-finger nucleases (ZFNs), meganucleases or transcription activator-like effector nucleases (TALENs), that are based on engineering of DNA-binding protein to recognize specific DNA sequence and induce a double-strand break (Silva *et al*, 2011). But the discovery of the CRISPR (clustered regularly interspaced short palindromic repeats) bacteria defense system made much easier redirecting the nuclease, because the CRISPR associated protein 9 (Cas9) exploited by this system is guided by an RNA molecule rather than DNA-binding domain, and consequently is simpler to engineer. The guide RNA (gRNA) molecule has complementarity to the DNA target sequence in proximity of a PAM (protospacer adjacent motif) site. The incredible potential of this system is demonstrated by the fact that in less than 10 years from the pioneering discovery of CRISPR (Jinek *et al*, 2012), it has already been awarded by a Nobel Prize in chemistry and has already many clinical trials ongoing for multiple diseases (Doudna, 2020), both for *in vivo* and *ex vivo* genome editing. Lately, new technologies have been developed coupling a mutated form of Cas9 (only inducing single-strand DNA break) to adenine or cytosine deaminase domains to generate adenine base editors (ABEs) or cytosine base editors (CBEs), respectively. ABEs and CBEs can catalyze the conversion of A•T-to-G•C base pairs or C•G to T•A base pairs

respectively, thus opening the possibility to introduce site-specific point mutations (Huang *et al*, 2021b).

### **1.1.2. Results, concerns and future perspectives**

To summarize, in 50 years of history and 30 years of clinical applications, gene therapy has achieved 9 market authorization by FDA or EMA for gene addition strategies, 6 of which consist on *ex vivo* transduction of HSC by  $\gamma$ -retroviral vector or LV to target hematological diseases (ADA-SCID and  $\beta$ -thalassemia) or diseases affecting CNS (CALD and MLD), or by CAR-T engineering to target B-cell malignancies, and the other 3 (2 on the market, 1 withdrawn for commercial reasons) involve local (in eye or muscles) or systemic administration of AAV vectors (targeting mainly CNS). Therefore, gene therapy represents the first curative strategy for genetic diseases that became a clinical reality, and now efforts are underway to broaden its clinical applications. And this has been done by transforming pathogens such as viruses into an ally, in particular with HIV-derived LV, that have been developed during the first wave of spread of AIDS epidemic. For this reason and for its troubled history, gene therapy still faces many challenges and skepticism.

One of the main critical aspects of gene therapy, that came out also from the first phase of clinical trials, is the risk of genotoxicity by insertional mutagenesis. Indeed, it is known that the integration of viral DNA in the host genome can alter expression of neighbor genes, thus inducing a malignant transformation of cells, and this phenomenon has been observed for multiple viral infections (Bushman, 2020; Levrero & Zucman-Rossi, 2016). In gene therapy this aspect is of concern particularly for integrating vectors based on  $\gamma$ -retrovirus and lentivirus. As mentioned before, several cases of vector-induced insertional mutagenesis have been observed in multiple clinical trials by transducing hematopoietic cells with  $\gamma$ -retroviral vectors. At the time of the development of the first therapeutic strategies and clinical trials the entire sequence of the human genome was not available yet, and it was not easy to accurately study the integration pattern of viral genome, therefore it was believed that integration of the viral DNA in the host genome was random. Conversely, it was later shown that  $\gamma$ -retroviruses integrate their genome preferentially in close proximity to transcription start sites (Wu *et al*, 2003), therefore potentially dysregulating the expression of the neighbor genes. Indeed, in 2 patients of the SCID-X1 clinical trial that developed leukemia there was an expansion of clones with transgene integration near the transcription start site of LMO2 gene, that is crucial for hematopoietic development, and which expression was found to be upregulated (Hacein-Bey-Abina *et al*, 2003). A third patient showed enrichment of clones with

integration upstream of the *CCDN2* transcription start site, that encodes for cyclin D2, a known oncogene (Hacein-Bey-Abina *et al*, 2008). From this point of view LV resulted to be safer than  $\gamma$ -retroviruses because they preferentially integrate their genome in coding regions of active genes, but not in proximity of the transcription start site, thus reducing the risk of dysregulation of endogenous genes (Schröder *et al*, 2002; Wu *et al*, 2003). But as it has been shown in HIV-infected patients (Maldarelli *et al*, 2014), also LV cannot be considered completely safe, therefore it is important to deeply study vector-genome interactions to design vectors with the lowest possible risk of genotoxicity. As an example, improvement in vector safety has been obtained by the development of self-inactivating (SIN) long terminal repeats (LTR), that show a reduced genotoxicity risk compared to transcriptionally active LTR (Montini *et al*, 2009), but also the choice of the promoter can impact on genotoxic potential (Scholz *et al*, 2017). Despite these improvements, in 2021 a clinical trial for CALD exploiting transduction of HSC by LV has been placed on hold by FDA upon the report of a myelodysplastic syndrome in a patient more than 1 year after treatment, only a couple of months after EMA market approval in Europe. The sponsor stated that specific design features of the LV likely contributed to this event (Keam, 2021).

Despite they are considered non-integrating, AAV vectors are not exempt from the risk of causing insertional mutagenesis. Wild-type AAV2 genome integration has been retrieved in 11 of 193 hepatocellular carcinoma and occurred in known cancer driver genes (Nault *et al*, 2015). Despite AAV vectors lack Rep gene, that in wild-type virus has DNA integrase activity (Smith, 2008), they have been shown to integrate with low efficiency in the host genome, however, considering the high doses used for treatment also this low efficiency of integration might be worrisome. Recently an AAV-based pre-clinical study for hemophilia A gene therapy in dogs showed multiple integrations of entire or fragmented vector genomes 10 years after treatment, with a preference for transcription units and for cancer-related genes, that led to non-malignant clonal expansion of targeted hepatocytes and increase in transgene expression in 2 dogs (Nguyen *et al*, 2021).

Another major issue in gene therapy is the immune response to either the vector or the transgene, indeed the uncontrolled and excessive immune reaction to the vector particles has been demonstrated to be the cause of a gene therapy-related death, the one of Jesse Gelsinger. While immunogenicity of the vector is less of a concern for *ex vivo* gene therapy strategies because the vector does not directly enter the body, it is particularly relevant for *in vivo* gene therapy. The encounter of the vector with the immune system induces the formation of neutralizing antibodies

(NAB), but they can be present in the patient even before treatment if they have been infected by the wild-type virus. While pre-existing immunity to LV is very low in the population, seroprevalence of NAB against AAV varies from 5% to 60%, depending on the serotype (Jeune *et al*, 2013), therefore patients are typically screened before enrollment in clinical trials of systemic AAV vector administration. Moreover, administration of a 2<sup>nd</sup> dose of the vector might be needed to counteract transgene dilution over time in therapies with non-integrating vectors, but it can be inhibited by NAB and might be challenging also using a different serotype because of possible cross-reactivity of NAB. Injection of a 2<sup>nd</sup> dose of AAV vector is possible in the eye, thanks to an immune-privileged environment (Bennett *et al*, 2012). Immunosuppression may be needed also to control T-cell mediated reaction against transduced cells, that expose AAV capsid antigens on class-I major histocompatibility complex (MHC) molecules, and this led to transgene loss in the first liver-directed gene therapy trial for hemophilia B (Pien *et al*, 2009). Adaptive immune response can be induced also against the transgene product, both in terms of production of antibodies and CD8<sup>+</sup> T-cell response and can be developed independently from the type of vector used (Calcedo *et al*, 2017), and can also affect *ex vivo* gene therapy (Squeri *et al*, 2019). In *in vivo* gene therapy, immune response against the transgene can be induced by transduction of antigen presenting cells (APCs), that can express the transgene despite the use of a tissue-specific promoter. This can be avoided by adding micro-RNA (miRNA) targeting site downstream the transgene, and in particular miRNA 142, expressed in hematopoietic cells, has been used to avoid transgene expression in APCs (Brown *et al*, 2006; Muhuri *et al*, 2021). Moreover, another major limitation of *in vivo* transduction by systemic administration of LV is phagocytosis by tissue-resident macrophages. This can be reduced by displaying high amounts of CD47 anti-phagocytic molecules on vector surface (Milani *et al*, 2019).

These observations and partially unsolved hurdles of gene therapy indicate that, in order to achieve the safest and most effective treatment possible, it is fundamental to deeply understand vector biology and to characterize its interaction with the organism from all points of view. Notably, in 1995 a National Institutes of Health (NIH) advisory panel concluded that the low clinical efficacy obtained until then in gene therapy trials could be attributed to “an inadequate understanding of the biological interaction of these vectors with the host” and suggested to focus investigations on basic aspects of gene transfer and the study of disease pathophysiology (Orkin *et al*, 1995). Later in time, we could testify that these efforts were actually put in place and led to some very successful gene therapy applications.

It is now important to continue to study delivery vectors and vector-host interaction to guarantee safety and efficacy of new gene therapy treatments.

Besides all of these biological hurdles for gene therapy, the story of Glybera also tell us that challenges in gene therapy also derive from the economic and social point of view. Indeed, gene therapy has a very high cost for a single-shot treatment, that ranges from 400.000\$ for CAR-T therapies Yescarta and Kymriah and 690.000\$ for Strimvelis (Shukla *et al*, 2019) to more than 2 million \$ for Zolgensma (Garrison *et al*, 2021). However, alternative treatments, such as ERT, are costly too and are life-long expenses. For example, prophylactic hemophilia treatment in the USA ranges from 200.000\$ to 400.000\$ per year (Thorat *et al*, 2018). Therefore, a one-shot 2-million-dollar treatment would be cheaper than more than 10 years of current prophylaxis. Nevertheless, the high cost and the technical challenges of the gene therapy treatments, in particular for *ex vivo* therapies, and difficult deployment in developing countries, are all emerging problems that the field has to face now that the efficacy and potential of gene therapy has been demonstrated.

## **1.2. Gene therapy vectors**

To overcome the challenge of delivering nucleic acids into target cells, multiple viral and non-viral vectors have been developed. As mentioned above, the concept itself of gene therapy derives from the observation of the possibility to transfer genetic material exploiting viruses (Temin, 1961; Sambrook *et al*, 1968; Tatum, 1966), therefore viral vectors have been among the first to be developed. Despite they are very efficient in transferring genetic material, because of their origin they are also more likely to induce an immune response in the host organism, therefore they necessitate extensive engineering of their genome and could represent a hazard from safety point of view. Thus, non-viral vectors have also been extensively studied, and lately their development was fueled by the advent of genome editing technologies. The choice of the type of vector depends on which are the needs for the desired application and whether the characteristic of a vector matches those needs. Indeed, tropism and immunogenicity depend on the type of vector, and also the type (DNA or RNA) and amount of genetic material that can be packaged. Moreover, some applications require a stable long-term expression of the transgene, others might prefer transient expression.

To develop a safe viral vectors, it is fundamental to ensure that it cannot replicate in the host organism, as the virus of origin would do. In order to make them replication defective, cis- and trans- acting sequences are separated. Trans-acting elements are those part of the viral genome that encodes for proteins involved in

packaging of the virions and transfer of the genetic material in the host cell. In general, these elements are removed from viral vectors genome and provided separately to producer cell lines, in order to assemble an intact and functional vector that lacks the elements to generate other virions upon the defective infection referred to as transduction. On the other hand, cis-acting elements are responsible for encapsidation of the vector genome construct, infectious cycle and, in case of integrating vectors, integration into the host genome, therefore are maintained in the vector genome together with the therapeutic transgene (Naldini & Verma, 2000).

### **1.2.1. Non-integrating viral vectors: Adenoviral and AAV vectors**

AdV are one of the first non-integrating vectors considered for *in vivo* gene therapy. Adenoviruses are non-enveloped viruses made of an icosahedral protein capsid that contain a linear double-stranded DNA with length ranging from 25 to 45 kb. Viral genome encodes from 35 proteins and is flanked by inverted terminal repeats (ITR), hairpin structures that prime DNA replication and contain the packaging signal. The latest generation of AdV lacks all the viral genes, that are substitute by the transgene, and only ITR are maintained from the original genome, therefore AdV have a very large cargo capacity (up to 36kb). Moreover, many different serotypes have been identified in nature to infect humans, and 2 of them (human adenovirus 2 and 5) have been exploited to generate gene therapy vectors and have a broad tropism for human tissues (Bulcha *et al*, 2021). Natural infection form adenoviruses are very common in humans, especially in the upper respiratory tract, therefore there is a high prevalence of NAB in the population, and this represent an important obstacle to its application for systemic gene therapy (Mennechet *et al*, 2019). Moreover, their high intrinsic immunogenicity represents a safety concern, particularly after the serious adverse event in the OCT trial that brought to the death of Jesse Gelsinger. AdV have been extensively used for *in vivo* gene therapy clinical trials, targeting mainly lungs and liver (Bramson *et al*, 1995), but due to the immunogenicity of the vector and the adverse events, AdV progressively left the stage to AAV for gene addition strategies. Nonetheless, AdV found extensive application into vaccine development and cancer gene therapy and are used still today in 50% of viral vector-based clinical trials (Bulcha *et al*, 2021). The immunogenicity of AdV can indeed be exploited to stimulate an immune response against the transgene encoded in its genome, and this feature makes them effective vaccines against viruses such as Ebola and influenza virus (Milligan *et al*, 2016; Sebastian & Lambe, 2018). More recently AdV have been used also in 3 of the most used vaccines for SARS-CoV2 virus (Ad26.COVID-S, ChAdOX1-nCoV and Gam-COVID-



Vac/SputnikV) (Mendonça *et al*, 2021). In the same way, AdV are used as vectors for cancer vaccination, but are also exploited as oncolytic viruses or to carry immune-regulatory genes (Shaw & Suzuki, 2019).

Despite they do not cause any known human disease, AAV have been extensively studied since their discovery in 1965. Their name derives from the fact that they lack the genes necessary for replication and expression of their own genome, thus they need adenoviruses protein to provide these functions. AAV genome is smaller than adenoviruses being only 4.7kb long, and it contains 4 open reading frames (ORFs): the first encodes for replication genes (Rep), the second encodes for 3 capsid proteins, the third for and fourth are nested sub-genomic coding for AAP (assembly-activating protein), involved in capsid assembly, and MAAP (membrane-associated accessory protein), whose function is not completely understood. The genome is a single strand DNA (ssDNA) flanked by 145-nt ITRs that, as for adenoviruses, serve as self-priming structure for replication and contains encapsidation signal (Bulcha *et al*, 2021). After infection, ssDNA is transferred into the nucleus, where the second strand is synthesized and intra- or inter-molecular recombination can occur between ITRs to form concatemer or circular DNA, that increase stability of the viral genome, that remains mostly episomal (Duan *et al*, 1998). Nonetheless, it has been observed that AAV genome can be integrated into the host DNA (Nault *et al*, 2015), and a locus in chromosome 19 has been described as common site of integration of AAV, and therefore it has been called AAVS1 (Kotin *et al*, 1991). This locus has been widely used as a safe harbor locus for targeted integration in genome editing approaches (Ward & Walsh, 2012). AAV can be used as a vector by substituting all the viral ORFs with a transgene, flanked by ITRs, thus obtaining a recombinant AAV (rAAV) (Aponte-Ubillus *et al*, 2018). Given the small dimension of viral genome, an important limit of rAAV vectors remain the small cargo capacity, that cannot exceed 5 kb. Multiple strategies have been attempted to overcome this limit. ITRs recombination capacity can be exploited to join together 2 viral genomes in a dual-vector system, or alternatively recombination can be induced between homologous sequences (Nakai *et al*, 2000). Otherwise, larger transgene can be obtained through RNA trans-splicing (Lai *et al*, 2005) or protein splicing by fusing split inteins (Li *et al*, 2008). Synthesis of the second DNA strand is fundamental for transgene expression and is the limiting step in AAV vector transduction. Double-stranded genome can be packaged into the capsid by introducing a mutation in one of the ITRs, generating a self-complementary AAV vector (scAAV) with enhanced transduction efficiency (McCarty *et al*, 2003) but with a cargo capacity halved compared to single-stranded rAAV.

AAV can be categorized according to their capsid in different serotypes. AAV serotype determines virus tropism and recognition by the immune system, and therefore have been extensively studied for vector engineering. The first source of discovery of new AAV serotypes has been natural variants found in human and non-human primates, that led to isolation of more than 100 serotypes (Wu *et al*, 2006). New serotypes can be obtained also through rational design, by which some new capsids have been obtained (Yang *et al*, 2019) but it is generally very difficult to apply, or directed evolution, that is based on iterative selection of randomly mutated capsids (Dalkara *et al*, 2013).

AAV vectors are generally recognized as weakly immunogenic and very versatile thanks to the diverse tropism conferred by different serotypes, therefore have been used in more than 200 clinical trials for diseases affecting CNS, liver, eye, heart and muscles (Bulcha *et al*, 2021). However, recent findings of AAV vector genome integration into host DNA (Nguyen *et al*, 2021) and toxicity caused by undesired transduction of dorsal root ganglion (DRG) in multiple studies in non-human primates (NHP) (Hordeaux *et al*, 2020) and for high vector doses in humans (Wilson & Flotte, 2020) raised some questions about safety of these vectors. Because of the episomal nature of AAV genome, they would progressively diluted in actively replicating cells but have shown stable long-term expression in non-dividing cells (Nathwani *et al*, 2014). AAV vectors are currently used also for genome editing. The episomal vector can be used as a donor DNA template for HDR by including homology arms flanking a genomic target site, but can also provide transient expression of Cas9 nuclease in actively replicating cells (Wang *et al*, 2020).

### **1.2.2. Integrating viral vectors: retroviral vectors**

Together with AdV, the first wave of gene therapy was characterized by an extensive use of retroviral vectors that, conversely to AdV and AAV vectors, actively integrate their genome into the host DNA. Retroviruses have a lipidic envelope, which contain a proteic capsid and a homodimer of linear, single-stranded RNA genome of 7-10 kb. Genomic RNA is retro-transcribed into a double-stranded DNA by the viral reverse transcriptase that is packaged into the virion, and then it is integrated into chromosomes by the integrase expressed by the viral genome itself. Retroviruses can be divided in 3 groups: oncoretroviruses, lentiviruses and spumaviruses, all of which have been studied for gene therapy applications (Kim *et al*, 2000). Oncoretroviruses are known to induce tumor formation, instead lentiviruses (such as HIV) induce immunodeficiencies, while spumaviruses are not linked to any known disease. The genome of retroviruses contains 3 ORFs: gag (encoding for capsid

protein), pol (encoding for protease, integrase and reverse transcriptase) and env (encoding for the envelope glycoprotein) and is flanked by long terminal repeats (LTRs) that mediate integration.

Retroviruses can be transformed into vectors by removing viral ORFs, which are substituted by the transgene, but leaving LTRs and the packaging signals. Moreover, the viral envelope glycoprotein, that mediates entry into the host cell, can be substituted with another glycoprotein from a different virus to change or expand its tropism (pseudotyping) (Cronin *et al*, 2005). Therefore, one of the most diffused envelope glycoproteins for production of retroviral vector is the vesicular stomatitis virus G glycoprotein (VSV-G). VSV-G pseudotyped retroviruses are pantropic and their entry into cells is mediated by low-density lipoprotein receptor (LDL-R) and its family members (Finkelshtein *et al*, 2013). Moreover, they resulted to be more stable, allowing concentration by ultracentrifugation and long-term storage (Burns *et al*, 1993).

Integrating vectors give the opportunity to treat dividing cells without diluting the transgene and losing its expression over time, opening the possibility to induce a selective advantage of corrected cells, and thus reaching a therapeutic level of correction by targeting a small population of cells. This aspect contributed to the success of *ex vivo* gene therapy for ADA-SCID, a severe immunodeficiency characterized by the accumulation of a toxic metabolite of adenosine that leads to lymphocytotoxicity (Bradford *et al*, 2017). Hematopoietic cells corrected by the insertion of a functional copy of adenosine deaminase carried by Moloney murine leukemia virus (MMLV, an oncolytic virus belonging to the group of  $\gamma$ -retroviruses) derived vector do not accumulate the toxic metabolite and therefore can repopulate the immune system (Aiuti *et al*, 2003).

The initial success of retroviral vectors, and in particular  $\gamma$ -retroviruses, brought them to the 2<sup>nd</sup> place of most widely used vectors for gene therapy in clinical trials, but safety concerns emerged in 2000s because of genotoxic potential caused by viral genome integration. Retroviruses integrate their genome preferentially near promoters, with the risk of dysregulation of expression of the neighbor gene and malignant transformation of transduced cells, as it has been observed in SCID-X1 clinical trial (Hacein-Bey-Abina *et al*, 2008). Despite leukemia cases affected gene therapy clinical trials for other diseases (Stein *et al*, 2010; Braun *et al*, 2014), malignancy development has been shown to be related not only to the vector but also to transgene- and disease-specific characteristics (Cicalese *et al*, 2016).

As mentioned above, lentiviruses have a safer profile compared to  $\gamma$ -retroviruses, thanks to different integration pattern and improvement in vector design, therefore LV replaced  $\gamma$ -retroviral vectors in latest clinical applications (see paragraph 1.3).

### **1.2.3. Non-viral vectors**

Even if throughout the history of gene therapy progressively improved viral vectors have been generated with good safety and efficacy profiles, immune responses and genotoxicity remain concerns related to the use of viral vectors. Therefore, non-viral vectors have also been considered for gene delivery, because of the absence of virus-derived components, virtually unlimited cargo capacity and relatively easy and cheap manufacturing processes (Yin *et al*, 2014). Currently, the most used non-viral gene delivery technique is lipofection, that is based on lipid vesicle called liposomes or lipid nanoparticles (LNP), that consist of spheric single or multiple layers of phospholipids, incorporated with sterols, accommodating an aqueous core that contains the genetic material to be transferred (Ren *et al*, 2021). Lipid layers can be also modified to increase stability, by adding for example polyethylene glycols (PEG) or targeting ligands that redirect liposomes to specific cells (Cullis & Hope, 2017; Eloy *et al*, 2017). Being non-toxic, low immunogenic, and biodegradable, liposomes can be safely used both *in vivo* and *ex vivo* (Yin *et al*, 2014).

Multiple treatments based on drug-containing liposomes have been approved in the last 30 years, also for carrying small interfering RNA (siRNA) or DNA molecules (Bulbake *et al*, 2017). Both RNA and DNA can be loaded into liposomes, but in both cases transgene expression is transient following delivery. Therefore, one of the most studied application is the transfer of mRNA for *in vivo* genome editing, to achieve a transient expression of genome editing machineries (Zhen & Li, 2019).

However, non-viral particles still suffer of low efficiency in some cases. Indeed, viruses evolved for thousands of years to efficiently insert their genomes into host cells, escape defense mechanisms and efficiently express their genes, and all of these are lacking in non-viral vectors. This is true in particular for DNA, which after entering the cell would lack the tool to move from cytosol to nucleus. One of the main advantages of using LNPs or liposomes is that it may be possible to re-administer them multiple times.

An application of LNP-mediated gene transfer we are all aware of is represented by the COVID-19 vaccines (BNT162b2 and mRNA-1273), that in both cases consist of LNPs carrying mRNA coding for SARS-CoV2 spike protein. These COVID-19 vaccines obtained impressive results in terms of efficacy and safety (Huang *et al*, 2021a).

### 1.3. Lentiviral vectors

Lentiviruses belong to the family of retroviruses and are therefore enveloped viruses with 2 copies of a 9.7kb, single-strand sense RNA genome. The virion is spherical, with a diameter of 120nm, and contain a nucleocapsid bound to the genome, that also contains a reverse transcriptase, a protease and an integrase protein. The most commonly used LV for gene therapy is derived from HIV-1, but its genome has been split into different plasmids used to produce LV to reduce the risk of producing replication-competent viruses. The LV genome plasmid contains the transgene and the cis-acting sequences, that are necessary for encapsidation, retrotranscription and integration, while trans-acting sequences have been split in 3 packaging constructs, which are expressed by the producing cells but are not packaged in the virion. The first packaging construct contains HIV *gag*, *pro* and *pol* genes, that encodes the capsid proteins p24, matrix and nucleoprotein (*gag*), and for reverse transcriptase, protease and integrase (*pol*). Gag gene is translated in a single polyprotein, which is the cleaved by the protease. The second packaging construct contains *rev* gene, that encodes for Rev protein, which is necessary for nuclear export unspliced mRNA. The unspliced LV mRNA is encapsulated and serve as vector genome. Rev protein binds a specific HIV sequence called RRE (Rev responsive element), that therefore has to be present on LV genome to generate vector particles. The third packaging construct contains the gene encoding for the envelope protein, but HIV *env* gene is usually substituted by VSV-G, that expand LV tropism, as previously described for retroviral vectors. The fourth construct necessary for LV production is called transfer construct and produces the mRNA that is encapsulated in the LV particle and constitute its genome. LV genome is flanked by LTRs, that are necessary for integration in the host DNA. HIV LTRs are composed of 3 elements, U3, R and U5, that are present in both 5' and 3' LTRs. U3 element act as a promoter/enhancer for transcription of HIV genome but latest generations of LV have a partial deletion in U3 3' LTR that is called  $\Delta$ U3. During retrotranscription  $\Delta$ U3 is copied in the 5' LTR, therefore the enhancer/promoter activity is disrupted in both LTRs, and LVs containing this deletion are called self-inactivating (SIN). The U3 region just upstream of the R element in 3' LTR is also needed as a polyadenylation (polyA) signal, therefore it cannot be eliminated, but a 400 bp depletion of the promoter/enhancer sequences upstream of the polyadenylation signal, that also contain a TATA box, is well tolerated (Zufferey *et al*, 1998). The depletion of the HIV promoter allows the insertion of an internal promoter that regulates the expression of the transgene and reduces the risk of genotoxicity, while the transcription of the LV genome in the producer cells is controlled by a cytomegalovirus (CMV) promoter

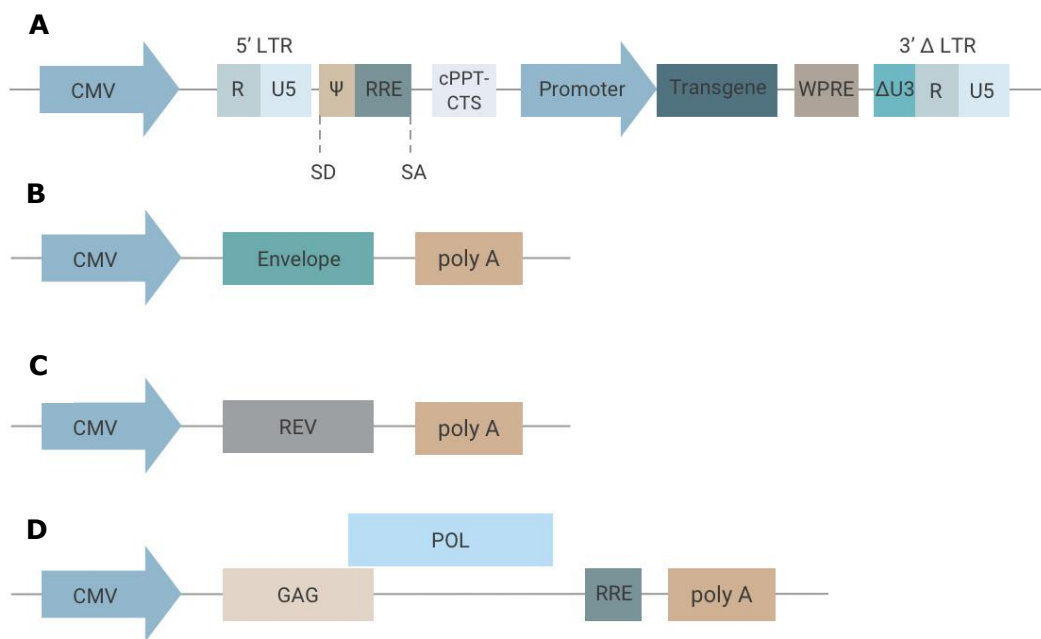


**Figure 1. Constructs for the production of 3<sup>rd</sup> generation LV.** A) LV genome transfer construct. CMV promoter control the transcription of the genomic mRNA. 5' LTR is depleted of U3 sequence and is composed only of R and U5 elements. Packaging signal ( $\Psi$ ) from gag gene is inserted in the transfer construct to allow encapsidation of LV genome, and contains a splice donor site (SD). RRE sequence is recognized by Rev protein during LV production and allows nuclear export of unspliced mRNAs, and is followed by a splice acceptor sequence (SA). Central polypurine tract (cPPT) and central termination site improve reverse transcription and nuclear import of LV genome. Transgene expression is controlled by an internal promoter, that can be tissue specific. WPRE is a post-transcriptional regulatory element that increase stability of transgene transcript and serve also as its polyadenylation signal. U3 of 3' LTR is depleted of 400bp to remove its promoter/enhancer function and increase safety. During retrotranscription it is copied in 5' LTR, and makes this construct self-inactivating (SIN). B) Envelope construct, usually expressing VSV-G. The polyA of this construct and packaging constructs derives from simian virus 40 polyadenylation signal. C) Packaging construct for expression of Rev protein. D) Packaging construct for expression of protein of capsid, matrix and nucleoprotein (gag gene), protease and reverse transcriptase and integrase (pol). Also in this construct there is an RRE sequence.

upstream of the 5' LTR, that is not incorporated in the genome. Downstream of the 5' LTR there is a fragment of gag gene that acts as a packaging signal ( $\Psi$ ), that is instead removed from gag gene in the packaging construct, and it also contains a splice donor. Next on the LV genome construct we find the RRE sequence, that is necessary for nuclear export of the full-length packaging competent vector genome by Rev protein during vector production, and a slice acceptor site. Other cis-acting sequences that are maintained from HIV genome are the central poly-purine tract (cPPT) and the central termination site (CTS), that increase efficiency of nuclear import of the vector genome and reverse transcription (Follenzi *et al*, 2000). Downstream of the transgene it has been added a post-transcriptional regulatory element from woodchuck hepatitis virus (WPRE), that stabilizes the transgene transcript, increasing substantially its level (Zufferey *et al*, 1999). Wild-type WPRE

contains part of the X protein sequence of woodchuck hepatitis virus (WHV), that has been reported to be potentially oncogenic (Kingsman *et al*, 2004), therefore it has been substituted with a mutated form (WPRE\*) in which that sequence has been disrupted (Zanta-Boussif *et al*, 2009).

HIV genome present a series of accessory genes (*vif*, *vpr*, *vpu*, *nef*) encoding for proteins that increase pathogenicity of the virus and escape from immune sensing, but are not necessary for production of functional viral particles, therefore have been eliminated. Moreover, the use of an external promoter for the transcription of the genomic RNA also allows the removal of *tat* gene, that encodes for a transcriptional activator protein necessary to start RNA synthesis from the promoter in the U3 element of the 5' LTR. Tat protein activity has been associated with Kaposi's sarcoma development (Buonaguro *et al*, 1994), therefore its removal further increased safety of LVs. This system of 4 plasmid represents the 3<sup>rd</sup> generation of LVs and reduces the risk of recombination of the plasmids that might lead to the generation of a replication-competent virus (Dull *et al*, 1998).

Scalable production of LV can be achieved by substituting the 4-plasmids system with a stable producer cell line, in which the constructs are stably integrated in the cell genome and are placed under the control of an inducible system, such as tetracycline operators (TetO). Addition of tetracycline to the culture medium would induce the expression of all of the constructs and therefore the production of LV particles. Inducible systems are required to pseudotype vectors with VSV-G, because its fusogenicity makes it toxic for the producer cells, therefore it cannot be expressed for a prolonged period of time (Chen *et al*, 1996).

Thanks to the presence of a lipidic envelope that is generated during budding of the viral particle, LVs surface can be engineered by editing producer cells, to induce the expression of protein of interest or removing others potentially harmful. Two examples have been described by our lab in the past. It is known that VSV-G pseudotyped vectors are inactivated by human serum (DePolo *et al*, 2000), limiting the possibility to administer LV intravenously. LV resistance to complement inactivation can be increase by reducing the number of VSV-G molecule expressed on vector surface, but also removing MHC-I molecules trough knock-out of  $\beta$ 2-microglobulin ( $\beta$ 2M) gene. MHC-I display on vector surface can indeed work as an allo-antigen and induce an antibody-mediated complement activation, but also activate a T-cell mediated immune response. LV produced by MHC-free cells results therefore to be less immunogenic (Milani *et al*, 2017). Another major limitation in LV *in vivo* administration is represented by phagocytosis of vector particles, in particular liver and spleen macrophages. Phagocytosis is mediated by a mix of positive and

negative signals sensed by phagocytic cells. CD47 display is one of these signals, that can inhibit phagocytosis through interaction with SIRP- $\alpha$  receptor present on plasma membrane of macrophages (Oldenberg *et al*, 2001). CD47 is normally expressed by producer cell lines but at low level, therefore its overexpression in LV producer cells results in increased amount on vector surface and shields the vector from phagocytosis (Milani *et al*, 2019).

Conversely to retroviruses that can transduce only dividing cells, LV have the advantage of transducing both dividing and non-dividing cells (Naldini *et al*, 1996), increasing the number of possible targets (Sakoda *et al*, 1999). Despite stimulation of HSC or T cell is still necessary for efficient *ex vivo* transduction, LV reach more easily cells with long-term repopulating potential, making them a better candidate for correction of hematopoietic stem cells (Naldini, 2011).

The genotoxicity adverse events due to  $\gamma$ -retroviral vectors in HSC gene therapy led to their progressive substitution with LV, which have improved efficiency of gene transfer and a safer profile (Schröder *et al*, 2002). In the last years, 5 advanced therapy drug products based on LV have been approved, all based on gene addition in HSC (Zynteglo for  $\beta$ -thalassemia, Skysona for CALD, Libmeldy for MLD) or T cell for CAR-T generation (Yescarta and Kymriah), making it the most widely used vector in clinical gene therapy applications. But *in vivo* applications of LV are under evaluation too, indeed seroprevalence anti-HIV or anti-VSV-G antibodies in the population is very low, thus avoiding the risk of pre-existing anti-viral immune response that often complicates AAV vector gene therapy. Moreover, the larger dimension of the LV genome allows accommodating longer transgene that do not easily fit into AAV genome. However, also LV are immunogenic, therefore NAB are developed upon systemic administration.

#### **1.4. The liver: architecture, function and tissue dynamics**

The liver is a unique organ involved in multiple functions, such as digestion, metabolism and protein secretion, but with also an important defense role thanks to detoxification of xenobiotic compounds and immunological functions. These variety of features are conducted by parenchymal cells, hepatocytes and cholangiocytes, that are supported by a number of non-parenchymal cells, mainly liver sinusoidal endothelial cells (LSEC), Kupffer cells (KC) and stellate cells. Liver functions can be carried out thanks to a peculiar vascular system, that has 2 vases carrying blood, the portal vein and the hepatic artery. The portal vein collects blood from the gastrointestinal tract, spleen, gallbladder and pancreas, therefore it is poor of oxygen but rich in nutrients and also toxins from food intake. Portal vein blood represent the



majority of the hepatic blood flow (about 75%) but is then mixed with that coming from the hepatic artery, that is a branch deriving from the abdominal aorta and therefore is oxygenated (Corbic *et al*, 1984). The 2 blood flows enter in the liver parenchyma and mix in capillaries between hepatocytes layers called sinusoids, giving rise to one of the 2 portal venous system in the human body. The blood is then drained by the hepatic veins that merge into the inferior vena cava to go back to the right atrium of the heart. The hepatic portal venous system represents a defensive mechanism of the organism from toxins and pathogens that can enter with food through the digestive system. Indeed, blood coming from the intestine goes directly into the liver before entering the systemic circulation, with a first-pass mechanism that allows hepatocytes to metabolize and detoxify xenobiotics entering into the body. For this reason, the liver is often the first defensive system encountered by external agents and therefore acquire a relevant role also from the immunological point of view. The importance of this defensive mechanism is evident in the case of the formation of portal-to-systemic collaterals (PSC), a series of blood vessels appearing between the portal vein and the systemic circulation in case of extensive liver damage that bypass the blood flow into the liver and its detoxification function, leading to an accumulation of toxin compounds that can cause a brain dysfunction known as hepatic encephalopathy (Chan, 2012).

Beside the blood vasculature, another "vessel" system is present in the liver, and is formed by bile ducts, which are a series of tubular structures composed by cholangiocytes that collect bile produced in the liver parenchyma and carry it outside the liver, through the common bile duct, to the duodenum, where it is involved in digestion.

Liver tissue is divided in functional units called lobules defined by the vascular systems. Lobules have a hexagonal shape, with a portal triad at every corner and a central vein in the center of the hexagon. Portal triads are composed of a portal vein, that is a venule branch of the portal vein that collects blood in the abdomen, an arteriole branch of the hepatic artery and a bile ductule. Sinusoids depart from portal vein and hepatic artery and reach the central vein, and blood rich of toxins and nutrients mix with the blood rich of oxygen. Blood runs in the sinusoids through the hepatocyte layers, that filter it, and finally reach the central vein, that carries it out of the liver. The exchange of compounds between blood and hepatocytes is facilitated by the presence of gaps called fenestrae between the endothelial cells forming the sinusoids. Hepatocytes form also small channels (canals of Hering) where bile is secreted and flows toward the bile ductule. Being the first organ encountered by pathogens that enters through the digestive system, liver presents the largest

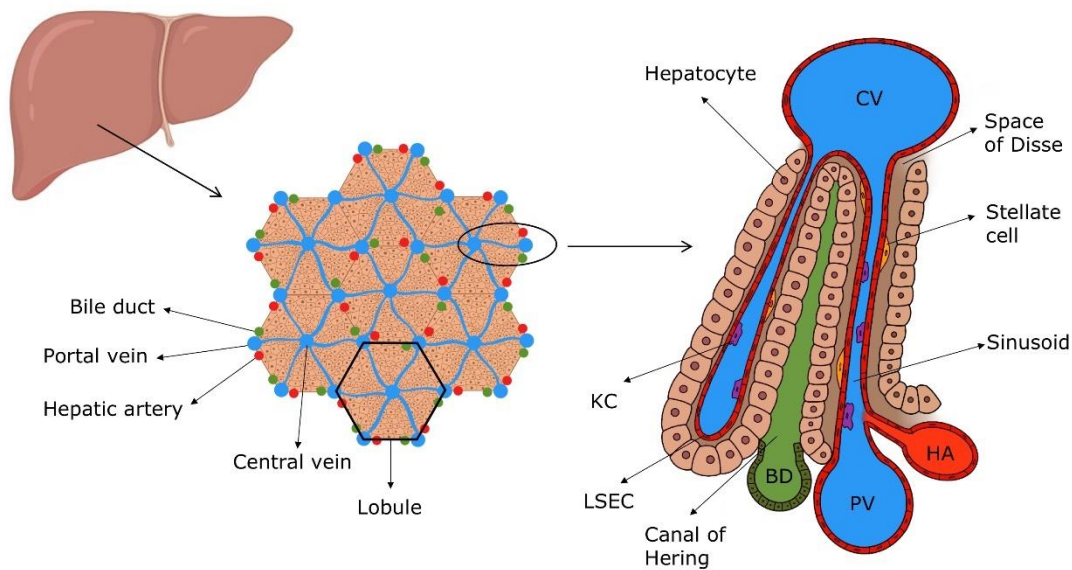


**Figure II. Liver structure.** Liver is made of repeated hexagonal structures called lobules. The lobule has a central vein in the center of the structure and a portal triad at each corner, in which there are a bile duct, a portal vein and a hepatic artery. Blood coming from the abdomen flows into the portal vein, then is mixed with oxygenated blood coming from the hepatic artery and is finally drained by the central vein. The vessels that run from portal to central veins are called sinusoids and are formed by a type of endothelial cells called liver sinusoidal endothelial cells (LSEC). Sinusoids are flanked by hepatocyte layers, but between hepatocytes and LSECs there is a space called space of Disse, in which stellate cells reside. Kupffer cells (KC) are located inside sinusoids and are liver tissue resident macrophages. Hepatocytes are polarized cells, one side overlook the space of Disse, while the other form the canal of Hering, in which bile is secreted and is drained into the bile duct. Abbreviations: CV=central vein; PV=portal vein; HA=hepatic artery; BD=bile duct; KC=Kupffer cell; LSEC=liver sinusoidal endothelial cell.

population of tissue-resident macrophages, which are called Kupffer cells, and are located inside the sinusoids. Moreover, hepatocytes are separated from LSEC by the space of Disse, in which stretch out hepatocytes' microvilli and reside hepatic stellate cells. These cells are quiescent in the normal liver, they constitute the major storage of vitamin A in the organism and in case of damage can turn into activated myofibroblast-like cells, and therefore play an important role in fibrosis (Yin *et al*, 2013).

#### **1.4.1. Hepatocytes metabolic functions**

Hepatocytes are the most abundant cells in the liver, comprising 80% of its volume and 60% of total cell number (Vekemans & Braet, 2005), and are responsible for almost all of the liver function. Hepatocytes are a secretory workhouse, as it is demonstrated by the extensive network of endoplasmic reticulum and Golgi. They

produce a variety of proteins, such as albumin, that is the most abundant protein in the blood, transferrin, an iron transporter,  $\alpha$ -1-antitrypsin (AAT), a protease inhibitor, and various coagulation factors, such as FIX. But hepatocytes also produce and secrete the bile, which is made mainly of fats (cholesterol and phospholipids), bile salts, bilirubin and inorganic salts dissolved in water (Schulze *et al*, 2019). The secretion of bile and blood protein occurs on different sides of the hepatocyte. Indeed, hepatocytes are highly polarized cells, with a basolateral plasma membrane domain that faces the space of Disse and an apical domain that constitute the bile canaliculi, each displaying a specific group of receptors, channels and surface proteins. Hepatocyte polarization is maintained also through intercellular tight junctions, that seal the space between hepatocytes (Kojima *et al*, 2003), but they are also rich of gap-junctions, that allows exchange of compounds between adjacent cells and have been demonstrated to be fundamental for multiple hepatocyte functions (Willebrords *et al*, 2015). On the apical plasma membrane are displayed ATP binding cassette (ABC) transporter and other bile salt efflux transporters, while the basolateral plasma membrane is rich of iron- and lipid-scavenger receptors such as LDL-R as well as other tyrosine kinase receptor (Schulze *et al*, 2019). The basolateral membrane is involved indeed in endocytosis of compounds arriving through the bloodstream, among which there are nutrients whose storage and metabolism is controlled by hepatocytes, such as glucose, lipids and iron (Wasserman, 2009; Rishi & Subramaniam, 2017; Alves-Bezerra & Cohen, 2017). Among the compounds that enter through the basolateral membrane there are also toxins and drugs, which are mostly lipid soluble. These compounds can be eliminated by a 2-stage processes of biotransformation that is accomplished by more than 50 proteins of the cytochrome P450 families (Zanger & Schwab, 2013). The first stage is the inactivation of the compound, that can also be exploited to transform a prodrug into its active form, while the second is the conversion of the metabolite into a hydrophilic agent that can be excreted more easily (Sikka, 2005).

Because of the peculiar structure of the liver lobule, microenvironment to which hepatocytes are exposed is different according to their position in the lobule. As an example, oxygenated blood enters in the lobule through the hepatic artery and flows in the sinusoid exchanging oxygen with hepatocytes until arriving at the central vein. Therefore, the concentration of oxygen in the blood goes from 60-65 mm Hg in the peri-portal area to 30-35 mm Hg when it arrives to the central vein, remarkably reducing its availability for hepatocytes in that area (Kietzmann, 2017). This difference in oxygenation leads to a differential expression of hypoxia-inducible factor (HIF), that regulates some metabolic liver functions (Kietzmann *et al*, 2001).

Differences in microenvironment in the liver lobule identify metabolically distinct hepatocytes in peri-portal and peri-central area, and this phenomenon has been termed liver zonation (Gebhardt, 1992). As for oxygen, also other nutrients and metabolites have the same portal-to-central gradient, but one of the signals that has been identified as a major regulator of liver zonation is  $\beta$ -catenin, which has been shown to be necessary for its establishment and maintenance.  $\beta$ -catenin is a transcription factor that in absence of signaling is targeted for ubiquitination and therefore degradation by phosphorylation from a complex formed by Axin, APC, GSK3 and CK1 proteins. The interaction of Wnt signaling protein to a receptor of the Frizzled (Fz) or LDL receptor-related proteins (LRP) families segregate Axin to the plasma membrane, disrupting the destruction complex and allowing  $\beta$ -catenin translocation into the nucleus (MacDonald *et al*, 2009). Benhamouche *et al*. demonstrated that non-phosphorylated (active)  $\beta$ -catenin is present in peri-central area while APC in peri-portal, and that conditional knock-out of APC induces activation of  $\beta$ -catenin in central area with consequently loss of differential expression of zonation markers in the lobule (Benhamouche *et al*, 2006). R-spondin (RSPO) ligands potentiate Wnt signaling by interacting with LGR4/5 receptors, which sequester Wnt/ $\beta$ -catenin pathway inhibitors RNF43 and ZNRF3, and therefore have been shown to be fundamental for liver zonation induction (Planas-Paz *et al*, 2016). It was also shown that pericentral LSEC express both WNT ligands and RSPO3, thus are considered responsible for the induction of liver zonation (Planas-Paz *et al*, 2016; Halpern *et al*, 2017).

Metabolic functions of hepatocytes are zoned according to the microenvironment in which cells reside. For example, the peri-portal area is more oxygenated thanks to the blood flowing from the hepatic artery, as mentioned above, therefore energy-demanding tasks such as protein secretion (including for example albumin and FIX), gluconeogenesis and cholesterol biosynthesis, are carried out by portal hepatocytes (Ben-Moshe & Itzkovitz, 2019). The opposite functions are inversely zoned, therefore peri-central hepatocytes are responsible for glycolysis and cholesterol consumption for bile acid synthesis. Metabolic zonation also allows spatial recycling of metabolites produced in peri-portal area by central hepatocytes. Enzymes contributing to a metabolic pathway can be expressed in sequential lobule layers, and utilize metabolites produced by the neighboring hepatocytes and transported through bloodstream or gap junctions. An interesting example is the neutral pathway of bile acid biosynthesis, that start with CYP7A1 and HSD3B7, abundant in pericentral layer, the following enzymes are CYP8B1 and CYP27A1, expressed in the sequential zone of liver, and ends with BAAT, which is found higher levels in portal area (Halpern

*et al*, 2017). Interestingly, cytochrome P450 enzymes are expressed by central hepatocytes, thus there is a zonation of damage caused by toxic intermediates in case of overdose of xenobiotics such as acetaminophen (Anundi *et al*, 1993).

Recently, a remarkable work by Halpern *et al.*, extended the concept of liver zonation further from the classical 3 zones (peri-portal or zone 1, mid-lobular or zone 2 and peri-central or zone 3), to identify up to 9 layers in the mouse lobule. This work was possible thanks to the combination of single-cell RNA sequencing (scRNAseq) and fluorescence *in situ* hybridization (FISH) analysis, that led to the identification of 6 markers whose expression has a gradient in the lobule. The authors propose that by the level of expression of each of these 6 markers it is possible to identify 9 layers with specific transcriptomic features (Halpern *et al*, 2017). A subsequent scRNAseq analysis performed on human liver proposed 6 hepatocyte layers, which showed similar functions to the 9 murine layers (MacParland *et al*, 2018). It is also interesting to notice that not only hepatocytes, but also LSEC have a different transcriptomic profile according to the lobule zone in which they are located (MacParland *et al*, 2018; Strauss *et al*, 2017).

Another peculiar feature of hepatocytes is their ploidy. Unlike most other cell types in humans, which have a single nucleus with 2 sets of chromosomes, hepatocytes can present multiple sets of chromosomes, and are therefore prevalently polyploid. Despite polyploidy is a common feature in other eukaryotes, such as plants, it is rarely encountered in the human body, being present only in a few cell types such as cardiomyocytes in the heart, megakaryocytes in the bone marrow, osteoclast in bones and hepatocytes in the liver (Sladky *et al*, 2021). Adult hepatocytes can have 1 or 2 nuclei, each of which can have 1 or 2 diploid genomes, therefore they can be mononucleated diploid cells (2n), mono or binucleated tetraploid cells (4n) or binucleated octoploid cells (8n). Polyploid hepatocytes have been shown to represent 90% of hepatocytes in the liver of adult rodent, of which 70% are tetraploid and 20% are octoploid, with about 20-30% of binucleated hepatocytes (either 2 x 2n or 2 x 4n) (Guidotti *et al*, 2003), while for human liver the percentage of total polyploid hepatocytes may be less than 30%, with 55% of them presenting 2 nuclei (Bou-Nader *et al*, 2020). The most well described mechanism for hepatocytes polyploidization is failure of cytokinesis. Post-natal mouse hepatocytes are almost all diploid, but at the age of weaning (2-3 weeks of age) most of them start mitosis without completing the last step that consists in the division of the cytoplasm of the 2 daughter cells (cytokinesis). Lack of cytokinesis leads to a single binucleated hepatocyte (Margall-Ducos *et al*, 2007) and to an increase in cell size proportional to the number of set of chromosomes (Martin *et al*, 2002). Other mechanisms lead to

the formation of polyploid mononucleated hepatocytes, such as endoreplication, that consist in duplication of cell DNA without entering mitosis (Zhang *et al*, 2019). By the combination of the 2 mechanisms binucleated octoploid cells are obtained. Whether polyploid hepatocytes have different functions or transcriptional features (Miettinen *et al*, 2014; Lu *et al*, 2007) or even distribution in the lobule compared to diploid (Tanami *et al*, 2017; Bou-Nader *et al*, 2020), remains debated, despite several different studies addressed these questions (Donne *et al*, 2020). Polyploid hepatocytes may also undergo to a process of ploidy reduction that has been observed both *in vitro* and *in vivo* (Miyaoaka *et al*, 2012), that also generates chromosome abnormalities and uniparental chromosome sets, leading to a vast genetic heterogeneity. This dynamic model has been named “ploidy conveyor” (Duncan *et al*, 2010).

#### **1.4.2 Tissue dynamics**

Unique proliferative features of livers have long been known, as it is demonstrated by the ancient Greek myth of Prometheus, who was chained to a rock while an eagle ate his liver, which grew back during night so that the eagle could eat it again every day. Indeed, it is well known that liver has a remarkable regenerative potential in pathological conditions, while it seems otherwise quiescent. Nevertheless, proliferation of hepatocytes is not understood completely.

Liver parenchymal cells (hepatocytes and cholangiocytes) derives from a common progenitor present during embryonic development called hepatoblast, which originates from the foregut endoderm and can be found already at embryonic day 8.5 (E8.5) in mice. Hepatoblasts commitment is driven by fibroblast growth factor (FGF) and bone morphogenetic protein (BMP) signaling, and they start to express liver-specific markers such as hepatocyte nuclear factor 4 $\alpha$  (HNF4 $\alpha$ ), albumin and  $\alpha$ -fetoprotein (AFP) (Ober & Lemaigre, 2018). At this stage hepatoblasts proliferate, and in the budding organ differentiation markers have been observed in the center, while the periphery presents higher proliferation rate, pushed by  $\beta$ -catenin (Suksaweang *et al*, 2004). The concept of reduced proliferation associated with maturation is often referred also to adult hepatocytes. Liver is also where hematopoiesis resides during fetal life, it contributes to hepatocytes maturation by induction of metabolic enzymes and therefore the shift of hematopoiesis to the bone marrow at the age of birth induce an important change also in liver (Kamiya *et al*, 1999). On the other hand, bile ducts specification from hepatoblasts is observed from hepatoblast only around the portal vein (Antoniou *et al*, 2009).

If hepatoblasts can be considered liver stem/progenitor cells in the fetal life, the existence of a similar population in the adult liver is controversial, despite multiple studies tried to address its existence and proposed several candidates. Indeed, it is not clear either if specific hepatocyte or cholangiocyte subsets sustain the tissue during homeostasis, or if all of them contribute equally to its maintenance, or if quiescent cells are reactivated in case of damage to replenish the parenchyma. It is known that hepatocytes are able to renew themselves in the adult liver, and therefore homeostasis is not driven by a different population such as cholangiocytes (Malato *et al*, 2011), but the characterization of lobule zones raised the question of whether the metabolic differences that we mentioned before apply also to proliferative potential. One of the first study that tried to address this question identified Axin2<sup>+</sup> pericentral hepatocytes has the major source of new hepatocytes during homeostasis, being able to regenerate more than 30% of liver area in 1 year, and expand toward periportal area acquiring specific features of the new zone (Wang *et al*, 2015). This work also identified Wnt signaling coming from central vein endothelial cells as the driver of Axin2<sup>+</sup> hepatocytes proliferation. These findings have been more recently challenged by evidence that attributed the higher proliferation of pericentral hepatocytes to the experimental model, given that different mouse strains for lineage tracing of Axin2<sup>+</sup> hepatocytes did not show the same proliferation rate (Wei *et al*, 2021; Sun *et al*, 2020). Similar results have been described by another group, that identified TERT<sup>high</sup> hepatocytes distributed in the lobule as responsible for the renewal of 30% of the tissue (Lin *et al*, 2018). Spread distribution of proliferating hepatocytes during homeostasis has been confirmed by marking hepatocytes randomly, with a slight predominance of mid-lobular zone, with 10% of hepatocytes that were able to duplicate in 1 year and 1% only that generate clusters with more than 2 cells (Chen *et al*, 2020). Lately, 2 interesting studies exploiting multiple lineage-tracing mouse models identified mid-lobular hepatocytes as the most active during homeostasis (Wei *et al*, 2021; He *et al*, 2021). In summary, the idea of spread or mid-lobular hepatocytes playing a major role in liver homeostasis seems the most prevalent at this time, but it is not clear yet whether there is a specific subpopulation among them that can be further characterized, and which is the contribution of these cells in tissue renewal over time.

If liver fetal development is well characterized and some knowledge is emerging on how homeostasis works in the adult liver, hepatocyte proliferation during post-natal growth has not been yet investigated deeply, and no clear description of tissue dynamics in the young liver is available to our knowledge. Nevertheless, some indications of proliferation of 1/3 of hepatocytes have been described in rats (Post &

Hoffman, 1964). Later on, evidence that DNA synthesis occurred in 18% of hepatocytes short after birth with a rapid decline during growth accompanied by a much lower mitotic activity, (Viola-Magni, 1972), led to the attribution of the increase in liver mass mostly to hypertrophy of hepatocytes (Sanjeev Gupta, 2000). Later studies confirmed that proliferation rate of mouse hepatocytes drops from the 2<sup>nd</sup> week of age or even before (Chang *et al*, 2008), and downregulation of a specific genetic program involving mainly cell cycle genes, driven also by miRNA-29 expression and accompanied by epigenetic changes, has been considered to determine the post-natal growth deceleration in multiple organs (Lui *et al*, 2014; Kamran *et al*, 2015; Lui *et al*, 2010).

Cell type	Origin	Characteristics	Reference
<b>Embryonic development</b>			
Hepatoblasts	Derived from endoderm	Bipotent precursors, generate both hepatocytes and cholangiocytes	Ober & Lemaigre, 2018
<b>Post-natal growth</b>			
Hepatocytes		Drop in proliferation rate short after birth	Chang <i>et al</i> , 2008
<b>Homeostasis</b>			
Axin2 <sup>+</sup> hep.	Central area	Repopulate 30% of liver tissue in 1 year	Wang <i>et al</i> , 2015
Tert <sup>high</sup> hep.	Spread	Repopulate 30% of liver tissue in 1 year	Lin <i>et al</i> , 2018
Mid-lobular hep.	Mid-lobular	10% of hepatocytes proliferate in 1 year	Chen <i>et al</i> , 2020 Wei <i>et al</i> , 2021 He <i>et al</i> , 2021
<b>Damage response</b>			
Hepatocytes	All areas	Hypertrophy in case of hepatectomy <1/3 of the liver Proliferation in case of moderate or acute damage, or 2/3 liver hepatectomy Can transdifferentiate into cholangiocytes in case of cholestatic injury	Michalopoulos & Bhushan, 2020 Schaub <i>et al</i> , 2018
Hybrid hep.	Portal area	Mild chronic damage Sox9 <sup>+</sup>	Font-Burgada <i>et al</i> , 2015
Oval cells LPC	(Rats) Portal area	Progenitor cells that give rise to both hepatocytes and cholangiocytes Activated in case of impairment of hep. proliferation	Farber, 1956 Miyajima <i>et al</i> , 2014
Cholangiocytes	Portal area	Transdifferentiate into hepatocytes in case of severe damage	Choi <i>et al</i> , 2014; He <i>et al</i> , 2014

**Table I. Liver tissue dynamics in different stages of life.** Liver cells proliferating during embryonic development, post-natal growth, homeostasis or in response to damage.



Despite the decrease in proliferation rate during growth and the quiescent state of the majority of hepatocytes in adults, the liver has a surprising ability to regenerate in case of damage. It is well known that most of the mass can be restored in around 7 days after hepatectomy of up to 2/3 of the total liver, with each of the liver subpopulation (hepatocytes, cholangiocytes, stellate cells, etc.) that are able to proliferate and originate daughter cells, while resections smaller than 1/3 of the liver leads to restoration of the mass only by hypertrophy of hepatocytes (Michalopoulos & Bhushan, 2020). But in response to other types of damage multiple mechanisms can be activated, that involve different hepatocyte or cholangiocyte subpopulations.

In case of moderate or acute damage hepatocytes can proliferate and regenerate the lost tissue, but in case of impairment of hepatocytes proliferation bipotent progenitors can be activated. A population of cells with bipotential differentiation capability has been first identified in rat, and has been shown to emerge in case of damage and generate both hepatocytes and cholangiocytes, and have been termed "oval cells" (Farber, 1956), and a similar population of liver progenitor cells (LPC) is present also in mouse liver in the canal of Hering in proximity of the portal vein (Miyajima *et al*, 2014). Similarly, Lgr5<sup>+</sup> cells, which are small cells that emerge near bile ducts in injured livers, have been described to contribute to regeneration of tissue in response to damage, and are also able to proliferate in vitro, originating organoids (Huch *et al*, 2013). On the other hand, periportal hybrid hepatocytes (HybHP), a specialized subtype of hepatocytes characterized by the expression of the ductal marker Sox9, have been shown to restore liver mass after chronic injury (Font-Burgada *et al*, 2015). The most updated model proposes that, while terminally differentiated hepatocytes can replenish the parenchyma in case of acute damage, specific hepatocytes subpopulations (such as HybHP) are recruited in case of a mild chronic damage, but can no longer contribute to regeneration if the injury is more severe and sustained, in which case bipotent cells (LPC) or bile duct cells can intervene (Gao & Peng, 2021). The capability of ductal cells to transdifferentiate into hepatocytes has been extensively described not only in mice but also in zebrafish, in which it is possible to ablate almost all of the hepatocytes by expressing the E. coli enzyme nitroreductase (NTR), that can convert Mtz (1-(2-hydroxyethyl)-2-methyl-5-nitroimidazo) into a cytotoxic agent. In these fish, the liver is regenerated by transdifferentiation of biliary epithelial cells (BEC) into mature hepatocytes (Choi *et al*, 2014; He *et al*, 2014), providing one of the first solid evidence of this phenomenon *in vivo*. It has been shown that also hepatocytes can transdifferentiate into mature cholangiocytes and form a functional biliary system in case of a strong cholestatic injury (Schaub *et al*, 2018). These findings indicate that, despite the quiescent state

of liver parenchymal cells, both cholangiocytes and hepatocytes have shown remarkable proliferative capability and plasticity, as a sign of their common embryonal origin.

Interestingly, despite polyploidy is generally considered as a hallmark of terminally differentiated hepatocytes, polyploid hepatocytes maintain proliferation potential. In case of partial hepatectomy binuclear hepatocytes undergo cell division to produce 2 mononuclear cells (Miyaoaka *et al*, 2012), and polyploid cells can be transplanted into a chronically injured liver and are able to expand, reduce their ploidy and re-polyploidize, also in presence of competing diploid hepatocytes (Matsumoto *et al*, 2020). Polyploid hepatocytes may even undergo multiple rounds of mitosis in injured liver without reducing their ploidy.

### **1.4.3 Liver immunological functions**

Because of its peculiar vascular system and its capacity to secrete proteins, the liver also plays an important immunological function. Indeed, hepatocytes are responsible for the production of 80-90% of the innate immune protein circulating in the bloodstream (Gao *et al*, 2008), but in the liver reside also a large number of immune cells that represent the first sentinels for pathogens, toxins and food antigens that enter the circulation through the digestive system. KC, which represent the vastest population of tissue resident macrophages in the body, are central for this role, but also other cell types, such as hepatocytes and LSEC, contribute to liver immune functions.

The liver is generally considered as a tolerogenic organ, mainly because the first liver transplantation experiments in pigs showed that it was better tolerated than other allogenic organs transplantations (Calne *et al*, 1969). Tolerance is maintained through the secretion of anti-inflammatory cytokines such as IL-10 and prostaglandins by KC and plasmacytoid dendritic cells (pDC) (Robinson *et al*, 2016), which downregulate expression of costimulatory molecules on antigen-presenting cells (APC), thus preventing the activation of T cells and the adaptive immune response (Groux *et al*, 1996). KC and DC are the main APC in the liver, but also LSEC and hepatocytes can present antigens directly to T cells. Presentation of antigens by these cells push T cells toward tolerance and induce the expansion of regulatory T cells (Lüth *et al*, 2008), thanks to the low expression of co-stimulatory molecules (Knolle *et al*, 1998). KC scavenge pathogens and pathogen-derived molecules present in circulation, but do not induce an inflammatory response, and have rather been shown to secrete IL-10 when exposed to lipopolysaccharides (LPS) (Knoll *et al*, 1995). LPS sensing is important also during liver growth to remodel KC distribution

in the liver lobule. Multiple studies have shown that KC are more concentrated in the peri-portal area (Bouwens *et al*, 1986; Sleyster & Knook, 1982), but recently it has been observed that this is not the case in newborn mice, and it is rather a mechanism developed at the age of weaning, when the switch in diet from mother milk to solid food induce also an increase in LPS in bloodstream coming from the gut, that leads to a shift of KC toward periportal area (Gola *et al*, 2021). In the same work it has been shown that higher concentration of KC in peri-portal area increases their overall phagocytic ability, reducing the probability for pathogens to reach peri-central area and reach the central vein, therefore gaining access to the systemic circulation. KC are an important barrier also for viral infections, indeed multiple viruses have been shown to be cleared from blood by KC (Zhang *et al*, 2002; Brunner *et al*, 1960). Phagocytosis by KC resulted in a half-life of 2 minutes of adenovirus in circulation in mice, while blockage of phagocytosis with gadolinium chloride (GdCl<sub>3</sub>) increases viremia (Alemany *et al*, 2000). This KC function is particularly important for *in vivo* gene therapy approaches, since clearance of viral vectors from blood reduces the efficiency of gene transfer to hepatocytes (van Til *et al*, 2005; Lieber *et al*, 1997). Uptake of viral particles by KC, and APC in general, induces the production of pro-inflammatory cytokines, such as tumor necrosis factor (TNF), interferon (IFN) and interleukin 6 (IL-6). TNF peak correlates with increase alanine transaminase (ALT) and aspartate transaminase (AST) blood levels, that reveal liver damage, while IL-6 can activate cytotoxic T cells. This mechanism is induced by sensing of viral genome by pattern recognition receptors (PRR) members such as TLR9, that through MyD88 induce Nf-kB activation, which results in expression of pro-inflammatory cytokines (Martino *et al*, 2011). Presentation of antigens by APCs on MHC class I and II in a pro-inflammatory environment induces an adaptive immune response through activation of CD8<sup>+</sup> and CD4<sup>+</sup> T cells respectively (Annoni *et al*, 2013). Pro-inflammatory conditions can also induce expression of MHC class II molecules on hepatocytes and induction of CD4<sup>+</sup> T cells activation (Herkel, 2003).

### **1.5. Liver gene therapy**

The liver has always been considered one of the most favorable organs for *in vivo* gene therapy for multiple reasons. As mentioned above, the liver has a peculiar and extensive blood supply that determines a high inflow of blood-borne particles such as gene therapy vectors. Moreover, fenestration on endothelial cells of liver sinusoids facilitate extravasation of viral particles, thus favoring transduction of hepatocytes. This is made evident by the high efficiency of liver transduction by multiple AAV serotypes (Zincarelli *et al*, 2008), LV (Follenzi *et al*, 2002), but also non-viral particles

such as LNPs (Shi *et al*, 2011). Moreover, liver cells, and in particular hepatocytes, are involved in multiple functions, which can be impaired by genetic mutations, leading to inherited genetic diseases, among which there are metabolic and coagulation disorders. For many of these diseases there is an unmet clinical need, with therapeutic strategies mostly based on treatment rather than curative approaches, therefore alleviating symptoms without intervening on the cause of the disease. Most of the treatments available for these diseases are based on enzyme replacement therapies or, in case of inborn error of metabolism, on dietary restriction or supplementation (Gambello & Li, 2018).

Liver is characterized by a tolerogenic environment. One of the main obstacles to an efficient application of gene therapy is the development of anti-transgene immune response, that is particularly relevant for patients that have never been exposed to the therapeutic protein and/or with mutations causing large losses of coding regions. By expressing the transgene in the tolerogenic environment of the liver, the induction of a transgene-specific adaptive immune response may be avoided, and an active immune tolerance may be induced (Mátrai *et al*, 2011; Mingozi *et al*, 2003a). Lastly, the low proliferation rate of hepatocytes in the adult liver also facilitates the use of non-integrating platforms such as AdV and AAV vectors, that may still allow long-term expression of the therapeutic transgene.

Taken together, these unique features favored application of liver-directed *in vivo* gene therapy for multiple therapeutic purposes, and many clinical trials have been already carried on. After an initial phase in which AdV have been exploited for gene transfer, in the last decades there has been an intensive study of AAV vectors for liver-directed gene therapy, but studies exploiting LV and non-viral vectors are undergoing too.

### **1.5.1. Hemophilia gene therapy**

The first disease that has been studied in the context of liver-directed gene therapy has been hemophilia, that is an X-linked coagulation disorder caused by mutations in factor VIII (FVIII, hemophilia A) or FIX (hemophilia B) genes. Both FVIII and FIX are physiologically expressed in the liver, but while FIX is normally synthesized by hepatocytes, FVIII is mostly secreted by endothelial cells including LSEC. Hemophilia patients have recurrent bleeding events, especially in joints, and their frequency and spontaneity correlate with the residual blood level of coagulation factor, that is <1% of normal levels in severe cases, between 1% and 5% in moderate and between 5% and 40% in mild cases of hemophilia (Mannucci & Tuddenham, 2001). The fact that an improvement of the pathological phenotype can be reached also with a partial

reconstitution of the clotting factor activity made hemophilia a favorable disease to start to explore liver gene therapy. Moreover, despite in western countries the improvement of standard of care and the introduction of ERT led to a constant increase of life expectancy of hemophilic patients from 10-15 years to almost the levels of the general population (Mannucci, 2020; Hassan *et al*, 2021), the health-related quality of life remains lower (WALSH *et al*, 2008), and accessibility to treatments might be limited by multiple factors, such as development of inhibitors against the coagulation factor. In the late 90's the first promising preclinical results have been achieved in the context of hemophilia B, with stable FIX activity for more than 1 year after a single intravenous administration of AAV vector expressing FIX in canine and murine models (Mount *et al*, 2002; Snyder *et al*, 1999). Unfortunately, the first clinical trial did not achieve the same result, and FIX expression lasted only for a few weeks (Manno *et al*, 2006). After a peak of clotting factor activity detected in the patients, the decrease was accompanied by a transient elevation of ALT and AST, later found to be caused by the reactivation of pre-existing CD8<sup>+</sup> T cells responding to AAV2 capsid, that attacked transduced hepatocytes (Mingozzi *et al*, 2007). Despite the ultimately negative outcome, still this trial represented the first demonstration of efficient *in vivo* gene transfer into human hepatocytes, and opened the way to the following clinical trials, that exploited improved vectors and transient immunosuppression regimen to inhibit anti-capsid immune response (Nathwani *et al*, 2011). In this case the vector used was an AAV8, and 3 doses were administered in different group of patients, from  $2 \times 10^{11}$  to  $2 \times 10^{12}$  vector genomes (vg)/Kg. In the high-dose group 4 of 6 patients showed increase in ALT levels, that was resolved by immunosuppression with prednisolone. A 4-year follow up showed a stable dose-dependent reconstitution of clotting factor, with 5% of activity observed in the high-dose group (Nathwani *et al*, 2014). The increase in circulating liver transaminases resulted to be dose-dependent, therefore improvements in safety of this liver gene therapy may involve the reduction of the effective vector dose. A significant improvement from this point of view came with the discovery of the Padua variant of FIX. A case of thrombophilia in a patient from the city of Padua has been described to be caused by the substitution of the arginine in position 338 of FIX with a leucine (R338L) (Simioni *et al*, 2009). This variant has been shown to increase FIX activity by 8- to 12-fold in hemophilic dogs, inducing immune tolerance, and achieving therapeutic levels with a significant lower dose of AAV vector (Crudele *et al*, 2015). Padua FIX was promptly tested in a clinical trial that exploited also an engineered AAV capsid (Spark100) by Spark Therapeutics at a dose of  $5 \times 10^{11}$  vg/Kg (George *et al*, 2017). The administration resulted to be safe, and patients showed a mean of FIX

activity of 33%, with therapeutic effects observed in all treated patients, demonstrating that improvement in vector and transgene design are crucial to reduce the administered dose without affecting the therapeutic outcome of the treatment.

Hemophilia A gene therapy is more appealing from a commercial perspective because of higher prevalence of cases, that is 17 cases every 100 000 male birth, 4.5-fold higher than hemophilia B (Iorio *et al*, 2019). But at the same time, it is also more challenging. First, FVIII is a bigger protein compared to FIX, it is encoded by a cDNA longer than 7kb, therefore exceeding the cargo capacity of AAV vectors. This problem has been circumvented by engineering a shorter but still active form of FVIII, B-domain-deleted (BDD) FVIII (Pittman *et al*, 1993). BDD-FVIII put the basis for most of the hemophilia A gene therapy trials, but its cDNA is still close to the maximum size of the transgene that can be inserted into the AAV vector genome, being 4.7kb long. FVIII is also more immunogenic, indeed 25-35% of severe patients under ERT develop antibodies against the exogenous coagulation factor (Patel *et al*, 2020). Lastly, FVIII expression resulted not to be stable over time in multiple gene therapy trials. The first clinical trial for hemophilia A started in 2017 and achieved physiological levels of FVIII activity in the high dose cohort ( $6 \times 10^{13}$  vg/Kg) (Rangarajan *et al*, 2017), but then decreased by 43% in the 2<sup>nd</sup> year and 10% in the 3<sup>rd</sup> year of follow-up (Pasi *et al*, 2020). Many other clinical trials are undergoing, but variability in transgene levels and short-term follow-up place hemophilia A gene therapy still in a stage of clinical development (Leebeek & Miesbach, 2021).

### **1.5.2. Gene therapy for inborn errors of metabolism**

Following the enthusiasm for the promising results achieved with AAV vectors for liver-directed gene therapy in the context of hemophilia, many groups started to explore other therapeutic applications for which transgene expression by hepatocytes could be helpful. The attention has been focused in particular on inborn errors of metabolism, a group of more than 1000 inherited genetic diseases (Ferreira *et al*, 2018) caused by the impairment of a biochemical pathway that affects 1 person every 2000 birth (Waters *et al*, 2018). One of the first metabolic diseases that have been studied for *in vivo* gene therapy was OTC deficiency, an X-linked metabolic disease that involves urea cycle and leads to blood hyperammonemia, whose severity depends on the level of residual activity of the enzyme and also determine the age of onset (early in severe cases, late in milder cases) (Caldovic *et al*, 2015). The interest on this disease started already in the 90's, and a clinical approach was tried using AdV, but was scarred by the first death of a patient directly caused by the gene

therapy (Raper *et al*, 2003). The attention was then moved to AAV vectors, leading recently to a clinical trial for adult patients with late onset (NCT02991144). Similarly, a clinical trial is currently ongoing for Grigler-Najjar syndrome (NCT03466463), in which a defect in UDP-glucuronosyltransferases gene (UGT1A1) leads to hyperbilirubinemia that can cause irreversible brain damage. Also in this case severity of the disease correlates with residual UGT1A1 enzymatic activity, and can be divided in type I (more severe) and type II (less severe). Other examples for gene therapy trials for correction of hepatocyte function are Wilson disease (NCT04537377) and glycogen storage disease type Ia (GSD1a, NCT03517085).

The liver can also be exploited to produce and secrete a therapeutic protein in the circulation to cross-correct other organs, and also for this strategy multiple clinical trials are ongoing. Mucopolysaccharidosis (MPS) type VI is caused by deficiency in arylsulfatase B (ARSB) enzyme, which is involved in glycosaminoglycans (GAG) degradation, that in affected patients accumulate in lysosomes, therefore it belongs to the group of lysosomal storage disorders (Harmatz, 2017). In physiological conditions lysosomal enzymes, besides being directed into lysosomes, are in part secreted and can be uptake by other cells that express mannose-6-phosphate (M6P) receptor, allowing therefore correction of cells by ERT (Sands & Davidson, 2006). Feasibility of cross-correction by expressing ARSB in hepatocytes transduced with AAV vector has been proved in mice and cats (Ferla *et al*, 2013), and is now under evaluation in a clinical trial (NCT03173521). In the same way, gene therapy-based cross-correction is possible in Pompe disease, in which glycogen is accumulated in lysosomes due to deficiency of the lysosomal acid  $\alpha$ -glucosidase (GAA) and leads to defects in cardiac and skeletal muscles, obtaining phenotypical amelioration of skeletal muscles and also inducing an active tolerance to GAA, whose immunogenicity could induce production of NAB in case of ERT (Han *et al*, 2017). A clinical trial is ongoing in late-onset patients (NCT03533673).

### **1.5.3. Current challenges and limitations of *in vivo* liver gene therapy**

The growing number of clinical trials of liver directed AAV-based *in vivo* gene therapy witnesses the huge potential of this platform and the vast expectations on its development. However, all these examples that we mentioned are also linked by common limitations, that are reflected in the inclusion criteria of clinical trials. Most patients have undergone ERT before being enrolled in the gene therapy trial, therefore some of them could have developed inhibitors to the protein encoded by the transgene, thus have to be excluded from the trial. Despite preclinical studies with AAV vectors and LV showed that gene transfer into hepatocytes can induce

immune tolerance toward the transgene product (Mingozzi *et al*, 2003b; Brown *et al*, 2007a) and also revert pre-existing immunity (Crudele *et al*, 2015), this effect has not been translated into the clinic yet, therefore presence of inhibitors remains an exclusion criterion (Samelson-Jones & Arruda, 2020).

As mentioned above, NAB against AAV capsid can be present in patients before treatment and represent a second important exclusion criterion from clinical trials, while not being an issue for potential use of LV. However, a recent hemophilia B clinical trial showed successful expression of FIX in 23 patients pre-immunized against AAV capsid, with only 1 that did not respond to therapy (Leebeek *et al*, 2021). Multiple strategies are under investigation to inhibit neutralization of the vector upon administration. Engineering new viral capsids can reduce the risk of encountering NAB in patient populations, but is not always effective due to the cross-reactivity of anti-AAV capsid antibodies (Pei *et al*, 2020). Transient immunosuppression or plasmapheresis can be exploited to reduce the amount of NAB in the circulation and allow efficient gene transfer into hepatocytes (Stone *et al*, 2021; Monteilhet *et al*, 2011). Another possible strategy that has been explored is the cleavage of IgG by the endopeptidase Imlifidase (IdeS), which enabled efficient gene transfer in mice with NAB against AAV capsid (Leborgne *et al*, 2020).

A third major exclusion criterion is the age of the patient. Being AAV a mostly non-integrating vector, exclusion of young pediatric patients is necessary to avoid transgene dilution over time caused by liver growth (Wang *et al*, 2011). For some metabolic diseases, the time of diagnosis and intervention is crucial to avoid progression of the disease and complications (Dietzen *et al*, 2009), but the episomal nature of AAV vectors challenges treatment in pediatric patients. Thus, most of the liver-directed AAV trials have to focus on late-onset diseases, such as mild forms of OTC deficiency and Pompe disease, which are generally less severe compared to early-onset diseases. Despite preclinical data have shown increased survival of Crigler-Najjar mouse model treated with AAV vector as newborn, bilirubin levels rose during growth, and in adult mice only a small fraction of hepatocytes still expressed the transgene (Greig *et al*, 2018), indicating dilution of AAV genome caused by liver growth.

This aspect deprives young patients of the possibility of being treated, forcing them to a lower quality of life associated with the currently available treatments for years before having access to a potentially curative gene therapy treatment. The same problem might be encountered also in presence of liver damage, in which case tissue regeneration may lead to a dilution of the transgene. The possible solutions to this problem can be narrowed to 2: re-administration of the drug product or stable



genetic correction. The induction of NAB upon administration of AAV vector limits the possibility of repeating the treatment, even if recently it has been shown that co-administration of tolerogenic rapamycin nanoparticles together with the vector prevents formation of AAV-specific antibodies, allowing successful vector re-dosing in preclinical models (Meliani *et al*, 2018; Ilyinskii *et al*, 2021).

Stable correction can be achieved by using integrating vectors, such as LV, or by exploiting novel strategies of targeted integration or *in locus* correction of the mutation. Therefore, these strategies are currently being investigated to extend clinical application of liver gene therapy to pediatric patients.

#### **1.5.4. LV-based liver gene therapy**

Despite there has not been any clinical application yet, the use of integrating vectors for *in vivo* transduction has been studied for multiple therapeutic purposes. Intravenous administration of LV has been shown to lead to efficient and quite selective transduction of the liver both in mice and NHP, despite the wide tropism of VSV-G envelope protein (Follenzi *et al*, 2002; Milani *et al*, 2019), therefore the liver is considered a good target for *in vivo* LV administration.

Initial experiments of i.v. LV delivery in mice showed efficient transduction of hepatocytes, together with LSEC and KC. Expression of hFIX was observed in adult immunodeficient mice, but not in immunocompetent mice (Tsui *et al*, 2002). This outcome was caused by transgene expression in APC due to the use of a ubiquitous CMV promoter, triggering therefore an adaptive immune response against the transgene, with production of anti-FIX antibodies and cytotoxic CD8<sup>+</sup> T cells that cleared transduced cells (Follenzi *et al*, 2002). Sustained transgene expression in immunocompetent mice was then achieved by narrowing transgene expression specifically in hepatocytes by using a hepatocyte-specific albumin promoter, but with a low expression level (Follenzi *et al*, 2002). Higher transgene levels were achieved by engineering new tissue-specific promoters, such as enhanced transthyretin (ET), that sustained hFIX expression at a therapeutic level (15% of normal), and detargeting from APC was improved by addition of multiple sites complementary to miRNA 142-3p in the 3' untranslated region of the transgene transcript (Brown *et al*, 2007b). This miRNA is selectively expressed in hematopoietic cells, and therefore also in APC, and binds to complementary target sites present on the transgene transcript to inhibit its expression, limiting antigen presentation and immune response against the transgene (Brown *et al*, 2006). Detargeting of transgene expression from APC resulted in stable transgene expression in a hemophilia B dog model with a significant improvement of clinical phenotype (Cantore *et al*., 2015). A

further improvement of LV has been obtained by increasing the amounts of “don’t-eat-me” signal on the vector surface to reduce phagocytosis from KC. CD47 has been described to act as a marker of self and inhibit phagocytosis by binding Signal Regulatory Protein  $\alpha$  (SIRP $\alpha$ ) receptor on macrophages (Oldenborg *et al*, 2000) and can be overexpressed in producer cells to increase its display on vector surface and generate CD47<sup>high</sup> LV. These LV have been shown to increase hepatocytes transduction and reduce phagocytosis in mice sensing human CD47, and increase transgene output also in NHP (Milani *et al*, 2019). This improved version of LV sustained expression human FIX in NHP (Milani *et al*, 2019; Cantore *et al*, 2015), paving the way for a possible clinical trial in the near future. Notably, integration site (IS) analysis and tumor-prone mouse model experiments showed that the therapeutic LV does not induce any clonal selection *in vivo* and does not increase the spontaneous incidence of hepatocellular carcinoma (HCC) (Cantore *et al*, 2015), highlighting the low risk of genotoxicity by LV.

Compared to other integrating viral vectors, such as  $\gamma$ -retrovirus, LV have been shown to efficiently integrate in both dividing and non-dividing cells. Initial reports on hepatocytes transduction observed that LV required cell cycling for *in vivo* transduction of hepatocytes (Park *et al*, 2000), but addition of cPPT and CTS in the transfer construct allowed nuclear translocation and resulted in efficient transduction of non-proliferating hepatocytes *in vivo* (Follenzi *et al*, 2000; VandenDriessche *et al*, 2002), therefore is suitable for a quiescent organ such as adult liver.

But because LV actively integrate its genome into the host DNA, it bears the potential to be maintained long-term, even life-long, following administration to newborn individuals. Despite most studies have involved adult animals until now, it has been previously shown that mice administered with LV expressing luciferase as newborns maintain high levels of transgene expression when reaching adult age (Yoshimitsu *et al*, 2004). A few studies also reported prolonged therapeutic effect of LV-mediated gene transfer in hepatocytes of neonatal animal models of Crigler-Najjar and Fabry disease (Yoshimitsu *et al*, 2004; Nguyen *et al*, 2005). Nevertheless, in-depth analysis of maintenance of LV-transduced hepatocytes following post-natal liver growth and homeostasis in adulthood is still lacking.

#### **1.5.5. *In vivo* genome editing**

In the last years novel strategies to achieve stable transgene integration or gene correction have been studied as an alternative to integrating vectors and to overcome the problem of transgene dilution of non-integrating vectors.

The development of genome editing platforms, and in particular CRISPR/Cas9 system, represented a revolution for the field and opened the way to new therapeutic opportunities. CRISPR/Cas9-based genome editing can be exploited either to introduce a mutation in the target gene through NHEJ, therefore disrupting its sequence and blocking its function, or to replace the mutated allele with a correct version of the gene exploiting HDR. Despite targeted correction of the gene through HDR is the most appealing strategy because it could be exploited for a wide range of diseases, it presents some issues. In addition to the CRISPR system, composed by Cas9 protein and a gRNA, it is necessary also to deliver the donor DNA, therefore 2 platform may be needed. One way to achieve this goal is a 2-AAV system, in which one brings Cas9 and gRNA, and the other carries the donor DNA (Richards *et al*, 2020; Ohmori *et al*, 2017). This system requires co-transduction of hepatocytes by both vectors, which may be challenging to achieve in humans, but the high transduction efficiency of AAV vectors facilitates this task in animal models. Alternatively, Cas9/gRNA can be delivered in form of mRNA exploiting LNPs, which also guarantee a transient expression that reduces the risk of off-target activity by the nuclease (Yin *et al*, 2016). The generation of DNA double-strand breaks can be deleterious, being able to induce DNA damage response (Schiroli *et al*, 2019) but can also induce integration of AAV vector genome in off-target loci. Therefore, targeted integration exploiting homology recombination has been studied also in the absence of nucleases. GeneRide system is based on homology arms flanking a promoterless donor DNA on AAV vector genome that direct its insertion in frame with albumin coding sequence, to produce a fusion protein that is cleaved thanks to the presence of 2A peptide (Barzel *et al*, 2014). Therapeutic application of homology recombination can be limited by the fact that it requires cell cycling (Scully *et al*, 2019). Therefore, HDR can be inefficient in a quiescent organ such as liver, but has been shown to be more active in newborn hepatocytes (de Caneva *et al*, 2019). Moreover, application of this strategy in a context where correction of cells induces a selective advantage can lead to a progressive increase in number of corrected hepatocytes over time, reaching a therapeutic benefit also starting from a low number of integration events (Chandler & Venditti, 2019). In some cases, a therapeutic benefit can be achieved by silencing of a mutated gene, therefore delivery of the Cas9/gRNA is sufficient to induce knock-down through NHEJ. Transient expression by mRNA delivered by LNP is the most advantageous solution, and after proving its efficacy in preclinical studies (Finn *et al*, 2018) has already reached the clinics to treat transthyretin amyloidosis (NCT04601051). In this disease, a mutation in the transthyretin (TTR) gene cause misfolding of the protein, with consequent accumulation in tissues. A single

intravenous administration of LNP carrying mRNA coding for Cas9 and the TTR-specific gRNA led to a dose-dependent reduction of TTR protein production, up to 96% in adult patients (Gillmore *et al*, 2021). In alternative to NHEJ-mediated knock-down, a single-base mutation can be induced by base editors to disrupt gene expression. Therapeutic potential of this strategy has been shown in NHP by introducing a mutation to knock-down proprotein convertase subtilisin/kexin type 9 (PCSK9) gene (an inhibitor of LDL-R) to treat familial hypercholesterolemia, obtaining 90% reduction in blood level of PCSK9 protein (Musunuru *et al*, 2021; Finn *et al*, 2018). These new genome editing strategies are extremely promising for the future of the field, to potentially overcome some of the long-lasting issues in gene therapy, however they generally are at an early stage of development and remain affected by some limitations, including off-target activity, off-target donor DNA integrations and incompletely predictable effects on target cells.

### 1.6. Liver gene therapy during liver growth

Recently we have administered LV expressing canine FIX (cFIX) in dog puppies of 2-4 months of age and observed a 4-fold decrease of cFIX protein in circulation in the first months after treatment, followed by a stabilization of the output that remained detectable for more than 3 years of follow-up (Figure III A). The decrease

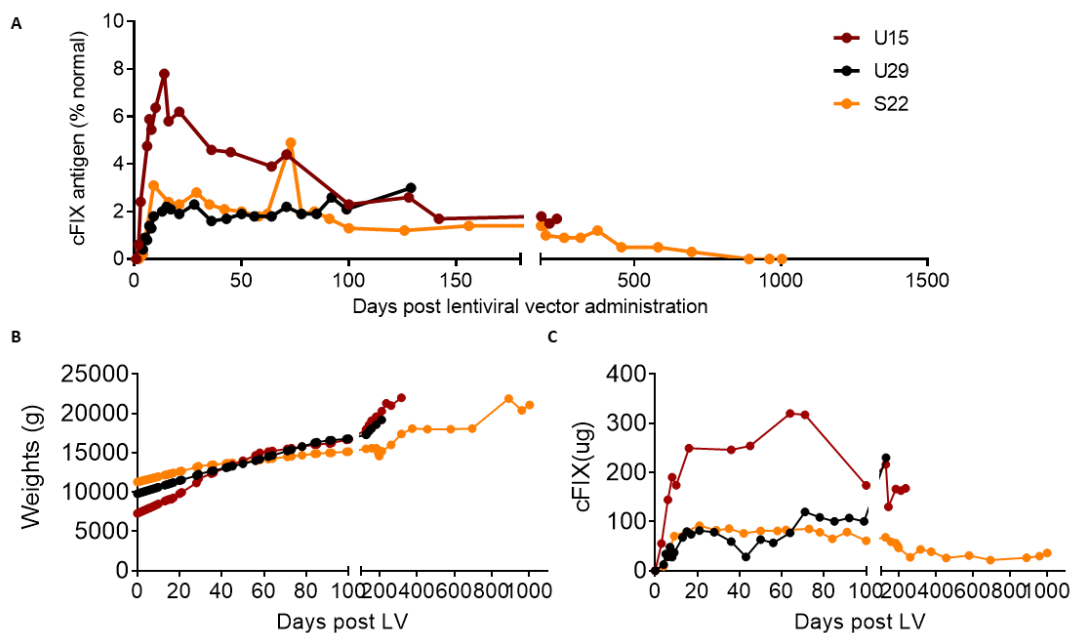


**Figure III: Decrease of cFIX during growth in young-treated dogs.** A) Concentration of cFIX expressed as percentage on normal level in blood of dogs treated as pups (2-4 months of age) with  $2.5 \times 10^{10}$  TU/Kg (S22) or  $5 \times 10^{10}$  TU/Kg (U29 and U15) of LV. B) Weight of dogs over time. C) Total amount of cFIX calculated using the estimated total blood volume based on dogs weight. Cantore, Milani, unpublished data.

of transgene output during liver growth could be explained either by the loss of a fraction of transduced hepatocytes or by the dilution of transduced hepatocytes due to a higher proliferation rate of untransduced hepatocytes. We determined the total amount of cFIX present in blood of treated dogs calculated from the estimated total blood volume based on their weight (Fig. III B). From this analysis the output of cFIX resulted to be stable during growth (Fig. III C), supporting the hypothesis of dilution rather than loss of transduced hepatocytes.

Starting from this observation we hypothesized that not all hepatocytes proliferate during post-natal liver growth to contribute to the generation of the adult liver. In the experiment described above, we might have transduced preferentially those hepatocytes that did not proliferate during growth, but are maintained anyway.

Overall, as mentioned above, how hepatocytes support post-natal liver growth remains largely unexplored, despite having important implications for liver-directed gene therapy strategies. Moreover, understanding the dynamic changes of the liver during growth and homeostasis is relevant to clarify the mechanism of maintenance of the therapeutic transgene and to establish the optimal time of treatment to maximize therapeutic benefit and ensure safety and durability towards application of liver gene therapy to pediatric patients.

## **2. Aim of the work**

The overall scope of this work is to study liver-directed *in vivo* gene therapy with LV in newborn and juvenile mice and the impact of post-natal liver growth on transgene maintenance. In particular, the specific aims of the project are:

1. To understand whether all hepatocytes in newborn mice proliferate and generate the adult liver or there are subpopulations preferentially supporting post-natal liver growth;
2. To compare the proliferation rate of LV transduced and untransduced hepatocytes at different ages;
3. To evaluate whether the efficiency of gene therapy is affected by the age of administration, specifically in terms of transduction of hepatocytes and transgene output;
4. To characterize the distribution of transduced hepatocytes in the liver lobule.

### 3. Results

#### 3.1 Hepatocytes proliferation during growth and homeostasis

We first set out to assess local proliferation of hepatocytes in mice and formation of clonal clusters during liver growth in physiological conditions. To do so, we took advantage of R26-Confetti mouse strain (Snippert *et al*, 2010), which allows clonal tracking of cells over time. These mice bear a construct in the Rosa26 locus that is composed of 4 cassettes coding for different fluorescent proteins: nuclear green fluorescent protein (nGFP), cytosolic yellow fluorescent protein (YFP) and red fluorescent protein (RFP) or membrane cyan fluorescent protein (mCFP) (fig. 1A). These coding sequences are spaced out by loxP sites, moreover between the CAG promoter and the coding sequences there is a floxed neomycin-resistance cassette with a stop codon that abrogates expression unless recombination by Cre recombinase occurs. Upon recombination by Cre, cells can be marked randomly by one of the four fluorescent proteins, maintaining its expression upon cell division. We crossed homozygous Confetti mice with AlbCreERT2<sup>+/+</sup> mice, which express the tamoxifen-inducible CreERT2 recombinase under the control of Albumin promoter (fig.1B). The resulting mouse progeny allowed time-controlled recombination of Confetti locus by a single intraperitoneal or subcutaneous tamoxifen administration with fluorescent protein expression restricted to hepatocytes. We observed that by administering a single dose of tamoxifen (0.1 mg/g) subcutaneously (s.c.) in newborn AlbCreERT2<sup>+/-</sup> Confetti<sup>+/-</sup> (AlbCre/Confetti) mice, on average 13% of liver tissue

#### A Confetti reporter construct



#### Outcomes upon Cre recombination

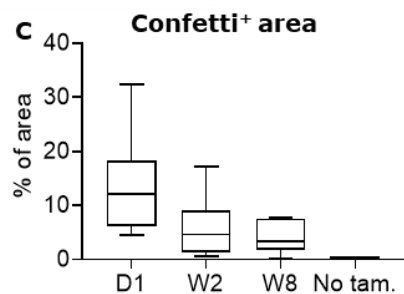
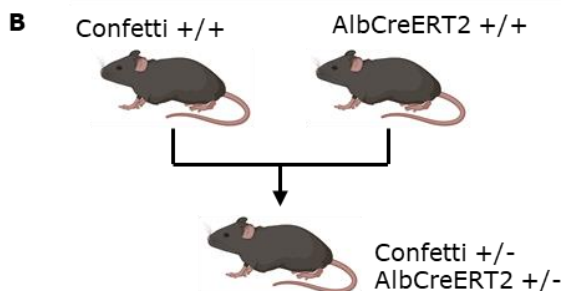
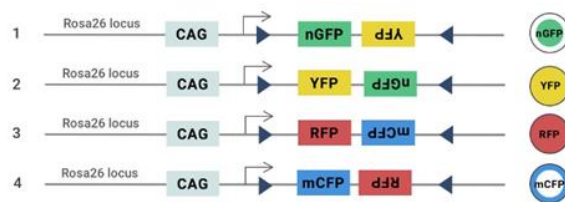


**Fig.1: Confetti mice to lineage trace marked hepatocytes.** A) Scheme of Confetti construct. Integrated in the Rosa26 locus, it is composed of a CAG promoter, followed by a loxP site, a neomycin resistance cassette and a second loxP site. Downstream, there is nuclear-GFP gene in forward orientation and YFP gene in reverse orientation, followed by a loxP site in reverse orientation and a second one in forward orientation. Finally, there is RFP gene in forward orientation and membrane-CFP in reverse orientation, followed by a loxP site in reverse orientation. Below, possible combinations of recombination of Confetti locus by Cre recombinase with their respective outcome of fluorescent protein expression. B) Crossing scheme of Confetti homozygous mice and AlbCreERT2 homozygous mice to obtain Confetti<sup>+/-</sup> AlbCreERT2<sup>+/-</sup> mice to be used for experiments. C) Median, interquartile range and range of percentage of total liver area that express one of the Confetti fluorescent reporters in AlbCreERT2/Confetti mice treated with a single dose of tamoxifen (0.1mg/g) in mice at D1, W2 or W8, or in untreated AlbCreERT2/Confetti (D1 n=16; W2 n=11; W8 n=10; no tam. n=3).

resulted to be positive for one of the four fluorescent proteins. Recombination efficiency was around 5% in 2-week old and 8-week old mice, in which tamoxifen is administered intraperitoneally (i.p.). No relevant marking of hepatocytes was observed in AlbCreERT2/Confetti mice not treated with tamoxifen. (fig. 1C). Since we aimed to track hepatocytes local expansion by evaluating the formation of single-color clusters at different time points after recombination induction, we preferred to have a partial activation of liver parenchyma, to reduce the probability of having close hepatocytes independently recombined but expressing the same fluorescent marker.

### **3.1.1 A fraction of proliferating hepatocytes in newborn mice gives rise to most of the adult liver**

To evaluate hepatocytes proliferation following post-natal liver growth and homeostasis in mice, we activated Confetti locus recombination in newborn mice at post-natal day 1 (D1) and analyzed livers at different time points (fig. 2A) to evaluate the percentage of expanded clusters and their dimension (fig. 2B). In our analysis, we did not include nGFP-expressing clusters, because the lack of a contiguous signal does not allow the identification of two adjacent cells as part of the same cluster. We observed an increase of cluster average size over time up to 1 year (Y1) of age, with a 4-fold increase already in the first 4 weeks of life and 17-fold at Y1 (fig. 2C), indicating local expansion of marked hepatocytes both during liver growth in the first phase of life and homeostasis in adult mice. Interestingly, we noticed that in the first 6 weeks of life there was an 8-fold increase in cluster average size, but between week 6 (W6) and Y1 the increase was less than 2-fold, indicating a decrease in proliferation rate in adult life. To determine which percentage of hepatocytes generates clusters, we calculated the number of hepatocytes composing each cluster based on cluster dimension and the average size of hepatocyte at each age (fig. 2D). At 3 days after activation of CreERT2 we observed almost exclusively clusters composed of 1 or 2 cells. At 1 week of age (W1) this group still represents around 80% of all the clusters,



with only 20% of clusters that are made of more than 2 hepatocytes. Interestingly, the percentage of 1-2 cell clusters, which we consider quiescent or slowly proliferating clusters, remains stable at 75% in all the others time points, suggesting that most of the hepatocytes in the newborn liver do not contribute to liver growth and remain quiescent also later in life. The remaining 25% of clusters increase their dimension over time, as we can observe by the progressive appearance of clusters with 6-10

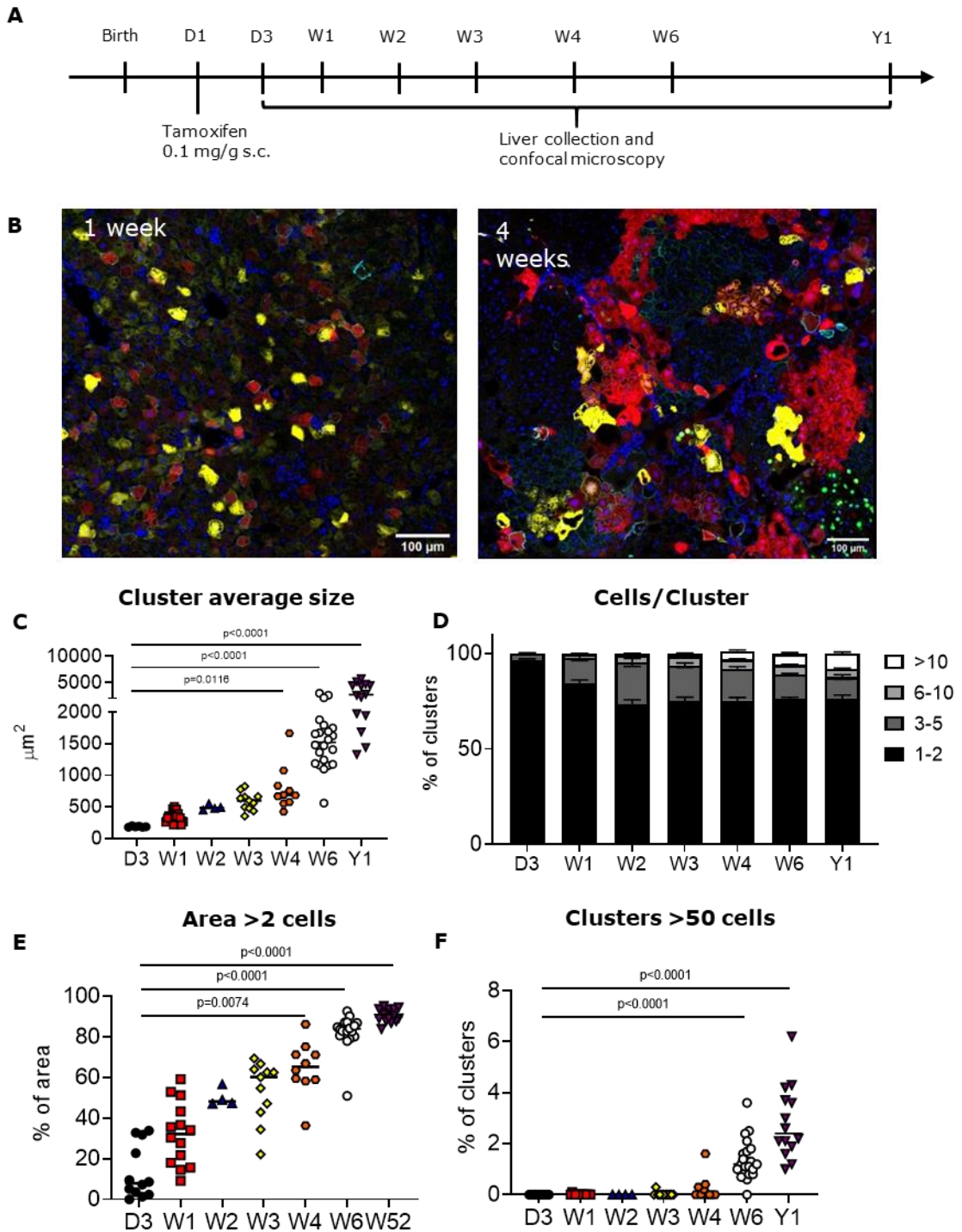


**Fig.2.: Monitoring clonal proliferation of hepatocytes following marking in newborn Confetti mice.** A) Scheme of the experiment: administration of 0.1mg/g of tamoxifen s.c. in AlbCre/Confetti mice at D1, liver collection and confocal microscopy analysis at different time points. B) Representative images of livers of AlbCre/Confetti mice treated with tamoxifen at D1 and analyzed 1 (left panel) or 4 (right panel) weeks post treatment. Nuclei are marked in blue by Hoechst. Scale bar=100 $\mu$ m. C) Single values and median of the average size of hepatocytes clusters in livers of mice treated with a single subcutaneous dose of tamoxifen (0.1mg/g) at D1, analyzed at D3 (n=6), W1 (n=20), W2 (n=4), W3 (n=11), W4 (n=10), W6 (n=22) or Y1 (n=14) of life from 6 independent experiments. For every mouse 2 images of 9 fields (3mm<sup>2</sup>) each has been acquired by confocal microscopy at 20X magnification. Kruskal-Wallis test with Dunn's multiple comparisons test vs. D3. D) Mean and standard error of the mean (SEM) of the percentage of clusters made of 1-2, 3-5, 6-10 or >10 cells. Number of cells per clusters have been calculated by measuring dimension of each cluster and dividing by the average size of hepatocytes at that age (D3=200  $\mu$ m<sup>2</sup>, W1=250  $\mu$ m<sup>2</sup>, W2=300  $\mu$ m<sup>2</sup>, W3=350  $\mu$ m<sup>2</sup>, W4, W6, Y1=450  $\mu$ m<sup>2</sup>). E) Single values and median of the percentage of area marked by Confetti colors that is made by clusters composed of more than 2 cells. Kruskal-Wallis test with Dunn's multiple comparisons test vs. D3. F) Single values and median of the percentage of clusters that are made of more than 50 cells. Kruskal-Wallis test with Dunn's multiple comparisons test vs. D3.

and then >10 cells, and are responsible for the observed increase in clusters average size. Moreover, the percentage of area occupied by clusters of more than 2 cells increases over time, going from 40% of the total marked liver area at W1 to more than 80% already at W6 and around 90% at Y1 (fig.2E). These data suggest that a relatively small percentage of hepatocytes proliferates during growth and generates the vast majority of the liver tissue of the adult mouse, thus resulting in a progressive reduction of clonality of the adult parenchyma. Furthermore, we observed some clusters that exceeded 50 cells already at week 4 (W4), and their percentage increased at W6 and represented 4% of the total number of clusters at Y1 (fig. 2F).

### **3.1.2 Reduced proliferation rate of hepatocytes from the second week of age**

We performed the experiment as above but activating recombination of the Confetti locus in 2-week-old AlbCre/Confetti mice (fig. 3A) to evaluate clonal expansion of hepatocytes during liver growth. Differently from what we observed in newborn mice, by marking hepatocytes in 2-week-old mice we observed a mild increase in cluster average size over time, that was lower than 2-fold at week 8 (W8) compared to week 3 (W3), and lower than 4-fold at Y1 (fig.3B). The percentage of quiescent clusters remained 80-85% throughout the follow up, and the expanding clusters were made mainly of 3-5 cells, with a few bigger clusters appearing only at W6 (fig. 3C). The percentage of marked area composed of expanding clusters (>2 cells) ranged from less than 20% at W3 to 40% at W8, confirming slower proliferation of hepatocytes in this phase of liver growth, and reaching 60% only at Y1 (fig. 3D). This last time point was also the only one in which we could observe clusters made

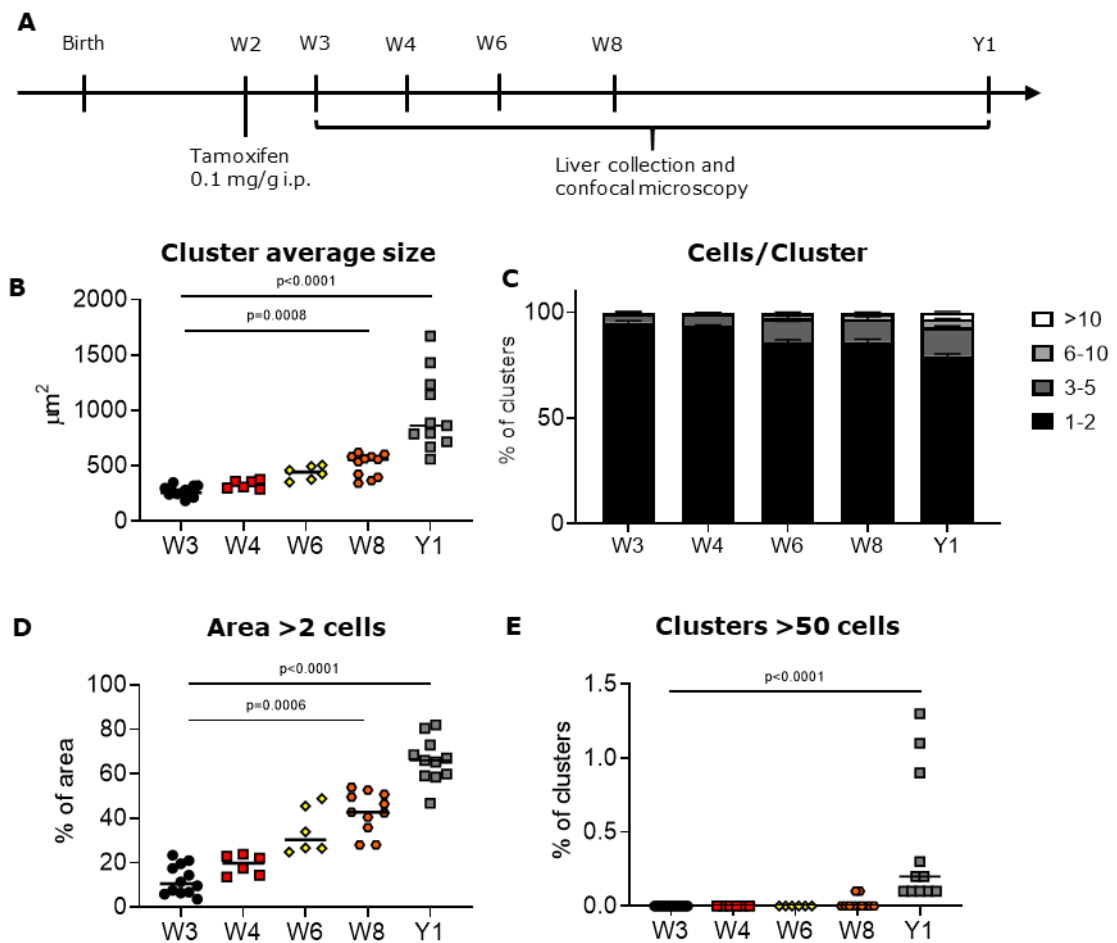


**Fig.3: Monitoring clonal proliferation of marked hepatocytes in juvenile Confetti mice.** A) Scheme of the experiment: administration of 0.1mg/g of tamoxifen *i.p.* in AlbCre/Confetti mice at W2, liver collection and confocal microscopy analysis at different time points. B) Single values and median of the average size of hepatocyte clusters in livers of mice treated with a single intraperitoneal dose of tamoxifen (0.1mg/g) at W2, analyzed at W3 (n=12), W4 (n=6), W6 (n=6), W8 (n=11) or Y1 (n=11) of life from 4 independent experiments. For every mouse 2 images of 9 fields (3mm<sup>2</sup>) each has been acquired by confocal microscopy at 20X magnification. Kruskal-Wallis test with Dunn's multiple comparisons test vs. W3. C) Mean and SEM of the percentage of clusters made of 1-2, 3-5, 6-10 or >10 cells. Number of cells per clusters have been calculated by measuring dimension of each cluster and dividing by the average size of hepatocytes at that age (W3=350  $\mu\text{m}^2$ , W4, W6, W8, Y1=450  $\mu\text{m}^2$ ). D) Single values and median of the percentage of area marked by Confetti colors that is made by clusters composed of more than 2 cells. Kruskal-Wallis test with Dunn's multiple comparisons test vs. W3. E) Single values and median of the percentage of clusters that are made of more than 50 cells. Kruskal-Wallis test with Dunn's multiple comparisons test vs. W3.

of more than 50 cells, which anyway represented less than 1% of total clusters (fig.3E). Taken together these data show that, despite the expansion of a minority of hepatocytes originates the adult liver, the proliferation rate of hepatocytes is reduced already from week 2 (W2). We then repeated the analysis by marking hepatocytes in 8-week-old AlbCreERT2/Confetti mice, to evaluate clonal expansion of hepatocytes during homeostasis. In this case we only observe a very mild increase in cluster

average size over time and at Y1 (fig. 4B). At week 14 (W14) (6 weeks post tamoxifen administration) the percentage of clusters with more than 2 cells was only 4%, and reached 10% at Y1 (fig. 4C), but with less than 2% of clusters made of more than 6 cells. The percentage of marked area made of expanding clusters was 10% at W14, and reached 30% at Y1 (fig. 4D), but we did not observe any cluster made of more than 50 cells at any time point (fig. 4E). Thus, we confirmed a reduction in hepatocyte proliferation rate over time that can be observed already at 2 weeks of age (Chang et al., 2008), and these data support previous evidence of very slow turnover of hepatocytes during homeostasis in the adult mouse liver (Chen et al, 2020).

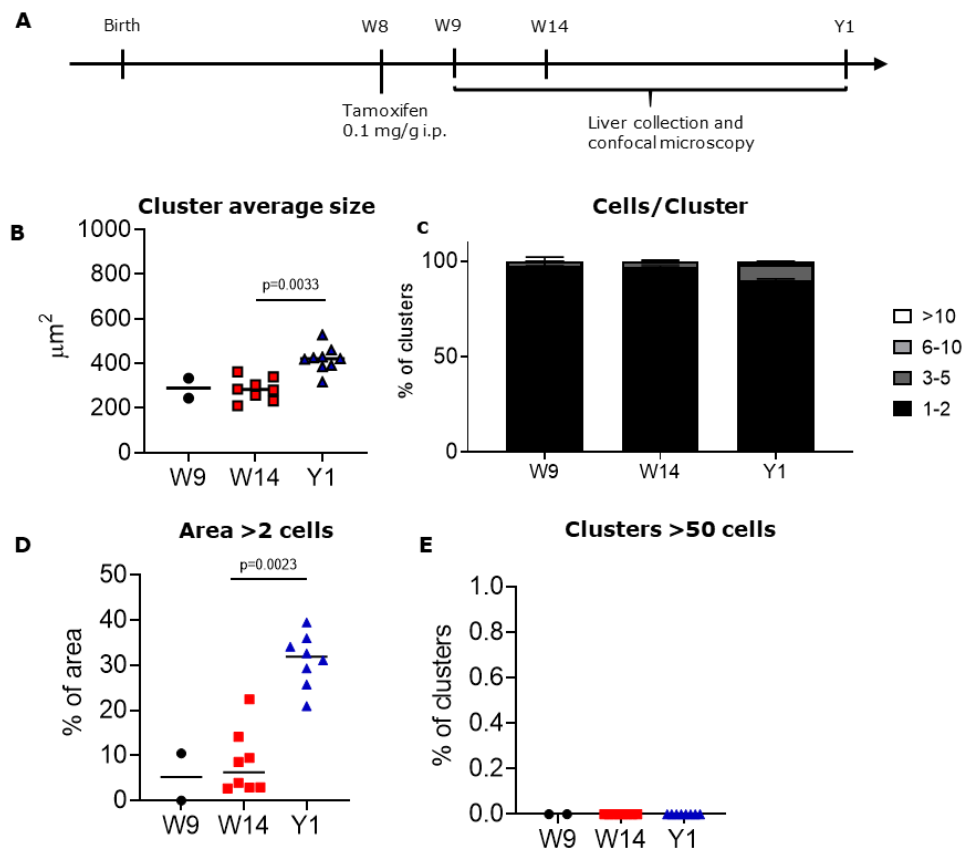


**Fig.4: Monitoring clonal proliferation of hepatocytes following marking in adult Confetti mice.** A) Scheme of the experiment: administration of 0.1mg/g of tamoxifen i.p. in AlbCre/Confetti mice at W8, liver collection and confocal microscopy analysis at different time points. B) Single values and median of the average size of hepatocytes clusters in livers of mice treated with a single intraperitoneal dose of tamoxifen (0.1mg/g) at W8, analyzed at W9 (n=2), W14 (n=9) or Y1 (n=9) of life from 2 independent experiments. For every mouse 2 images of 9 fields (3mm<sup>2</sup>) each has been acquired by confocal microscopy at 20X magnification. Kruskal-Wallis test with Dunn's multiple comparisons test vs. W3. C) Mean and SEM of the percentage of clusters made of 1-2, 3-5, 6-10 or >10 cells. Number of cells per clusters have been calculated by measuring dimension of each cluster and dividing by the average size of hepatocytes (W9, W14, Y1=450 µm<sup>2</sup>). Kruskal-Wallis test with Dunn's multiple comparisons test. D) Single values and median of the percentage of area marked by Confetti colors that is made by clusters composed of more than 2 cells. E) Single values and median of the percentage of clusters that are made of more than 50 cells. Kruskal-Wallis test with Dunn's multiple comparisons test vs. W3.

## 3.2 Proliferation of LV-transduced and untransduced hepatocytes

### 3.2.1 LV-transduced and untransduced hepatocytes proliferate at a similar rate

In order to understand if LV transduction of hepatocytes has an impact on their proliferation potential *in vivo*, we administered intravenously  $2.5 \times 10^{10}$  TU/Kg of LV expressing blue fluorescent protein (BFP) under the control of the hepatocyte-specific cassette comprising the ET promoter and miR142T (LV.BFP, see 1.5.4), to AlbCre/Confetti mice at D1, W2 or W8. We then activated CreERT2 with a single dose

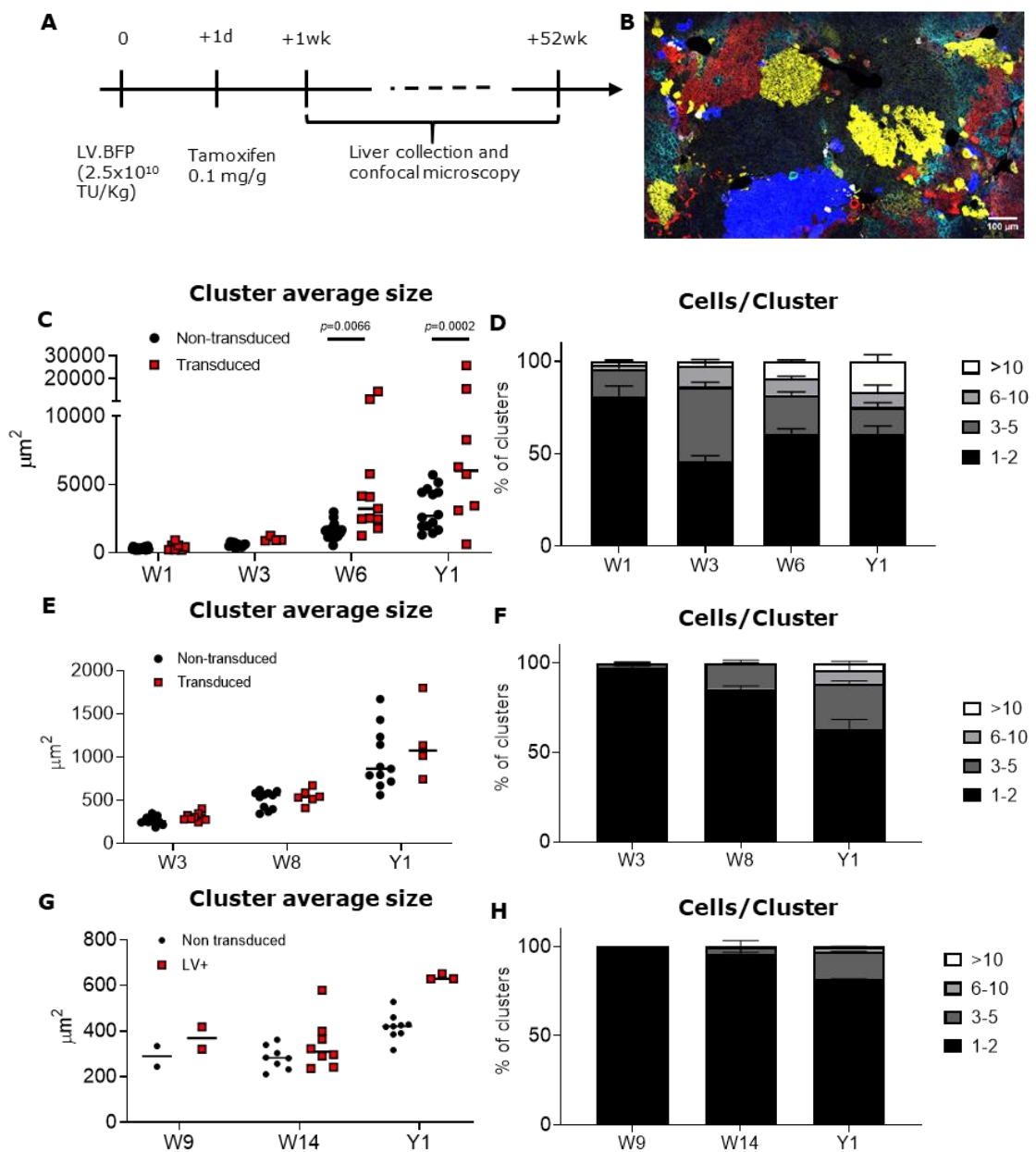


**Fig.5: Evaluation of proliferation of LV-transduced and untransduced hepatocytes.** A) Scheme of the experiment: administration of  $2.5 \times 10^{10}$  TU/Kg of LV.BFP in AlbCre/Confetti mice at different ages followed by administration of 0.1mg/g of tamoxifen the day after, liver collection and confocal microscopy analysis at different time points. B) Representative image of AlbCre/Confetti mouse treated at D1 and collected 3 weeks post treatment. Scale bar=100 $\mu$ m. C-D) Hepatocytes proliferation in newborn AlbCreERT2/Confetti mice treated with  $2.5 \times 10^{10}$  TU/Kg LV.BFP at D 1 and 0.1 mg/g of tamoxifen the day after. C) Single value and median of cluster average size formed from non-transduced (Confetti mice, same as fig.2) and transduced hepatocytes (W1 n=7, W3 n=4, W6 n=11, Y1 n=8). Two-way Anova with Sidak's multiple comparisons test. D) Mean and SEM of the percentage of LV<sup>+</sup> clusters made of 1-2, 3-5, 6-10 or >10 cells. E-F) Hepatocytes proliferation in AlbCreERT2/Confetti mice treated with  $2.5 \times 10^{10}$  TU/Kg LV.BFP at W2 of age and 0.1 mg/g of tamoxifen the day after. E) Single value and median of cluster average size formed from non-transduced (Confetti mice, same as fig.3) and transduced hepatocytes (W3 n=9, W8 n=6, Y1 n=4). Two-way Anova analysis with Sidak's multiple comparisons test. F) Mean and SEM of the percentage of LV<sup>+</sup> clusters made of 1-2, 3-5, 6-10 or >10 cells. G-H) Hepatocyte proliferation in AlbCreERT2/Confetti mice treated with  $2.5 \times 10^{10}$  TU/Kg LV.BFP at W8 of age and 0.1 mg/g of tamoxifen the day after. G) Single value and median of cluster average size formed from non-transduced (Confetti mice, same as fig.4) and transduced hepatocytes (W9 n=2, W14n=8, Y1 n=3). H) Mean and SEM of the percentage of clusters made of 1-2, 3-5, 6-10 or >10 cells.

of tamoxifen the day after, and monitored cluster formation from untransduced (marked by RFP, YFP, or mCFP) or transduced (marked by BFP) hepatocytes (fig. 5A-B). Newborn-treated mice showed a gradual increase in the average size of BFP<sup>+</sup> clusters, which became higher than non-transduced clusters at W6 and Y1 post treatment (fig. 5C). Moreover, we observed that clusters of non-proliferating transduced hepatocytes decreased from 81% of total clusters at W1 to 60% at W6 and Y1, with a percentage of clusters with more than 10 cells reaching 9% at W6 and 16% at Y1 (fig. 5D). For mice treated at 2 weeks of age we did not observe any differences in average size of transduced clusters compared to non-transduced ones, confirming a lower proliferation rate from this age (fig. 5E). Quiescent clusters resulted to be 85% at 8 weeks of age and 60% at 1 year, but most of the expanding clusters displayed a reduced number of cells compared to mice treated as newborns, with very few clusters with more than 10 cells at W8 (fig. 5F). Mice treated at 8 weeks of age did not show any increase in average size of transduced clusters between W9 and W14, and only a mild increase at Y1 that was higher compared to what has been observed for non-transduced clusters (fig. 5G). In terms of cluster composition, adult-treated mice showed 95% of quiescent clusters at W14, and 81% at Y1, with most of the proliferating clusters that remained small in dimension (fig. 5H). These data indicate that transduced hepatocytes are able to proliferate locally maintaining the transgene and its expression. The differences observed between cluster size and composition of transduced and non-transduced hepatocytes can be considered minor, given that transduced hepatocytes are marked with only one fluorescent protein (BFP), while non-transduced hepatocytes are marked with 3 different colors. This difference results in a lower probability of having fusion of two

independent clusters expressing the same fluorescent reporter for untransduced hepatocytes, while fusion of independently marked clusters may be more common for LV<sup>+</sup> clusters, thus overestimating the proliferation of transduced hepatocytes by this analysis.

### ***3.2.2 3D analysis show local proliferation and expansion of transduced and untransduced hepatocytes***

To confirm that only a portion of hepatocytes proliferate in the first week of life of mice, we marked cells in active proliferation using EdU (5-ethynyl-2'-deoxyuridine), an analog of thymidine that is incorporated into the chromatin during DNA synthesis (S phase of cell cycle). We administered LV.GFP in mice at D1, followed by administration of 3 doses of EdU (50µg/g each) at day 3, 4 and 5, and livers were collected at day 6 to evaluate the percentage of proliferating hepatocytes in the first week of life (fig. 6A-B). We counted that 28% of total hepatocyte nuclei (HNF4a<sup>+</sup>) and 33% of GFP<sup>+</sup> cells were also EdU<sup>+</sup> (fig. 6C), confirming the previous observation that about 25-30% of hepatocytes generate clusters. We set to evaluate local proliferation of transduced hepatocytes also by 3-dimensional (3D) imaging of livers of newborn mice treated by intravenous administration of 2.5x10<sup>10</sup> TU/Kg or 5x10<sup>9</sup> TU/Kg of LV expressing GFP under the control of the same hepatocyte-specific expression cassette described above (LV.GFP). We exploited X-clarity technology to clear fixed livers and acquired 3D images by 2-photon microscopy (fig. 6F). By measuring volume of GFP<sup>+</sup> clusters in livers collected at different time points after treatment (up to 1 year) in multiple experiments, we observed that the percentage of GFP<sup>+</sup> tissue is maintained stably over time, at both LV doses (fig. 6D). Moreover, we measured the dimension of each GFP<sup>+</sup> cluster and arbitrarily defined small, middle, and high-volume clusters to evaluate their increase in dimension over time. We observed mainly small-volume clusters at W1, corresponding to 80% of the total, followed by an increase in middle and high-volume clusters over time, that together represent more than 90% of the clusters (fig. 6E). The same pattern was observed also in mice treated with the lower dose of LV, with only a slightly lower percentage of high-volume clusters measured at Y1. 3D analysis confirmed that transduced hepatocytes are maintained in liver during growth and homeostasis, and proliferate locally maintaining transgene expression. Despite both Confetti and 3D imaging experiments showed local expansion of transduced hepatocytes, the fraction of clusters that increase their dimension over time was different, being the vast majority in the former experiment and a minority in the latter. This apparent discrepancy between the results obtained by 3D and 2-dimensional (2D) imaging analysis may



be due to the arbitrarily defined volume threshold set for the classification of small, middle, and high-volume clusters in 3D images, which does not take into consideration the increase in size of hepatocyte during growth. To assess whether we might be underestimating the percentage of proliferating hepatocytes, by missing 3-dimensional clusters growth (on the Z axis) by the 2D analysis, we acquired 3D images of livers of AlbCre/Confetti mice 6 weeks after the administration of a single dose of tamoxifen as newborn. Quantification of dimension and number of clusters was not possible due to technical reasons, but we could still perform a qualitative

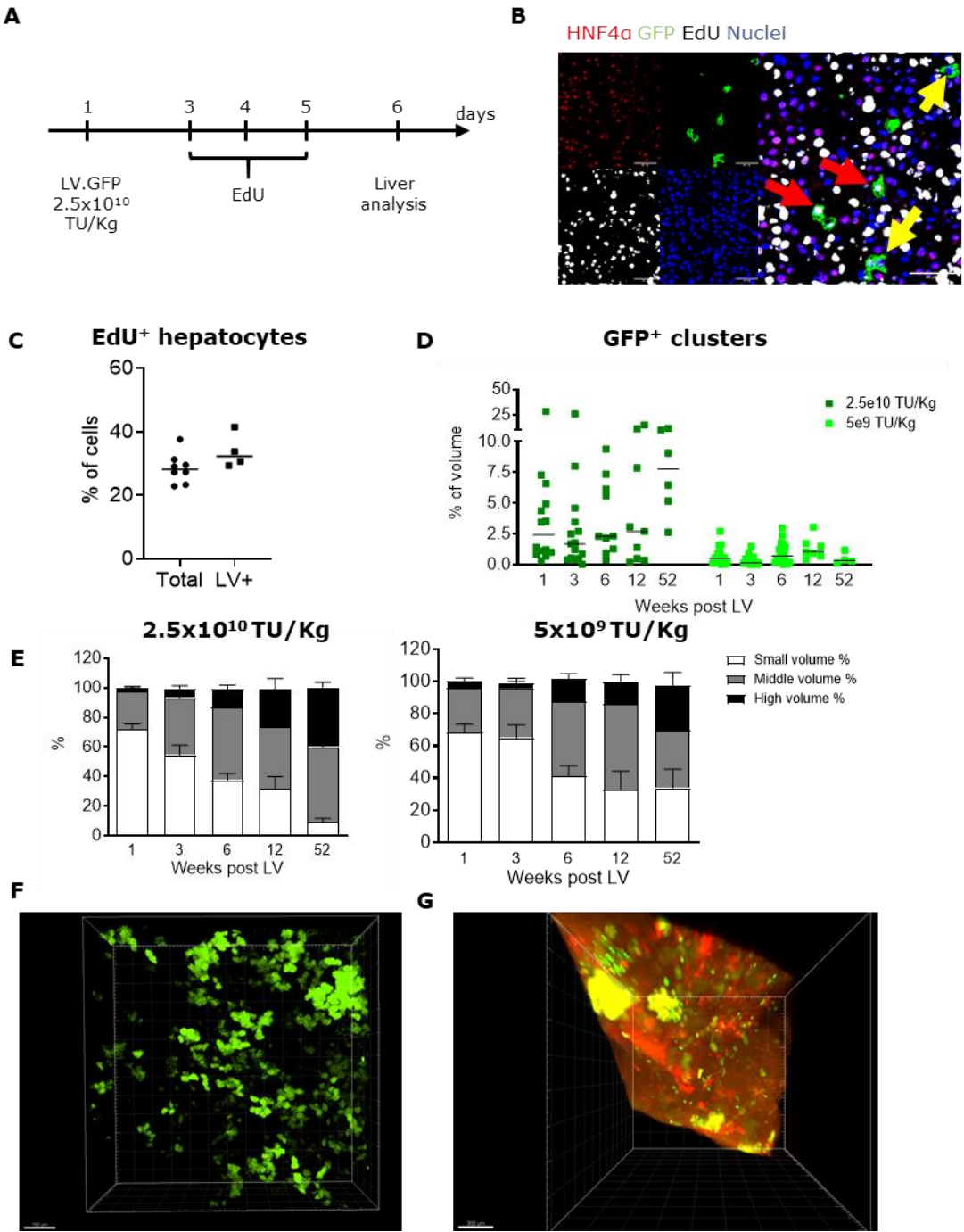




**Fig.6: 3D imaging of proliferating transduced and non-transduced hepatocytes.** A) Scheme of the experiment: newborn wt mice were treated i.v. with LV.GFP at D1 and subcutaneously with EdU 50 $\mu$ g/g at D3, D4 and D5, livers were collected and analyzed at D6. B) Representative image. From left to right: HNF4a (red), GFP (green), EdU (white), nuclei (blue), merged. Red arrow: GFP<sup>+</sup> HNF4a<sup>+</sup> EdU<sup>+</sup> cells. Yellow arrow: GFP<sup>+</sup> HNF4a<sup>+</sup> EdU<sup>-</sup> cells. Scale bar= 50  $\mu$ m. C) Single values and median of percentage of total hepatocytes (n=8 mice) or transduced hepatocytes (n=4 mice) positive for EdU staining. D) Single values and mean of quantification of percentage of GFP<sup>+</sup> area in 3D images of cleared livers of mice treated with 2.5 $\times 10^{10}$  TU/Kg or 5 $\times 10^9$  TU/Kg of LV.GFP at D1 and analyzed 1 (low dose n=16, high dose n=14), 3 (low dose n=15, high dose n=15), 6 (low dose n=19, high dose n=12), 12 (low dose n=7, high dose n=9) or 52 (low dose n=4, high dose n=6) weeks post LV administration. Kruskal-Wallis test with Dunnett's multiple comparisons test vs. week 1. E) Mean and SEM of percentage of clusters identified as small (white bar), middle (grey) or high (black) volume in mice in C treated with 2.5 $\times 10^{10}$  TU/Kg (left panel) or 5 $\times 10^9$  TU/Kg (right panel) of LV.GFP. F) Representative image of cleared liver of a mouse treated with 2.5 $\times 10^{10}$  TU/Kg of LV.GFP at D1 acquired with 2-photon microscope at W3. Scale bar=150  $\mu$ m. G) Representative 3D image of cleared liver of AlbCre/Confetti mice treated with tamoxifen (0.1 mg/g) at post-natal day 1 and analyzed after 6 weeks by Lightsheet microscope. Scale bar=300  $\mu$ m.

analysis. In the representative image in fig. 6G we could clearly observe the presence of several single-cell clusters, in addition to high-volume clusters, suggesting appropriate identification of the small clusters by the 2D analysis.

### **3.2.3. Reduction of proliferation rate of hepatocytes inside single-cell derived cluster**

The similar proliferation rate between transduced and untransduced hepatocytes observed in previous experiments reassured over the use of LV as a tool to study liver tissue dynamics in vivo. We set out to investigate proliferation of hepatocytes in two windows of time by first administering LV expressing CreERT2 in newborn heterozygous Confetti mice and then activating recombination of Confetti locus at W2 by tamoxifen administration and subsequently analyzing livers at W6. In this way we could expect to see multi-color clusters, each of which has been generated by the proliferation of a single transduced hepatocytes, and composed of multiple single-color clusters, originated by hepatocytes activated with tamoxifen administration at W2. The dimension of the multi-color clusters depends on the proliferation occurred between D1 and W6, while dimension of single-color clusters depends on the proliferation occurred between W2 and W6 (fig. 7A). Unfortunately, the low recombination rate of transduced hepatocytes did not allow us to have reliable quantitative data from this experiment, but we can still draw a qualitative picture from it. In figure 7B we can observe the liver of a Confetti mouse treated with LV.CreERT2 at D1 and with 3 doses of tamoxifen at 2 weeks of age, then analyzed at W3. We can see a low number of cells expressing Confetti colors, with very few

clusters made of cells expressing different colors. Instead, livers collected at W6 show some multi-color clusters made of multiple cells, while single-color clusters are small and made mainly of 1 or 2 cells, indicating that growth from the 2<sup>nd</sup> to the 6<sup>th</sup> week of age was characterized by a low number of replication cycles per cell, thus confirming the reduction in proliferation rate of hepatocytes over time.

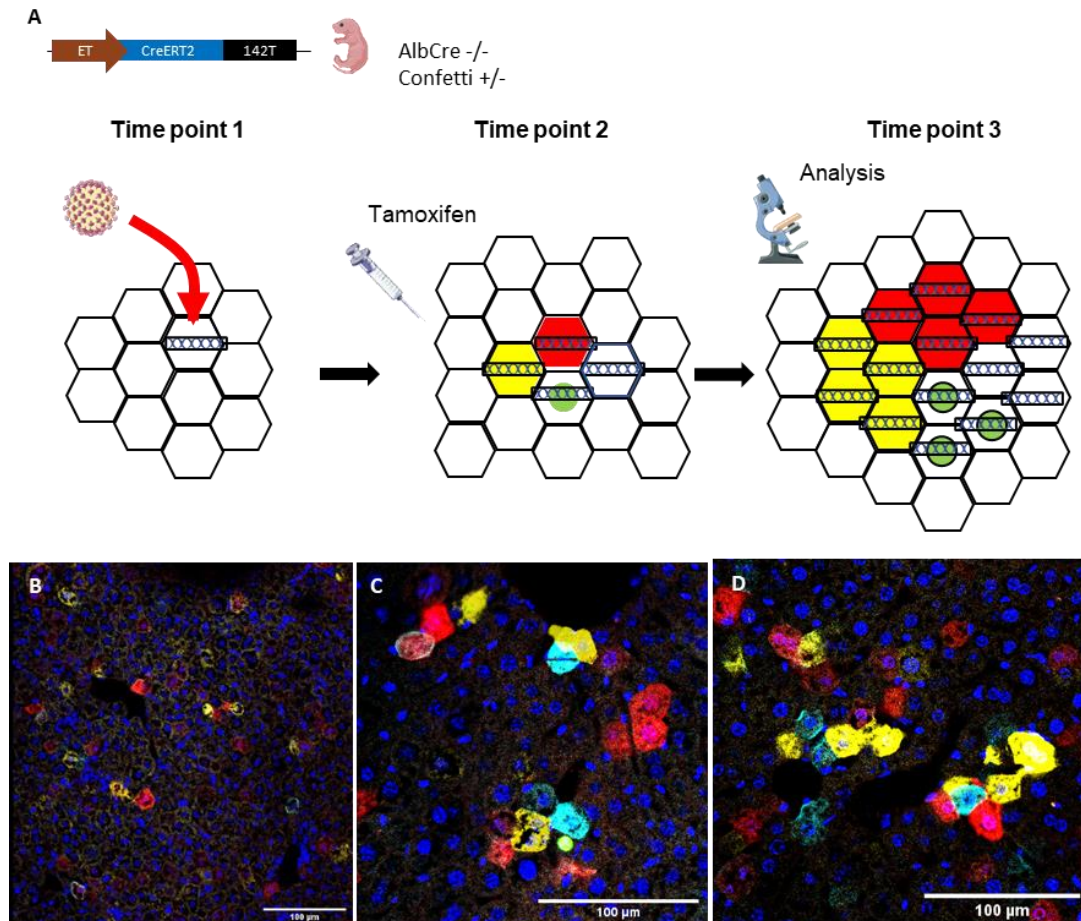


**Fig.7: Evaluation of hepatocytes proliferation in two windows of time in Confetti mice.** A) Experimental scheme exploiting LV expressing CreERT2 recombinase under the control of ET hepatocyte-specific promoter to study *in vivo* hepatocytes proliferation in two windows of time. LV.CreERT2 is administered *i.v.* in Confetti<sup>+/-</sup> newborn mice. Between time point 1 and 2 hepatocytes proliferate and generate clusters, then tamoxifen is administered to activate recombination of Confetti locus only in hepatocytes carrying the Cre transgene. Inside a cluster, each hepatocyte will be marked with a different fluorescent reporter. Between time point 2 and time point 3 expansion of clusters continues. At the moment of analysis, we will observe single-color clusters formed between time point 2 and 3, and multi-color clusters formed between time point 1 and 3. B, C, D) Representative images from the experiment described in A) from 2 independent experiments. Newborn Confetti<sup>+/-</sup> mice were treated with  $2.5 \times 10^{10}$  TU/Kg LV.CreERT2 and 2 weeks later with 3 doses of tamoxifen (0.1mg/g each). Images have been acquired 1 week (B) or 4 weeks (C, D) post tamoxifen administration. Scale bar =100  $\mu$ m.

### **3.3. Age-dependent differences in liver-directed LV gene therapy**

#### ***3.3.1. Administration of LV to newborn and juvenile mice improves hepatocyte transduction efficiency and transgene output***

Considering the different proliferation rate between hepatocytes in newborn vs. 2-week- or 8-week-old mice, we wondered whether this difference has an impact on the efficiency of gene therapy in mice of different ages. We hypothesized that higher proliferation rate of transduced hepatocytes in newborn mice may result in an increased transduction, resulting also in a higher output of a therapeutic transgene product, such as hFIX. Moreover, we asked if proliferation of transduced hepatocytes led to an increase of transgene output over time. To evaluate efficiency of gene therapy at different ages, we administered LV.hFIX i.v. to wild-type (wt) mice at D1, W2, W3, W4 or W8, at  $2.5 \times 10^{10}$  TU/Kg dose, collected plasma samples over time and measured the concentration of hFIX (fig. 8A). At the end of the experimental follow up the group with the highest transgene output was 2-week-old treated mice, with a total output 2-fold higher compared to mice treated at D1 and 6-fold higher compared to adult-treated mice (week 8). Interestingly, we noticed that 3-week-old treated mice have a high output of hFIX, close to 2-week-old treated mice, while administration of LV already at 4 weeks of age resulted in a strong reduction in transgene output, similarly to adult-treated mice. Moreover, by plotting hFIX levels as a fold on the value at the first time point analyzed (W2 post treatment), we noticed that all the treated groups have a stable transgene output over time, except for mice treated as newborn. In this group we observed a 4-fold increase in hFIX levels at W6 compared to W2, followed by a slight decrease and a stabilization of the output at a 3-fold higher level compared to W2 (fig. 8B). In order to understand the biodistribution of LV in liver subpopulation of mice treated at different ages, we isolated hepatocytes, KC, LSEC and pDC, and a pool of all nPC by FACS sorting at the end of the experiments (12-33 weeks post LV administration). Despite the differences in transgene output, vector copy number (VCN) per diploid genome in sorted hepatocytes was similar among groups, but newborn-treated mice have a reduced LV VCN in nPC, and in particular in KC and pDC (fig. 8C). Moreover, we performed gene expression analysis to evaluate transgene expression in sorted hepatocytes, and we observed higher transgene mRNA levels in young compared to adult-treated mice (fig. 8D), in accordance with the higher transgene protein output. To assess LV transduction of liver subpopulations short after transduction, we isolated by FACS sorting hepatocytes, nPC, KC, LSEC and pDC 3 days post LV administration, to avoid confounding factors due to cells turn-over, proliferation and polyploidization over

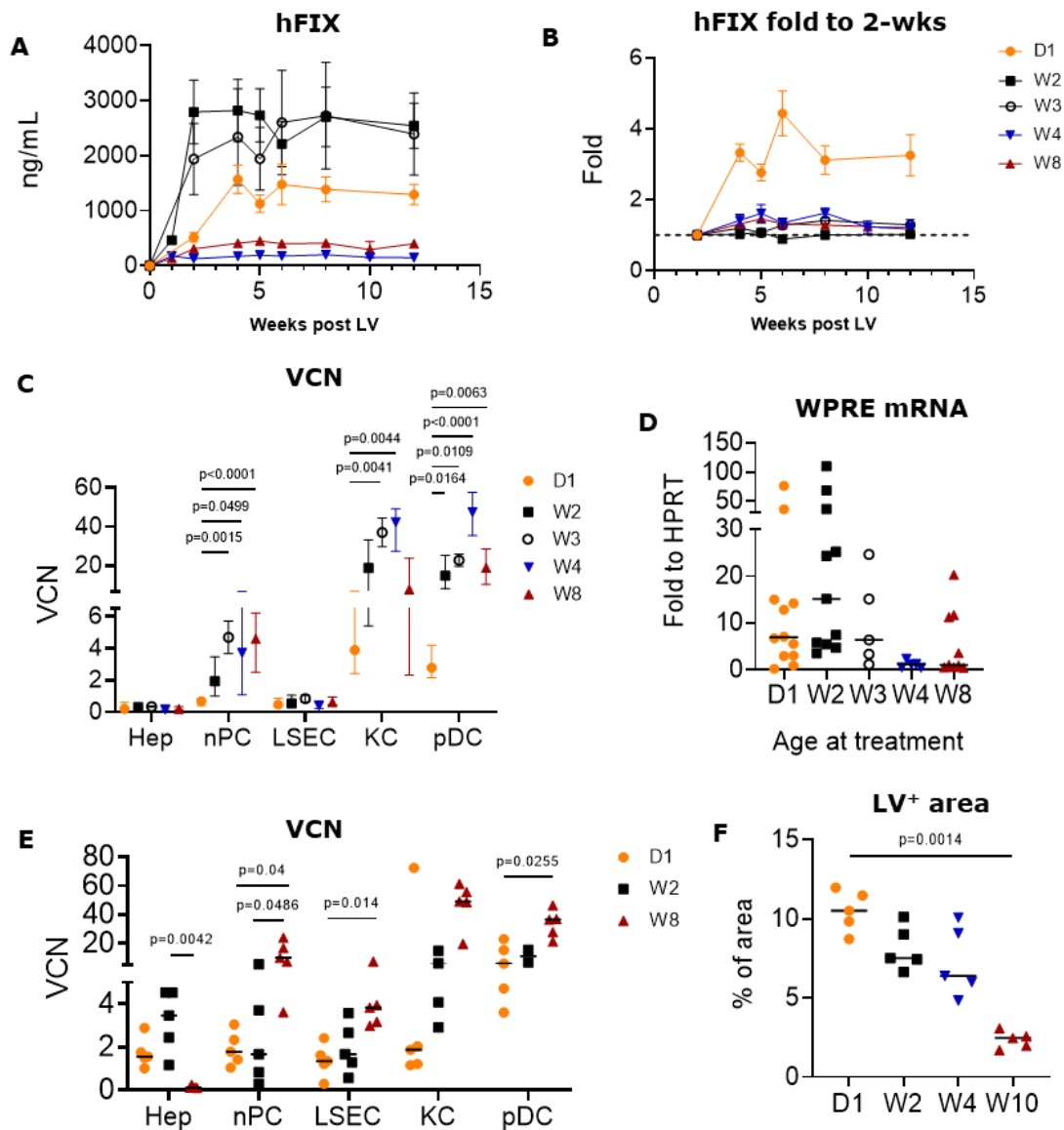


**Fig.8: Evaluation of LV-based gene therapy efficiency at different age of treatment.** A) Mean and SEM of hFIX plasma concentration in mice treated with i.v. administration of  $2.5 \times 10^{10}$  TU/Kg LV.ET.hFIX at D1, W2, W3, W4 or W8 and B) fold of hFIX concentration on the value measured 2 weeks post-LV administration. Pool of 3 independent experiments. D1 n=22, W2 n=19, W3 n=5, W4 n=5, W8 n=15. In A Mixed effect analysis with Bonferroni's correction: D1-W2  $p=0.0020$ ; D1-W8  $p=0.0022$ ; W2-W4  $p<0.0001$ ; W2-W8  $p<0.0001$ ; W3-W4  $p=0.0111$ ; W3-W8  $p=0.0012$ . C) Median and interquartile range of VCN of sorted hepatocytes, LSEC, KC and pDC measured at the end of the experiments shown in A and B 12 to 33 weeks post LV administration. Kruskal-Wallis test with Dunn's multiple comparisons test. D) Single values and median of transgene mRNA level measured as a fold on HPRT housekeeping gene expression of some of the mice shown in A-B-C. D1 n=12, W2 n=13, W3 n=5, W4 n=5, W8 n=9 Kruskal-Wallis test with Dunn's multiple comparisons test. E) Single values and median of VCN of sorted hepatocytes, total nPC, sorted LSEC, KC and pDC 3-day post i.v. administration of  $2.5 \times 10^{10}$  TU/Kg LV in mice at D1 (n=5), W2 (n=5) or W8 (n=5). Kruskal-Wallis test with Dunn's multiple comparisons test. F) Single values and median of percentage of liver area expressing mCherry by immunofluorescence analysis 3 days post administration of  $2.5 \times 10^{10}$  TU/Kg LV.ET.mCherry in mice at D1 (n=5), W2 (n=5), W4 (n=5) or W10 (n=5). Kruskal-Wallis test with Dunn's multiple comparisons test.

time (fig. 8E). We focused our attention on newborn, 2-week-old and 8-week-old treated mice. These data showed a higher VCN in sorted hepatocytes in young (newborns and 2-week-old) compared to adult (8-week-old) mice, indicating a more efficient transduction of parenchymal cells that may explain the higher transgene output observed in these mice. Moreover, total nPC in adult-treated mice showed a significantly higher VCN compared to young mice, and in particular pDC, KC and LSEC, indicating that the age of administration of LV impacts on its biodistribution among liver cell types. To confirm the higher level of transduction of hepatocytes in young-treated mice, we administered  $2.5 \times 10^{10}$  TU/Kg of LV expressing mCherry fluorescent reporter in wt mice at D1, W2, W4 or W8, and analyzed 2D images of livers to measure the percentage of mCherry<sup>+</sup> area 3 days post treatment. We confirmed that transgene-positive liver parenchyma was higher in newborn and 2-week-old mice compared to adult-treated mice (4.5 and 3.4-fold respectively), while 4-week-old treated mice showed an intermediate level of liver transduction despite the lower transgene output at this age (fig. 8F).

### ***3.3.2. Mono- and bi-nucleated hepatocytes are transduced with the same efficiency at all ages***

Differences in transgene expression and protein output between mice treated at different ages with LV.hFIX may also be due to physiological changes of hepatocytes that occur during mouse growth. Indeed, at around 3 weeks of age important metabolic changes occur in hepatocytes, caused mainly by the change in diet following weaning, but one of the most significant alteration is the polyploidization of the majority of hepatocytes. We hypothesized that transduction occurring before or after this important phase of liver life can determine a difference in transgene output: indeed hepatocytes targeted before polyploidization will duplicate the number of transgenes present *per* cell (without altering the number of LV copies per genome or the percentage of LV<sup>+</sup> area), while those that are transduced after polyploidization may have a lower amount of LV genetic material. If LV preferentially transduces hepatocytes during polyploidization when administered at W2 or W3, then there will be a duplication of the total number of transgenes in parallel to duplication of all the genetic material, without modifying the VCN, thus possibly increasing transgene output. To test this hypothesis, we produced an LV expressing both hFIX and GFP, separated by an internal ribosome entry site (IRES), and administered  $2.5 \times 10^{10}$  TU/Kg in mice at D1, W2, W3 and W8 in order to monitor transgene output over time for 12 weeks and then acquire IF images at the end of the experiment to correlate

FIX output with the percentage of GFP<sup>+</sup> area and the count of mono- and bi-nucleated hepatocytes, as a surrogate for diploid and polyploid cells. We observed a strong correlation between the percentage of GFP<sup>+</sup> area and the total output of FIX measured at the end of the experiment, which was true for age groups analyzed independently or all together (fig. 9A). Interestingly, the relation between transduced area and transgene output appeared to be linear, but we could not detect major differences in the slope of linear regression for mice treated at different ages, suggesting no differences in transgene output *per cell* in mice treated at different ages. Moreover, we found that among GFP<sup>+</sup> hepatocytes, about 75% have a single nucleus and 25% have two nuclei, independently on the age of treatment, and that the same percentages were observed also among non-transduced hepatocytes (fig. 9B). These data indicate that LV transduces with the same efficiency mono- and bi-nucleated hepatocytes in adult mice, while in the growing liver there is no preference for transduction of hepatocytes that are about to become bi-nucleated. Therefore, transgene output correlated with the transgene-positive tissue, but it did not seem to depend on the number of polyploid transduced cells

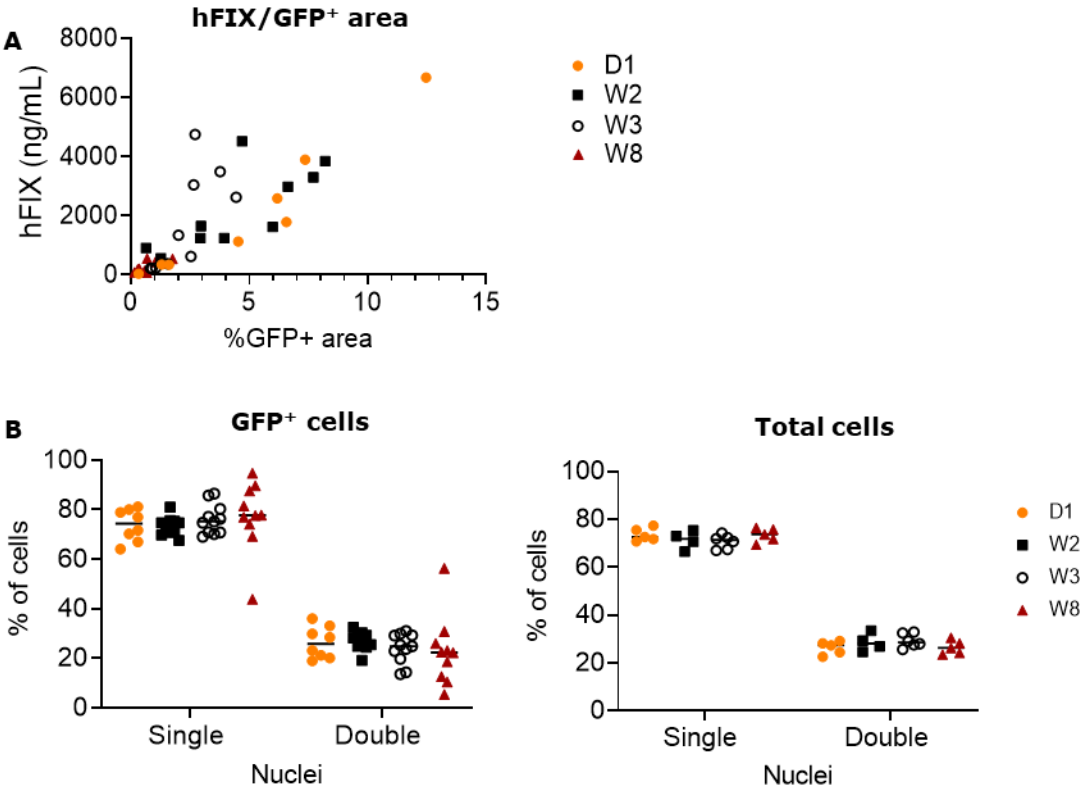


**Fig.9: Evaluation of transduction of mono- and bi-nucleate hepatocytes.** A) Single values of total hFIX bloodstream concentration and percentage of GFP<sup>+</sup> area at W12 post treatment in mice treated with  $2.5 \times 10^{10}$  TU/Kg of LV.hFIX.IRES.GFP at D1 (n=8), W2 (n=10), W3 (n=10) or W8 (n=10). Spearman's correlation: pool  $r=0.8873$   $p<0.0001$ ; D1  $r=0.9524$   $p=0.0011$ ; W2  $r=0.8182$   $p=0.0058$ ; W3  $r=0.8909$   $p=0.0011$ ; W8  $r=0.6848$   $p=0.0347$ . Pearson's correlation pool:  $r=0.8837$   $p<0.0001$ ; D1:  $r=0.9612$   $p=0.0001$ ; W2:  $r=0.7512$   $p=0.0123$ ; W3:  $r=0.7482$   $p=0.0168$ ; W8:  $r=0.7482$   $p=0.0128$ . Linear regression slopes: D1=543.6; W2=392.8; W3=990.1; W8=254.4; pool=480.3. B) Single values and median of percentage of GFP<sup>+</sup> (left panel) or total hepatocytes (right panel) with 1 or 2 nuclei in mice of experiment shown in A. Two-way Anova with Tukey's multiple comparisons test.

### **3.4. Analysis of the distribution of LV transduction in the liver lobule at different ages of treatment**

#### **3.4.1 The LV transduction preference switches from peri-central to peri-portal during growth**

It is known that position of hepatocytes in the liver lobule plays a major role in the determination of their metabolic functions (see 1.4.1). Therefore, we evaluated the distribution of LV-transduced hepatocytes in the liver lobule of mice treated at D1, W2 or W8 with LV.GFP at a dose of  $2.5 \times 10^{10}$  TU/kg. We annotated portal veins by identification of bile ducts next to them, while central veins by the lack of bile ducts in IHC images of livers. We identified peri-portal and peri-central areas by drawing a circle around portal and central veins (fig. 10A), with a radius that varied according to the dimension of the liver lobule at each age of analysis ( $r=187\mu\text{m}$  for mice analyzed at W1,  $r=200\mu\text{m}$  for mice analyzed at W3,  $r=225\mu\text{m}$  for mice analyzed at W9 or later). We measured the percentage of GFP<sup>+</sup> tissue in peri-central and peri-portal area and calculated the fold between these two values (fig. 10B). Mice treated as adults, showed a 1.8-fold higher percentage of GFP<sup>+</sup> tissue in peri-portal compared to peri-central area 1 week post treatment, while mice treated at D1 or W2 showed a more homogeneous distribution of GFP<sup>+</sup> area across the lobule. The higher percentage of LV<sup>+</sup> area in peri-portal compared to peri-central area in adult-treated mice may be due to either a transduction bias or to silencing of the transgene only in peri-central area. To test this hypothesis, we repeated this zonation analysis on mice treated with LV.GFP at  $2.5 \times 10^{10}$  TU/Kg by collecting livers at different time points over time. Lobules of newborn and 2-week-old treated mice showed a homogeneous distribution of GFP<sup>+</sup> area up to 12 weeks post treatment, indicating that the transgene was not silenced in peri-central area of adult mice. The peri-portal bias of GFP<sup>+</sup> tissue was observed in adult treated mice up to 1 year post treatment. To confirm this transduction bias, we also used immunofluorescence (IF) to analyze liver sections. We evaluated LV distribution in liver lobules of mice treated at D1, W2,



W3, W4 or W8, 3 to 7 days post-treatment at a dose of  $2.5 \times 10^{10}$  TU/Kg. Periportal and pericentral areas were identified by performing IF staining for glutamine synthetase (GS, marks peri-central hepatocytes) and cytokeratin-7 (CK7, marks bile ducts) and drawing an area around the marked cells with the same dimension used in IHC analysis (fig. 10 C). We measured the percentage of transduced tissue exploiting fluorescent reporters and calculated the fold between the peri-portal and peri-central areas (fig. 10D). We observed that this fold was below 1 (peri-central bias) for newborn and 2-week-old treated mice (median 0.72 and 0.67 respectively), and above 1 (peri-portal bias) for mice treated at 4 or 8 weeks of age (median 1.45 and 2.23 respectively), in multiple experiments, indicating a mild pericentral transduction bias for young-treated mice, and confirming peri-portal transduction bias previously observed for adult-treated mice. To further characterize position of

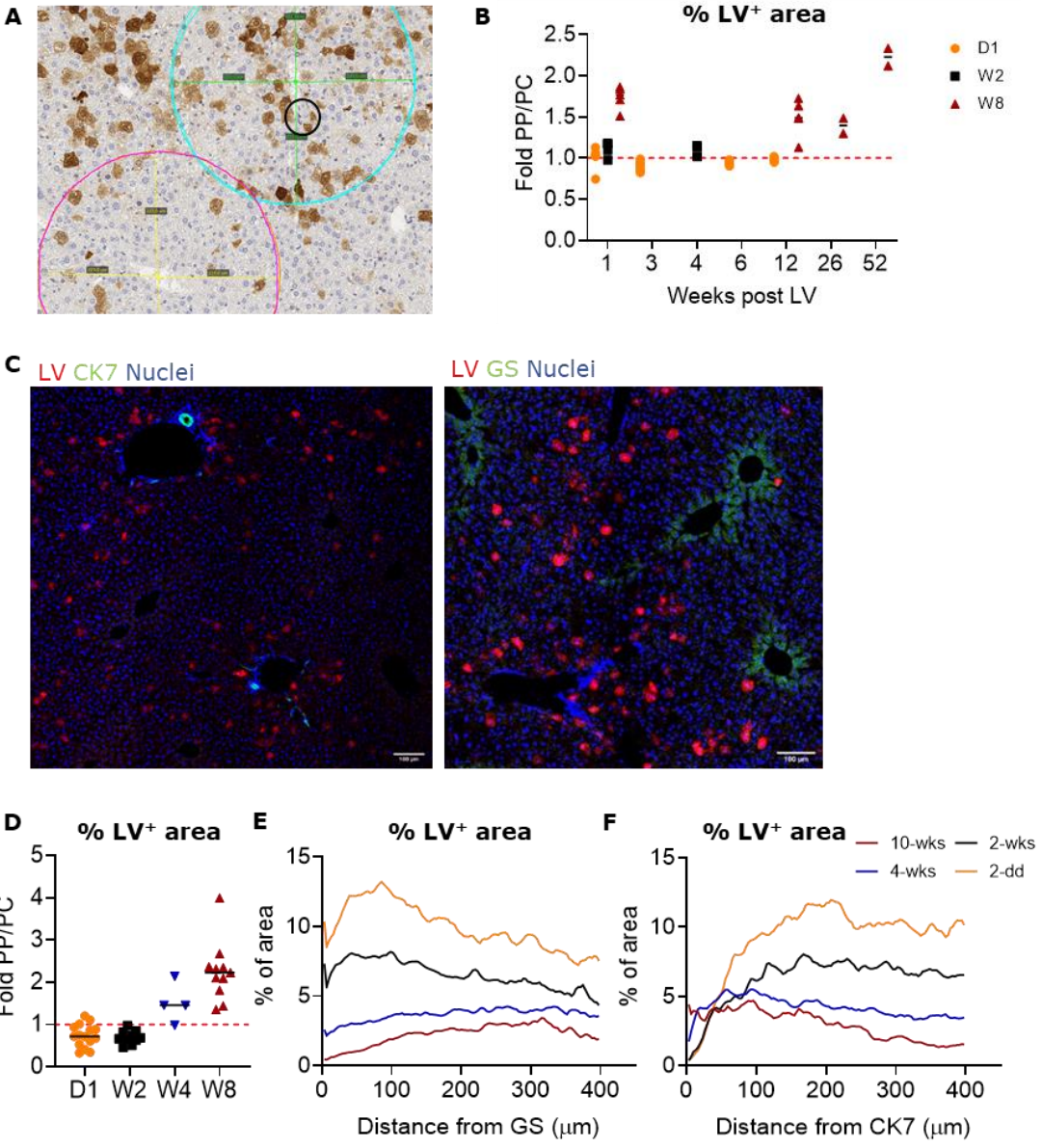




**Fig.10: Zonation of LV<sup>+</sup> hepatocytes in mice treated at different ages.** A) Representative images of immunohistochemistry analysis of LV transduction bias performed on mice treated with  $2.5 \times 10^{10}$  TU/Kg of LV.GFP at 8 weeks of age. After immunostaining with anti-GFP antibody (brown), portal veins are identified by the presence of bile ducts (black circle) next to them, while central veins are identified by absence of bile ducts next to them. Peri-portal (light blue circle) and peri-central (pink circle) areas are considered as the areas in a radius around portal and central veins respectively, whose dimensions depends on the age ( $r=187\mu\text{m}$  at W1,  $r=200\mu\text{m}$  at W3,  $r=225\mu\text{m}$  at W4 or later). B) Single values and median of fold between percentage of GFP<sup>+</sup> tissue in peri-portal (PP) vs. peri-central (PC) areas in mice treated with  $2.5 \times 10^{10}$  TU/Kg LV.GFP at D1, W2 or W8 and analyzed at different time points post-LV administration. For mice treated at D1: W1 n=5, W3 n=, W6 n=4, W12 n=3; for mice treated at W2: W1 n=4, W4 n=3; for mice treated at W8: W1 n=5, W12 n=5, W26 n=2, W52 n=2). C) Representative images of immunofluorescence analysis of LV transduction bias performed on mice treated with  $2.5 \times 10^{10}$  TU/Kg of LV.mCherry at 8 weeks of age. Immunostaining with anti-mCherry (red), anti-cytokeratin 7 (CK7, in green in the left image) and anti-glutamine synthetase (GS, in green in right image) has been performed to mark respectively transduced hepatocytes, bile ducts and central hepatocytes. Nuclei are marked in blue by Hoechst staining. Peri-portal areas have been identified in a radius around CK7<sup>+</sup> bile ducts, while central areas have been identified in a radius around GS<sup>+</sup> central hepatocytes. Dimension of radius is the same used in IHC analysis. Scale bar=100  $\mu\text{m}$ . D) Single values and median of fold of percentage of transgene positive area between peri-portal (PP) and peri-central (PC) areas in mice treated with  $2.5 \times 10^{10}$  of LV at D1 (n=15), W2 (n=10), W4 (n=4) or W8 (n=11). Red dashed line = 1. Pool of 3 independent experiments. One sample Wilcoxon test vs. 1 with Bonferroni's correction D1  $p=0.0104$ , W2  $p=0.008$ , W8  $p=0.004$ . E-F) Mean of percentage of transduced tissue as a function of the distance from GS<sup>+</sup> area (E) or CK7<sup>+</sup> area (F) in mice treated with  $2.5 \times 10^{10}$  of LV.mCherry at D1 (n=5), W2 (n=5), W4 (n=5) or W10 (n=5) and analyzed 3 days post LV administration.

transduced hepatocytes in liver lobule, we measured the percentage of LV<sup>+</sup> tissue at every point of liver lobule, according to the distance from CK7<sup>+</sup> or GS<sup>+</sup> area. Transgene-positive hepatocytes showed a peak in an area of 150  $\mu\text{m}$  around the GS<sup>+</sup> pericentral hepatocytes, in mice treated at D1 or W2, while they were few in close proximity to CK7<sup>+</sup> bile ducts and increased until reaching a plateau at a distance of 150  $\mu\text{m}$ . On the other hand, for older-treated mice there was a peak of LV<sup>+</sup> area in the first 150  $\mu\text{m}$  around bile ducts, followed by a decrease, while it increased moving away from GS<sup>+</sup> area for older treated mice (fig. 10E-F).

### **3.4.2 KC distribution in the liver lobule follows LV transduction bias**

We have shown that the lower transduction of hepatocytes obtained by treating mice as adults is due at least partially to an increased uptake by non-parenchymal cells, and mostly tissue-resident macrophages (see 3.3.1). Moreover, it has been recently published that distribution of KC across liver lobule changes during mouse growth, with a shift towards peri-portal area in adult mice that occurs around the age of weaning, and this zonation increase the ability of KC to capture pathogens that enters through the portal vein (Gola *et al*, 2021). For these reasons, we decided to investigate the possible role of KC in determining the transduction bias in LV-treated mice. First, we investigated KC distribution in liver lobule. We measured the

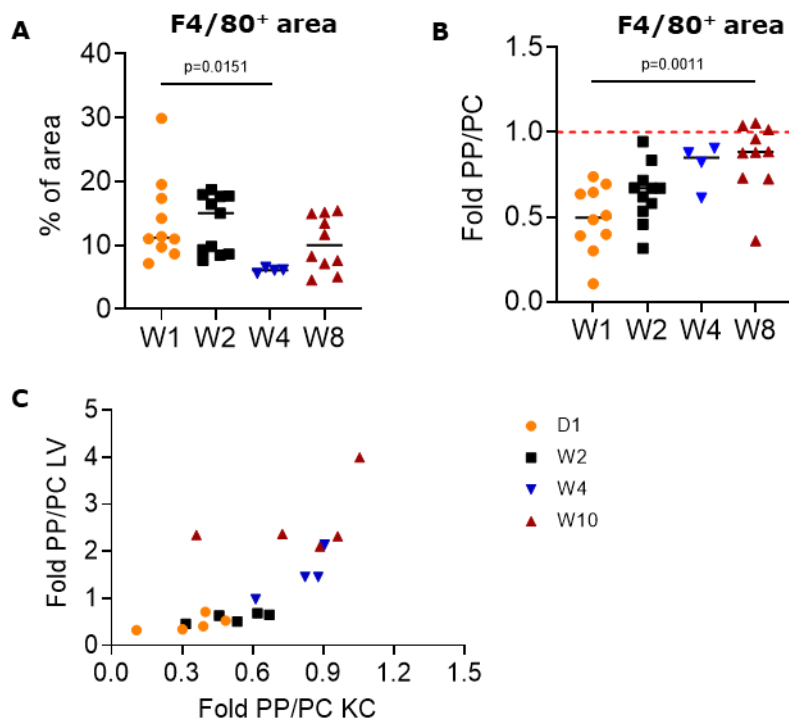


**Fig.11: KC distribution in the liver lobule.** A) Single values and median of percentage of liver tissue marked by F4/80 immunostaining in mice of 1 (n=10), 2 (n=11), 4 (n=4) or 8 (n=10) weeks of age. Pool of 2 independent experiments. Kruskal-Wallis test with Dunn's multiple comparisons tests vs. W1. B) Single values and median of fold between percentage of transduced tissue in peri-portal (PP) vs. peri-central area identified as in fig. 11, in mice of 1, 2, 4 or 8 weeks of age (same as A). Kruskal-Wallis test with Dunn's multiple comparisons tests vs. W1. One sample Wilcoxon test vs. 1 with Bonferroni's correction D1 p=0.008, W2 p=0.004. C) Correlation between fold of percentage of marked tissue in peri-portal (PP) vs. peri-central (PC) area by immunostaining for mCherry transgene (LV) or F4/80 (KC) in mice treated with  $2.5 \times 10^{10}$  TU/Kg LV.mCherry at D1 (n=5), W2 (n=5), W4 (n=4) or W10 (n=5). Spearman's correlation test r:0.7561; p=0.0002.

percentage of F4/80<sup>+</sup> tissue in per-central and peri-portal area, identified as previously described by IF. We observed a similar amount of KC in mice at all ages, expressed as percentage of area marked by F4/80 immunostaining (fig. 11A). Our data suggest that mice in the first week of life have a higher concentration of KC in peri-central compared to peri-portal area, that persist also in the 2<sup>nd</sup> week of life, but later on (4<sup>th</sup> and 8<sup>th</sup> week of life) there is a shift towards the peri-portal area that leads to a more homogenous distribution of KC (fig. 11B). Interestingly, the change in KC distribution parallels the observed switch of transduction bias from the peri-central area in young mice to the peri-portal area into adult mice. Indeed, performing the zonation analysis of transduced hepatocytes and KC distribution in the lobule in mice treated with  $2.5 \times 10^{10}$  TU/Kg of LV.mCherry at different ages, we can notice a strong correlation between LV transduction bias and KC zonation (fig 11C).



**Fig.12: LV transduction bias in KC-depleted adult livers.** A) Representative images of liver of adult mouse treated with 2 doses of clodronate liposomes (left) or PBS liposomes (right) 48 and 24 hours before IF analysis. In red F4/80 immunostaining to identify KC, in blue nuclei stained with Hoechst. Scale bar =100µm. B) Single values and median of quantification of percentage of F4/80+ area in liver of adult mice treated with two doses (48 and 24 hours before analysis) of clodronate liposomes (n=6), PBS liposomes (n=3) or untreated (n=3). C) Scheme of the experiment: adult wt mice treated with  $2.5 \times 10^{10}$  TU/Kg LV.GFP after 2 doses (48 and 24 hours before LV administration) of clodronate liposomes (n=6), PBS liposomes (n=6) or no pre-treatment (n=6), and analyzed 7 days post LV.D) Single values and median of percentage of transduced peri-portal (PP), peri-central (PC) or total liver area. Kruskal-Wallis test with Dunn's multiple comparisons test vs. clodronate liposomes group. E) Single values and median of fold of percentage of transduced area between PP and PC area. Kruskal-Wallis test with Dunn's multiple comparisons test vs. Clodronate liposomes group.

showed a lower percentage (3.2-fold) of GFP<sup>+</sup> tissue compared to LV-only group, probably determined by the increase in macrophages concentration (fig. 12D). Surprisingly, we observed no increase in percentage of GFP<sup>+</sup> tissue in peri-central area in KC-depleted mice compared to control groups, but a 4.9-fold increase in peri-portal area compared to LV-only group and 15.4-fold increase compared to PBS-liposomes group. This increase also determined a stronger peri-portal transduction bias that in KC-depleted mice was 8.9-fold higher compared to LV-only group and 10.5-fold higher compared to PBS-liposomes group (fig.12E). These data suggest that LV phagocytosis by tissue resident macrophages is not the cause of the preferential transduction of peri-portal hepatocytes in adult mice, and that their depletion does not improve transduction of the peri-central area.

### 3.5. Multiple transduction of hepatocytes

#### 3.5.1 The frequency of multiple-transduction events is lower in adult-treated than young-treated mice

We have shown that administration of LV in young mice leads to a higher percentage of transduced liver parenchyma compared to adult-treated mice, but the percentage of transgene-positive area observed is still a minor part of the total tissue (about 10%). We therefore expect to have a single LV for each transduced hepatocyte, and for this reason the observation of hepatocytes transduced at multiple copies might be an indication of a subset of hepatocytes that are more prone to be transduced. Furthermore, differences in percentage of multiple-transduced hepatocytes between mice treated at different ages might contribute to explain differences in transgene output. To evaluate the presence of hepatocytes transduced independently by multiple LV we administered a mix of 3 LV expressing different fluorescent reporters (GFP, mCherry or BFP) in newborn, 2-week-old or 8-week-old

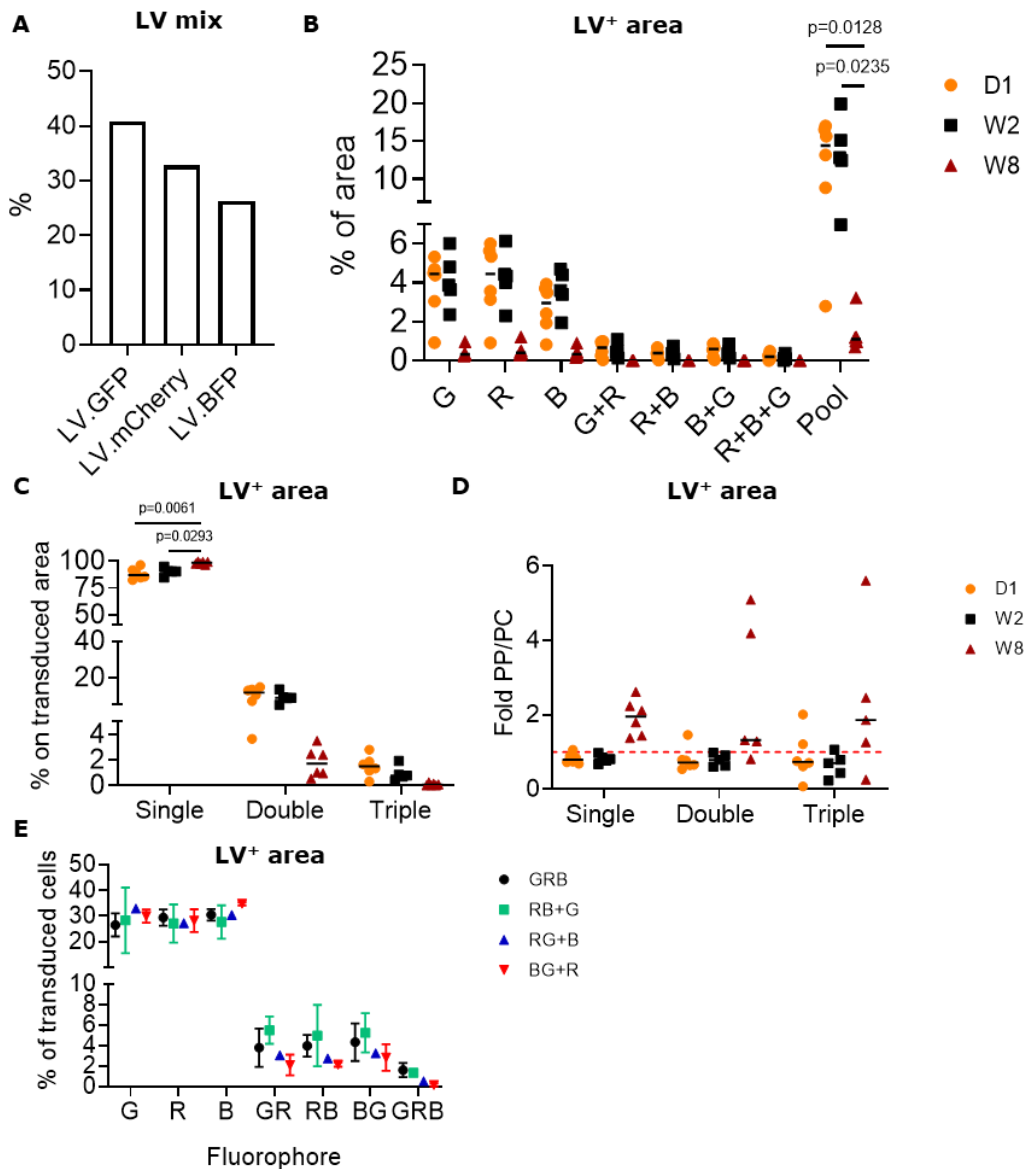


**Fig.13: Evaluation of multiple transductions of hepatocytes.** A) Mean of percentage of each LV in the mix of LV.GFP, LV.mCherry and LV.BFP. Percentage, calculated based on results of FACS analysis of 293T cells transduced with LV mix at MOI 0.1, 0.05 or 0.01. B) Single values and median of percentage of tissue area marked in green (G), red (R), blue (B) and the combination of 2 or 3 fluorescent protein, or by any color (Pool) in mice treated with  $2.5 \times 10^{10}$  TU/Kg of the mix of LV.GFP, LV.mCherry and LV.BFP (same as A) at D1 (n=6), W2 (n=5) or W8 (n=6). Kruskal-Wallis test with Dunn's multiple comparisons test for pool group. C) Single values and median of percentage of transduced area marked by 1 (single), 2 (double) or 3 (triple) fluorescent reporters (same experiment as B). Kruskal-Wallis test with Dunn's multiple comparisons test on single-positive area. D) Single values and median of fold of percentage of single, double, or triple-positive area in peri-portal (PP) vs. peri-central (PC) area (same experiment as B and C). One sample Wilcoxon test vs. 1 with Bonferroni's correction. E) Mean and standard deviation (SD) of percentage of cells positive for GFP (G), mCherry (R) or BFP (B) or combination of 2 or 3 fluorescent reporter in mice treated with  $2.5 \times 10^{10}$  TU/Kg of the mix of 3 LV, or by the mix of 2 LV and the 3<sup>rd</sup> injected independently, at D1 and analyzed 1 week post LV administration. GRB n=4, RB+G n=3, RG+B n=1, BG+R n=3.

mice to determine the presence of hepatocytes expressing 1, 2 or 3 fluorescent markers. LV were mixed before injection, thus we controlled the composition of the mix by transducing 293T cells in vitro at multiplicity of infection (MOI) 0.1, 0.05 or 0.01 and analyzed them at FACS. We confirmed that the mix between the 3 LV was acceptably balanced, with 40% of LV.GFP, 33% of LV.mCherry and 27% of LV.BFP (fig. 13A). We collected livers 1 week post LV administration and measured the percentage of green, red, and blue area, and the percentage of area positive for the combination of 2 or 3 colors. We observed that the percentage of transduced area was higher in mice treated at D1 and W2 (13% of total liver area), while 9-fold lower in adult-treated mice (fig. 13B) as expected from the data shown above (see fig. 8F). Moreover, we observed a good balance between the percentages of area positive for each color, which was around 4% for each of them, confirming the balanced composition of the LV mix. By measuring the percentage of transduced area that expresses one, two or three fluorescent proteins, we observed that mice treated at D1 or W2 had 89% of the transduced area marked by a single color, 10% marked by two colors and 1% marked by three colors. Adult-treated mice, on the other hand, had on average 98% of transduced area positive for one color, 1.9% positive for two and only 0.1% positive for three colors (fig. 13C). These data show that administration of LV in young mice leads to a higher percentage of hepatocytes with multiple copies of vector compared to adult-treated mice. We then evaluated the distribution of single and multiple-transduced hepatocytes in the liver lobule. Newborn and 2-week-old treated mice showed a ratio of percentage of transduced tissue between peri-portal and peri-central area lower than 1, for single-, double- and triple-transduced area. In adult mice the ratio peri-portal to peri-central was on average higher than 1 for single, double, and triple-transduced hepatocytes, thus confirming the transduction bias described before also for multiple-transduced hepatocytes (fig. 13D). To exclude that pre-mixing of LV before injection can create aggregates between viral particles that increases the probability of entry of more than 1 LV in a single hepatocyte, we injected in newborn mice either the mix of 3 LV or a mix of 2 LVs and immediately after the 3<sup>rd</sup> was administered separately. If pre-mixing creates aggregates of the different LVs, increasing the probability of having multiple transduction events, we would find reduced percentage of triple-transduced hepatocytes in those groups in which one vector was missing from the mix and, by contrast, these groups would show a higher number of hepatocytes transduced by the two pre-mixed LV compared to the combination with the LV injected separately. By analyzing livers one week post administration of the various combination of the 3 LV, we observed that in all the groups the percentages of double-positive hepatocytes

transduced with one vector present in the mix and the one administered separately were similar to the percentage of the hepatocytes transduced by the two vectors pre-mixed together. Moreover, the percentages of double and triple transduced hepatocytes were similar in mice injected with mix of 2+1 LV or mix of 3 LV, indicating that pre-mixing the LV did not impact on the percentage of observed multiple-transduced hepatocytes (fig. 13E).

### 3.5.2. LV transduction does not induce a proliferative advantage in hepatocytes

To evaluate proliferation potential of hepatocytes transduced by one or multiple LV, we administered the mix of 3 LV in newborn mice, and then collected livers 1-, 3- or 6-weeks post-treatment to measure cluster dimension and composition over time. We observed an increase in the percentage of transduced area between W1, W3 and W6, suggesting a mild proliferative advantage of transduced hepatocytes compared to non-transduced ones, or a preferential transduction of those

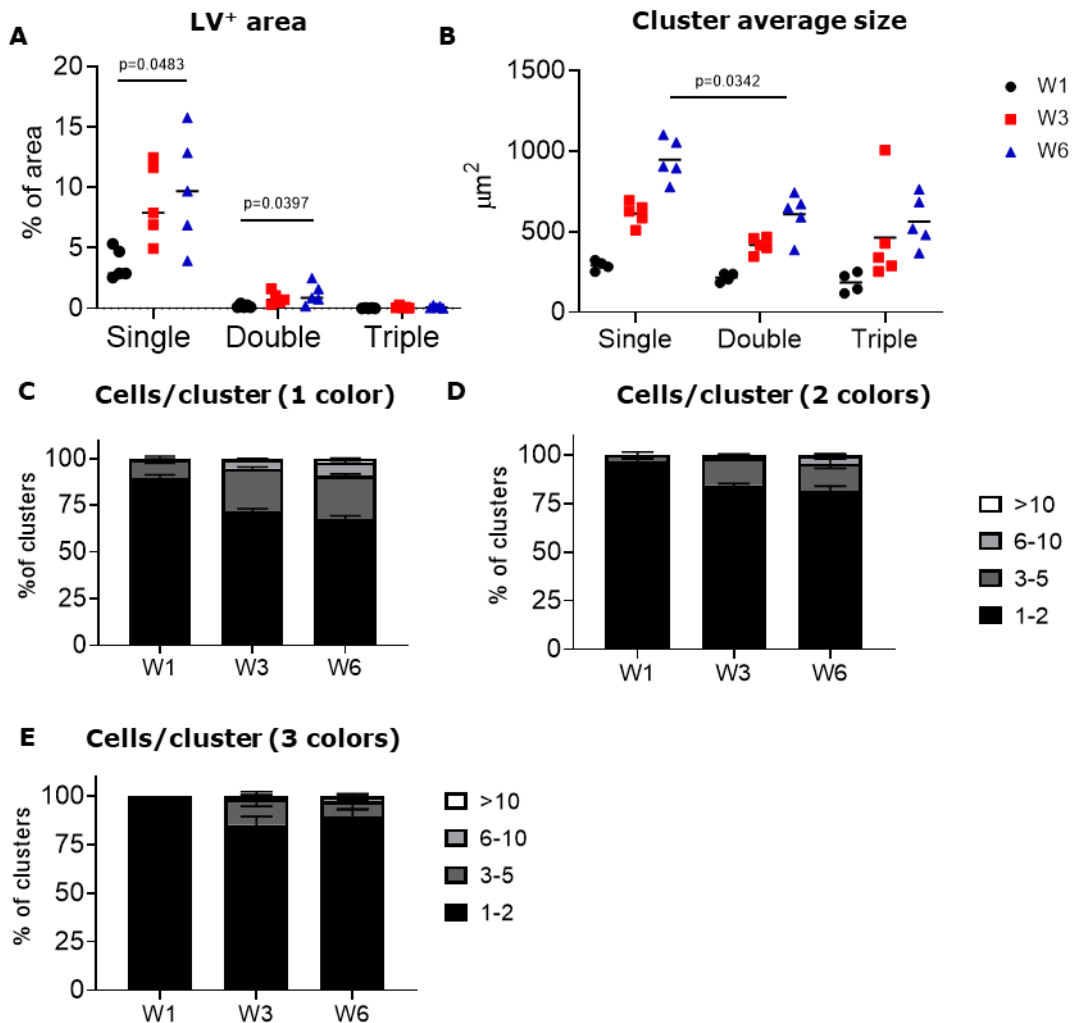


**Fig.14: Analysis of the proliferation of multiple transduced hepatocytes.** A-B) Single values and median of percentage of total liver tissue (A) positive for one, two or three fluorescent reporters and cluster average size (B) in mice treated with  $2.5 \times 10^{10}$  TU/Kg of a mix of 3 LV (LV.GFP, LV.mCherry, LV.BFP) at D1 and analyzed 1 (n=5), 3 (n=5) or 6 (n=5) weeks after treatment. Kruskal-Wallis test with Dunn's multiple comparison test in A. Friedman's test with Dunn's multiple comparison's test in B. C-D-E) Mean and SEM of the percentage of clusters positive for 1 (C), 2 (D) or 3 (E) fluorescent reporters and made of 1-2, 3-5, 6-10 or >10 cells. Number of cells per clusters have been calculated by measuring dimension of each cluster and dividing by the average size of hepatocytes at that age ( $W1=250 \mu\text{m}^2$ ,  $W3=350 \mu\text{m}^2$ ,  $W6=450 \mu\text{m}^2$ ).

hepatocytes that are proliferating (fig. 14A). We also observed an increase of cluster average size, indicating proliferation of transduced hepatocytes, as expected, but this increase resulted to be less evident for hepatocytes expressing two or three transgenes (fig. 14B). Indeed, by looking at cluster composition we counted that 25% of single-color cluster are generated by proliferating hepatocytes, also showing clusters with more than 10 cells at week 6, while the percentage of proliferating multi-color clusters was lower, and clusters appeared to be smaller, both for double- and triple-transduced hepatocytes (fig. 14C). These observations suggest that transduction did not induce a proliferative advantage *per se*. Moreover, proliferation of transduced hepatocytes was confirmed to be similar to that observed in non-transduced Confetti hepatocytes.

### **3.6. Role of pseudotype, promoter and integration on gene therapy efficiency at different ages of treatment**

In the experiments described above we used an integration-competent VSV-G pseudotyped LV, with transgene expression controlled by the hepatocyte-specific promoter ET. In this setting, we observed differences in transduction efficiency of liver parenchyma among mice treated at different ages, paralleled also by different level of transgene output when using LV expressing hFIX. Moreover, we observed a mild peri-central transduction bias in young-treated mice and a peri-portal transduction bias in adult-treated mice. Transduction properties and transgene expression are also known to be dependent on the pseudotype of LV or its promoter, thus we repeated the experiments using LV expressing hFIX or mCherry under the control of ET promoter and pseudotyped with Baculovirus-derived GP64 glycoprotein, or VSV-G pseudotyped LV expressing hFIX or GFP under the control of the human alpha 1-antitrypsin (hAAT) hepatocyte-specific promoter, coupled with hepatocyte control region (HCR) enhancer. We observed that transduction with both GP64-pseudotyped LV (fig. 15A) and LV with HCR/hAAT promoter (fig.15B) resulted in similar age-related differences to those we observed for VSV.G pseudotyped LV with the ET promoter, i.e. similar percentage of transgene-positive area for mice treated at D1 and W2, and a lower transduction efficiency in adult-treated mice. These data



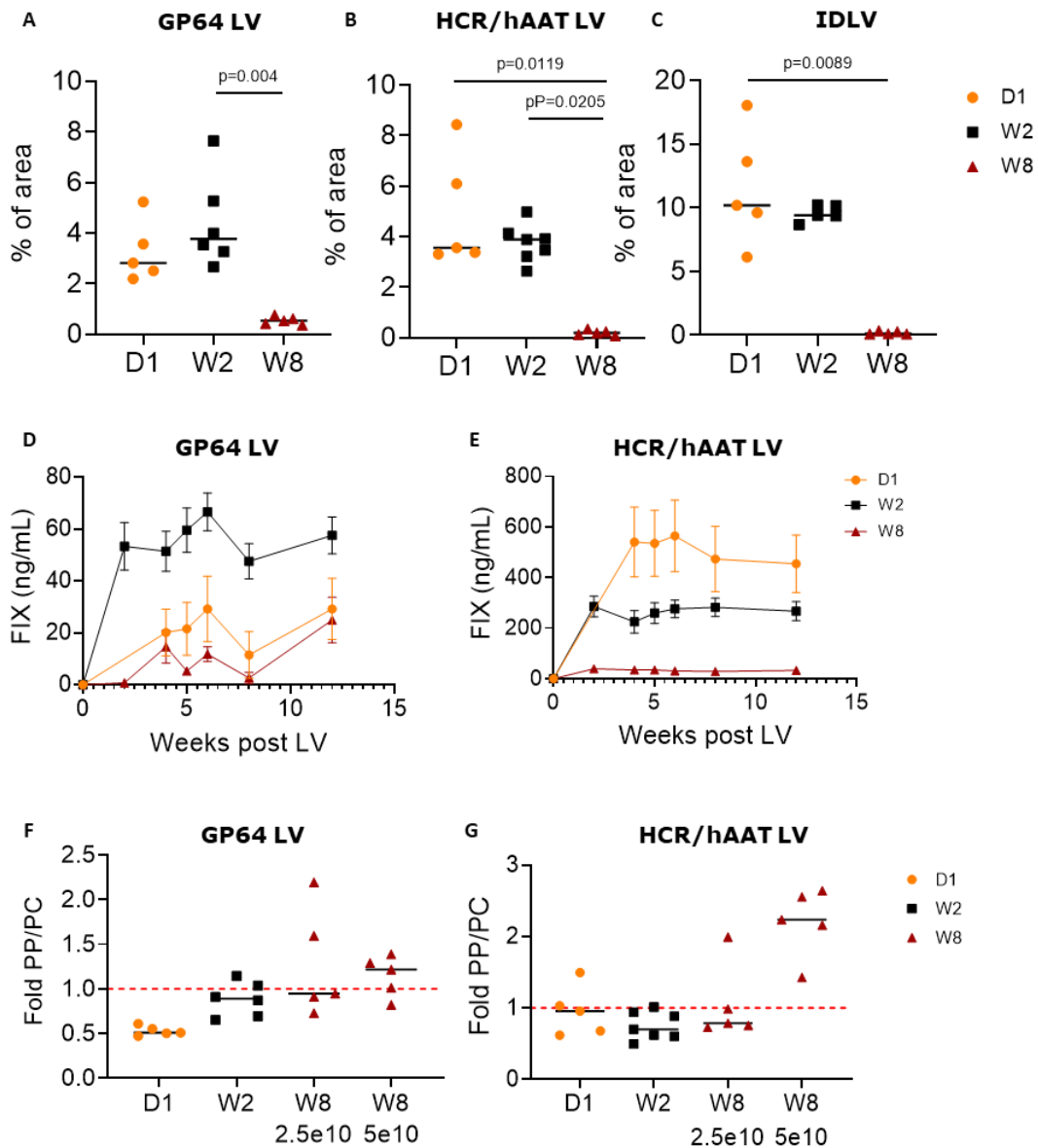


**Fig.15: Efficiency of gene therapy by LV containing different envelope proteins or promoters.** A-B-C) Single values and median of percentage of transgene-positive area in mice treated with  $2.5 \times 10^{10}$  TU/Kg of GP64-pseudotyped LV.ET.mCherry (A), VSV-G-pseudotyped LV.HCR/haAT.GFP (B) or VSV-G-pseudotyped IDLV.ET.mCherry (C) at D1 ( $n=5$  for GP64 LV,  $n=5$  for LV.HCR/haAT,  $n=5$  for IDLV), W2 ( $n=6$  for GP64 LV,  $n=7$  for LV.HCR/haAT,  $n=5$  for IDLV), or W8 ( $n=5$  for GP64 LV,  $n=5$  for LV.HCR/haAT,  $n=5$  for IDLV) and analyzed 3 days post-LV administration. Kruskal-Wallis test with Dunn's multiple comparisons test. D-E) Mean and SEM of hFIX plasma concentration in mice treated with i.v. administration of  $2.5 \times 10^{10}$  TU/Kg LV.ET.hFIX pseudotyped with GP64 (D) or LV.HCR/haAT.hFIX pseudotyped with VSV-G (E) at D1 ( $n=4$  for GP64 LV,  $n=10$  for LV.HCR/haAT), W2 ( $n=7$  for GP64 LV,  $n=12$  for LV.HCR/haAT), or W8 ( $n=5$  for GP64 LV,  $n=10$  for LV.HCR/haAT). In B) pool of 2 independent experiments. F-G) Single values and median of fold of percentage of transgene positive area between peri-portal (PP) and peri-central (PC) areas in mice treated with  $2.5 \times 10^{10}$  TU/Kg or  $5 \times 10^{10}$  TU/Kg of GP64-pseudotyped LV.ET.mCherry (F) or VSV-G-pseudotyped LV.HCR/haAT.GFP (G) at D1 ( $n=5$  for GP64 LV,  $n=5$  for LV.HCR/haAT), W2 ( $n=6$  for GP64 LV,  $n=7$  for LV.HCR/haAT) or W8 ( $n=5$  for GP64 LV,  $n=5$  for LV.HCR/haAT, at each dose). Red dashed line = 1. One sample Wilcoxon test vs. 1 with Bonferroni's correction.

indicate that the lower percentage of transgene-positive tissue area observed in adult-treated mice is not dependent on LV pseudotype or promoter. Moreover, the same pattern was observed using a VSV-G pseudotyped integrase-defective LV (IDLV) expressing the fluorescent reporter mCherry under the control of ET promoter, suggesting that integration of the viral genome is not a limiting step in transduction of hepatocytes in adult mice (fig. 15C). GP64-pseudotyped LV.ET.hFIX also showed a pattern of expression of the transgene in mice treated at different ages very similar to the one observed using a VSV-G pseudotyped LV, with the highest levels of hFIX observed by administering LV at W2, intermediate levels at D1 and the lowest at W8 (fig. 15D). On the other end, by changing the promoter from ET to HCR/hAAT, we observed that newborn-treated mice reached a higher level of transgene output compared to 2-week-old treated mice, while adult-treated mice showed one more time the lowest levels of hFIX (fig. 15E). These data indicate that the choice of promoter has an impact on the transgene output that can be obtained by treating mice at different ages of life. Lastly, we observed a slight peri-central transduction bias in young-treated mice by administering both GP64-pseudotyped LV.ET.mCherry and VSV.G pseudotyped LV.HCR/hAAT.GFP, while the peri-portal bias became apparent in adult-treated mice only by increasing the dose of LV administered (fig. 15F-G), suggesting that when transgene-positive hepatocytes are few, it is more difficult to properly identify their distribution in the lobule.

### **3.7. LV transduce the same hepatocyte subset in newborn and 2-week-old mice**

The differences in transgene output observed in young-treated mice by using different promoters might suggest that different hepatocyte subpopulations are targeted by administering LV at D1 or W2. These two hepatocyte subpopulations could have different metabolism and thus promoter activity. To test this hypothesis, we set out to evaluate if, by administering two LV expressing different fluorescent reporters in the same mouse at D1 and W2, we detect multiple-transduced hepatocytes. If so, it would mean that the hepatocytes targeted at these time points are similar, otherwise the absence of double-positive hepatocytes might indicate that we reached different subpopulations. To this end, we analyzed the presence of anti VSV-G immunoglobulin M (IgM) and G (IgG) from blood samples of mice treated at D1 or W6 (as positive control), to determine if it was induced an immune response against the administered LV that would prevent effective LV re-administration. We detected a transient IgM response in mice treated as adults, as expected, while levels

of IgM 2- and 9-weeks post LV administration in newborn-treated mice were comparable to untreated mice (fig. 16A). IgG were present at low level in serum of adult-treated mice already 3 days post-treatment, and increased 2 and 9 weeks after, as expected while they were absent in newborn-treated mice at all time point

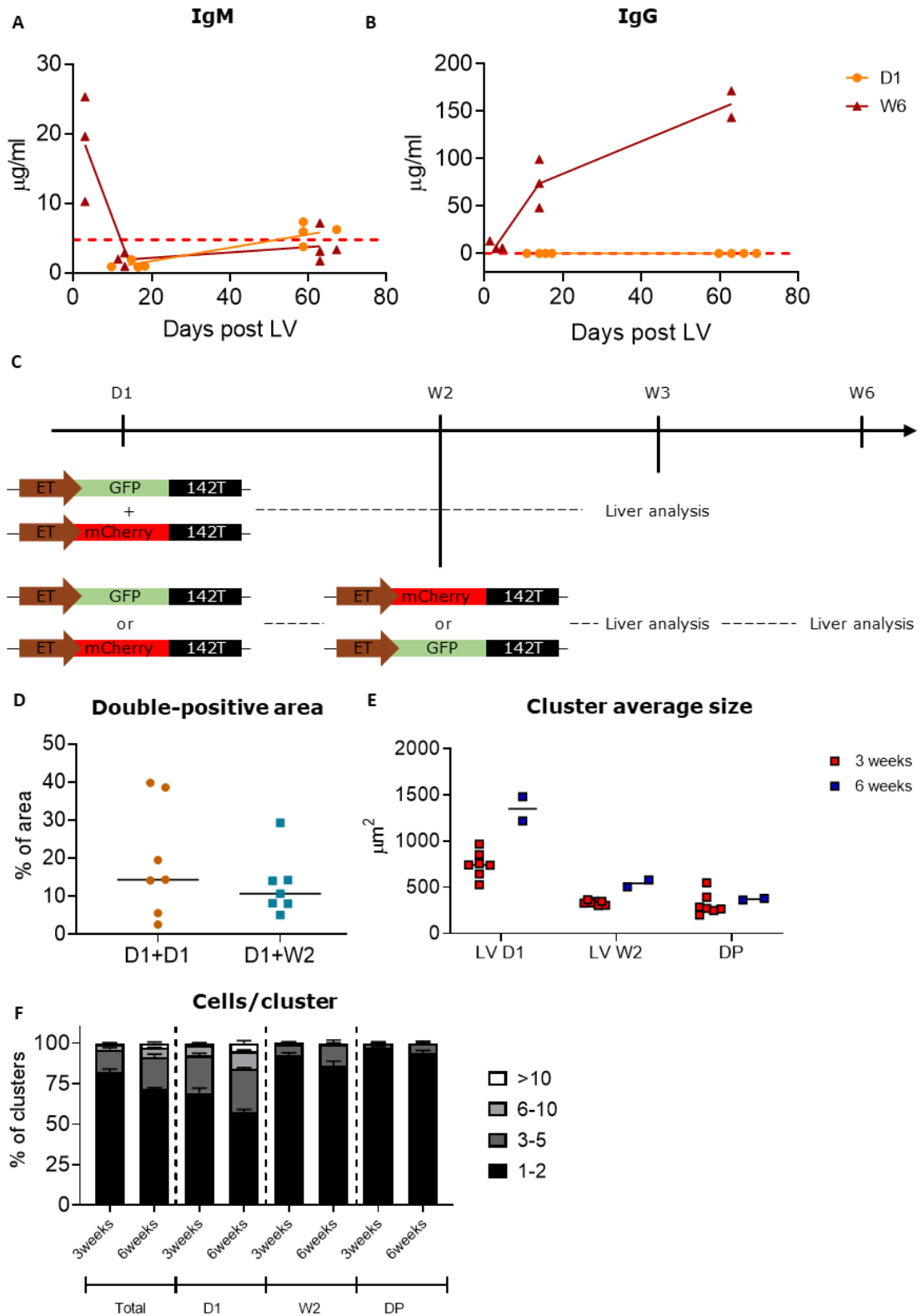


**Fig.16: Sequential administration of different LV at two different ages during growth.** A-B) Single values and mean of IgM (A) and IgG (B) antibodies detected in plasma of mice treated with LV at D1 or W6 and analyzed 3 (D1 n=0; W6 n=3), 14 (D1 n=3; W6 n=3) and 64 (D1 n=3; W6 IgM n=4 IgG n=2) days after treatment by ELISA. Red dashed line represents UT value (n=1). C) Scheme of the experiment: mice treated with LV.mCherry and LV.GFP ( $2.5 \times 10^{10}$  TU/Kg each) administered together at D1 (D1+D1) or administered separately at D1 and W2 (D1+W2), analyzed at W3 (D1+D1 n=7, D1+W2 n=7) or W6 (D1+W2 n=2). D) Single values and median of percentage of mCherry<sup>+</sup> area marked also by GFP in livers analyzed at W3. Mann-Whitney test. E) Single values and median of average size of clusters generated by LV administered at D1 (LV D1) or W2 (LV W2) or both (double positive, DP). F) Mean and SEM of the percentage of clusters positive for the fluorescent reporter expressed by the vector administered at D1, W2 or both, and made of 1-2, 3-5, 6-10 or >10 cells.

analyzed (fig. 16B). These data indicate that newborn mice do not develop a humoral immune response against LV particles, thus allowing administration a second dose of LV. Therefore, to evaluate if by administering LV at day 1 or week 2 we reach different hepatocyte subpopulations, we administered in the same mice LV expressing GFP or mCherry at D1 and W2, switching vectors in different experiments, and used newborn mice administered with both vectors at the same time as controls. We collected livers at W3 and W6 of age to evaluate multiple transductions and monitor proliferation of single and multiple transduced hepatocytes (fig. 16C). We measured the percentage of clusters mCherry<sup>+</sup> that were positive also for GFP 1 week after the administration of the last dose of LV, and observed about 15% of double-positive clusters, with no differences between mice treated with the two LVs at the same time or at D1 and W2 (fig. 16D), indicating that the targeted hepatocytes are likely the same at the two ages. We then measured average size of clusters formed by hepatocytes transduced at D1, W2 or double-transduced hepatocytes. We noticed that at W3 the clusters generated by hepatocytes transduced at D1 are already larger than those generated by hepatocytes transduced at W2, as also shown above (see fig. 5). Moreover, only in the former group there was an increase of cluster average size between W3 and W6 (fig. 16E). By looking at cluster composition, we observed the presence of clusters with >5 cells at W3 for LV administered at D1, and a further expansion at W6 with generation of clusters made of more than 10 cells. Instead, clusters from hepatocytes transduced at W2 were mainly made of 1-2 cells, with only a small percentage with more than 2 cells both at W3 and W6 (fig. 16F). Double-positive clusters showed the lower rate of proliferation, with no increase in cluster average size and a very small percentage of clusters with more than 2 cells at W3 and W6. These data suggest that upon administration at D1 or W2 LV transduces the same hepatocyte subset, as also supported by the observation that at these time points of treatment we observe the same peri-central transduction bias. Moreover, we confirmed also in this setting that hepatocytes marked in the newborn liver generate larger clusters compared to those

marked at W2, and that this pattern is similar for LV-transduced and non-transduced hepatocytes as shown in the Confetti mouse strain.

### 3.8. Physiological protein expression in the growing liver

As mentioned above, the transgene output in mice transduced as newborns with LV.hFIX has a different pattern compared to mice treated at an older age. While mice treated at W2 or older show a stable concentration of hFIX in plasma over time, in newborn-treated mice we observed a 4-fold increase between W2 and W6, followed by a slight decrease and stabilization of the output (see fig. 8B). Given the important physiological changes that happen in the liver during growth, we wondered whether transgene output pattern reflect these changes, and therefore can be considered as physiological, or it is an effect specific of the transgene. Thus, we investigated mRNA and protein levels of 3 genes normally expressed by hepatocytes in mice at different ages. In particular, we measured LDL-R, albumin and PCSK9 mRNA and protein

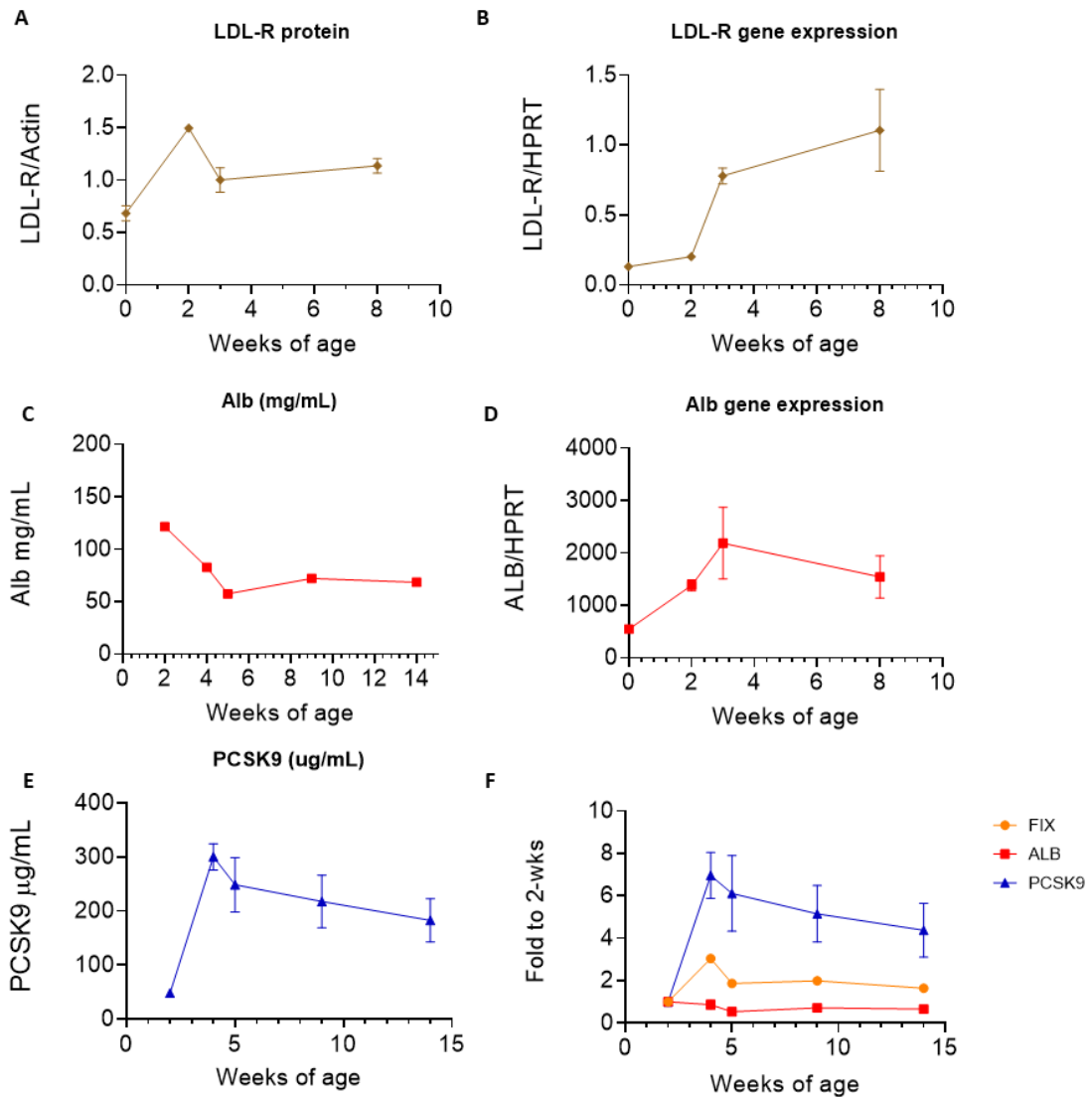


**Fig.17: Physiological expression of endogenous proteins by hepatocytes during growth.** A) Mean and SEM of LDL-R protein levels in total liver of mice collected as newborns (n=5) or at 2 (n=5), 3 (n=4) or 8 (n=4) weeks of life, quantified by Western blot. B-D) Mean and SEM of LDL-R and Albumin mRNA levels in total livers of mice in A and expressed as fold on HPRT mRNA levels. C-E-F) Mean and SEM of concentration of albumin (C-F), PCSK9 (E-F) and FIX (F) in plasma samples of mice treated at D1 with  $2.5 \times 10^{10}$  TU/Kg LV.hFIX and collected at 2, 4, 5, 9 or 14 weeks of life (n=8).

expression in the liver or in the blood over time. For all these 3 analyzed proteins we observed changes in both mRNA and protein levels over time, indicating metabolic changes in hepatocytes during growth. In particular, LDL-R show a pattern of protein expression that resemble what we observed for the hFIX transgene, with an initial increase in the first 2 weeks, followed by a slight drop and a stabilization of the total amount of protein (fig. 17A). On the other hand, mRNA levels showed a different pattern, with low expression in the first 2 weeks of life, followed by an increase between W2 and W3 (fig. 17B). Also albumin concentration in blood showed a decrease greater than 2-fold between W2 and W5, followed by a stabilization of the amount of protein (fig. 17C). But also for albumin we observed a different pattern for mRNA in total liver, with a 4-fold increase between birth and W3, followed by mild drop (fig. 17D). PCSK9 protein plasma levels resulted to be low in 2-week-old mice, then increase of 6-fold at W4, and then decrease slightly, similarly to what has been observed for hFIX (fig.17E). Taken together, this data suggest that the pattern of transgene output observed in LV.hFIX-treated newborn mice may be due to general metabolic changes occurring in hepatocytes during growth that influence expression and production of hFIX transgene resulting in the observed pattern over time (fig.17F).

## **4. Discussion**

### **4.1 Hepatocyte proliferation rate during growth and homeostasis**

Despite multiple studies have investigated proliferation of hepatocytes in adult liver during homeostasis or in response to damage, to our knowledge little is known about tissue dynamics in newborn mice. Here, we report a model of proliferation of hepatocytes during post-natal liver growth exploiting the Confetti mouse strain, in which we mark hepatocytes by activating the recombination of the Confetti locus in newborn (1-day old), juvenile (2-week-old) or adult (8-week-old) mice and then monitor the number and dimension of clusters generated by marked hepatocytes. We observed that the increase in cluster average size is higher in newborn-activated mice (8-fold in the first 6 weeks of life and 17-fold in 1 year) compared to mice activated at 2 weeks of age (2- and 4- fold at 6 weeks and 1 year post treatment respectively) and 8 weeks of age (1.5-fold between W14 and Y1), indicating a progressive reduction in the proliferation rate of hepatocytes over time. This reduction is also confirmed by the observation that in newborn-activated mice the increase observed during growth (first 6 weeks of life) is much higher than the one observed in the homeostatic phase. Moreover, in mice activated at all ages we observed only a minority of clusters that were made of more than 2 cells, thus deriving from proliferating hepatocytes. We can therefore speculate that proliferating hepatocytes in the newborn liver generate clusters of cells, some of which are able to duplicate themselves, but at a progressively slower rate. The low percentage of proliferating clusters in juvenile-activated mice suggests that a fraction of the daughter cells generated by a single proliferating hepatocyte in the newborn liver is then able to duplicate themselves, and these cells will do a low number of cycles in the rest of the mouse life, as it is suggested by the small dimension of the clusters generated from that time onwards. Interestingly, in newborn-activated mice the fraction of expanding clusters (25%) is stable over time, indicating that quiescent hepatocytes do not start to proliferate later in time, but that at the end of the growth phase the proliferating clusters may occupy 90% of the liver tissue. The active proliferation of only a fraction of hepatocytes in the first week of life has been confirmed also exploiting EdU incorporation, which marked 28% of hepatocytes between post-natal day 3 and day 5. Our work provides the first, to our knowledge, description of a relatively oligoclonal composition of the adult mouse liver originating from a small subset of proliferating hepatocytes. These observations are of particular

interest for the application of liver directed *in vivo* gene therapy. Indeed, the therapeutic genetic modification, whether obtained by gene transfer or gene editing, needs to be maintained over physiological post-natal growth. Thus, it is necessary to target the specific hepatocytes subset responsible for these processes, to ensure durability of the gene therapy. Otherwise, inefficient modification of this crucial subpopulation of hepatocytes may lead to progressive reduction or loss of the therapeutic effect.

#### **4.2. Proliferation of transduced hepatocytes**

One of the aims of our study was the investigation of the consequences of liver growth on maintenance of LV-transduced hepatocytes and its effect on transgene output over time. We showed in multiple settings that hepatocytes transduced in newborn mice proliferate locally and generate clusters of cells expressing the transgene. This evidence has been also obtained at different ages. More importantly, proliferation of transduced hepatocytes did not substantially differ to that of untransduced mice, with the generation of large clusters over time from a fraction of proliferating hepatocytes in newborn-treated mice, and the formation of smaller clusters in mice treated at 2 or 8 weeks of age. Therefore, we consider that transduction does not induce an overall proliferative advantage to hepatocytes, even in long-term follow up (up to 1 year). This observation is reassuring, considering the potential concern of insertional mutagenesis in gene therapy based on integrating vectors. Moreover, we showed that hepatocytes transduced by multiple vector particles proliferate less compared to single-transduced hepatocytes, further confirming that LV transduction does not stimulate proliferation *per se*. This reduced proliferation of multiple transduced cells might be a consequence of multiple factors: on one hand, being multiple-transduction a rare event, it is very unlikely that two clusters expressing the same couple of fluorescent reporters are close to each other and merge after proliferation, which could be a more common event for single-transduced clusters and might increase the percentage and dimension of proliferating clusters; another explanation could be that the subset of hepatocytes that are more prone to be transduced are not those that generate the biggest clusters over time; lastly, multiple-transduction events might actually impair proliferation. This last hypothesis might be tested by exploiting models of liver damage, to assess whether this subset of hepatocytes can be recruited to repair liver parenchyma in a different experimental setting. However, we consider unlikely that LV transduction, at the tested doses, induce a permanent impairment in proliferation, given the formation of large clusters that we observed in multiple experiments. Indeed, in



AlbCreERT2/Confetti mice treated with LV.BFP we observed a modest increase in the percentage of transduced proliferating clusters and their dimension compared to non-transduced ones. Since, however, transduction does not seem to induce a proliferative advantage as highlighted by the lower proliferation of multiple transduced hepatocytes, we may then explain this discrepancy either by a preferential transduction of proliferating hepatocytes by LV or by a consequence of fusion of clusters. The former hypothesis seems to be supported by the observation that the percentage of transduced area increases over time (fig.14 A) and by the slightly higher percentage of EdU<sup>+</sup> transduced hepatocytes (33%) compared to non-transduced, while the latter is supported by the lower percentage of proliferating clusters observed by administering a mix of 3 LV expressing for different fluorescent reporters (fig.14 B). Overall, our interpretation is that LV transduction is generally neutral for hepatocytes proliferation rates and that differences in hepatocyte clusters size and growth are likely due to the different experimental settings used.

Our work suggests that LV transduction of hepatocytes can also be exploited as a tool to study liver tissue dynamics. We took advantage of this tool by administering two LV expressing for different fluorescent reporters at different stages of growth, to monitor proliferation of hepatocytes in different windows of time in the same mice, and we confirmed the reduction in proliferation rate over time. For a similar purpose, we also administered a CreERT2-expressing LV in newborn Confetti mice and then treated them with tamoxifen 2 weeks later. By this experimental design, we may be able to establish if the proliferating capacity is maintained by all or only some of the daughter cells derived from proliferating hepatocytes.

We have shown that transduced hepatocytes can proliferate locally and are maintained during growth and homeostasis. It has been previously shown that LV-transduced hepatocytes are maintained following partial hepatectomy (Mátraai *et al*, 2011). However, the effect of different types of liver damage on maintenance of the transgene remains to be evaluated. Different liver cells have been identified to be responsible for the regeneration of liver after damage, among which both hepatocytes and cholangiocytes (Miyajima *et al*, 2014). We have observed that i.v. administration of LV also allows transduction of ductal cells that maintain their capacity to generate organoids *in vitro* and engraft in mice (unpublished data), suggesting the potential maintenance of the transgene in case of transdifferentiation of ductal cells into hepatocytes and regeneration of liver parenchyma, but this evidence has still to be obtained *in vivo*.

### **4.3. Effect of age at treatment on liver transduction**

In this work we provided for the first time a comprehensive analysis of LV-based liver-directed gene therapy efficiency in mice treated at different ages, both in terms of transduction and transgene output. We show here that the age of administration of LV impacts its biodistribution to liver cell types and lobule zones. Based on our results, we can distinguish between transduction in young (first 2-3 weeks of life) vs. adult mice. In the first group we observed a high transduction of hepatocytes accompanied by low VCN in non-parenchymal cells, in particular KC, LSEC and pDC. In adult mice we confirmed our previously reported data that there is a higher uptake by non-parenchymal cells (mainly KC) that leads to a reduced transduction of hepatocytes (Milani *et al*, 2019). This observation has been confirmed also in terms of percentage of transgene positive area by IF analysis in mice treated at different ages with LV expressing a fluorescent reporter.

Higher transduction of liver parenchyma in young mice is confirmed also by the higher frequency of multiple-transduction events, that represent more than 10% within transduced hepatocytes in young mice compared to 2% in adult mice at the tested LV dose. This higher percentage might also indicate the presence of a subset of hepatocytes that is more prone to be transduced, otherwise we should not observe a higher percentage of multiple transduced hepatocytes within transduced hepatocytes in the group treated at young age. Moreover, considering that the probability of a cell to be transduced by 3 LV expressing for 3 different fluorescent reporter is the same to be transduced 3 times by LV expressing the same reporter, we can expect the percentage of multiple-transduced hepatocytes to be higher than the observed one. It might be interesting to study the characteristics of hepatocytes that make them more prone to be transduced compared to the others.

Here we also describe a non-homogenous transduction of liver lobule by LV, with a zonation of transduced hepatocytes that varies according to the age of LV administration, a finding with important implications for gene therapy. Young-treated mice show a higher percentage of transduced cells in peri-central area, contrary to adult-treated mice which show a peri-portal transduction bias. Likely the zonation of transduced hepatocytes is due to a transduction bias rather than silencing of the transgene expression specifically in a lobule zone, because we did not observe the appearance of peri-portal bias in young-treated mice analyzed up to 12 weeks post treatment. Interestingly, we observed that KC are not responsible for the determination of transduction bias, particularly in adult mice, and that their depletion actually increases the transduction in peri-portal but not in peri-central area.

Transduction biases have also been described for AAV vectors using AAV7 or AAV8 serotypes and multiple promoters and transgenes, with adult mice showing peri-central bias, while no bias detected in newborn mice (Bell *et al*, 2011). In adult-treated NHP, on the other hand, has been observed a peri-portal bias, by AAV vectors, while newborn NHP instead have a homogeneous transduction of liver lobule. The causes of these differences have not been fully elucidated, but we speculate that transduction bias of AAV vectors and LV might be determined by the same factor or set of factors. In this case, having already excluded the involvement of KC, we might consider the role of fenestrae, which have been described to vary in number and dimension according to the age and the position in the liver lobule. In particular, fenestrae in peri-portal sinusoids of adult rats have been described to be larger than peri-central ones, but lower in total number (Wisse *et al*, 1983). Therefore, LV particles might be limited in transduction of peri-central hepatocytes by the small dimension of fenestrae, while AAV vectors, being smaller, could transduce them more easily thanks to the higher porosity of sinusoids. Moreover, fenestrae in young mice are bigger in peri-central area (Barberá-Guillem *et al*, 1986), thus allowing a higher transduction by LV in young mice. We will investigate the role of fenestrae dimension and distribution in young and adult mice to determine their role in transduction efficiency and bias, in order to then translate this information possibly to the human liver.

It has long been debated the existence of a subset of proliferating hepatocytes in the adult liver that play a major role in renewal of liver parenchyma. Wang *et al* proposed that Axin2<sup>+</sup> hepatocytes located around the central vein are predominant in liver turnover (Wang *et al*, 2015). Other groups could not confirm these data later on (Wei *et al*, 2021; Sun *et al*, 2020). Our finding of a preferential transduction of peri-portal hepatocytes in adult mice may support the cause against the role of Axin2<sup>+</sup> peri-central hepatocytes in liver homeostasis. If those cells replace 35% of liver parenchyma in 1 year, starting from central area and expanding toward portal area, we will probably lose the peri-portal transduced hepatocytes. Conversely, we showed that they are maintained long term and they are able to proliferate and generate small clusters. We have also shown in this and previous works that also transgene output is stably maintained up to 1 year post LV administration in adult mice (Brown *et al*, 2007a; Cantore *et al*, 2015).

#### **4.4. Effect of age at treatment on transgene output**

The therapeutic potential of gene transfer for non-cell autonomous diseases depends on the amount of transgene that is produced by transduced cells. We

focused our attention on hFIX, a transgene with which our group has previous experience (Cantore *et al*, 2015; Milani *et al*, 2019). As mentioned above, hemophilia is a good candidate for gene therapy (see 1.5.1). The goal of gene therapy is to reach the therapeutic threshold of FVIII or FIX activity with the lowest possible vector dose. We show here that administration of LV.hFIX in young mice allows reaching a level of transgene output up to 6-fold higher compared to adult-treated mice with the same LV dose on a per weight basis. In our experiments, we administered  $2.5 \times 10^{10}$  TU/kg dose, that has been shown to provide 30% of normal clotting factor activity in adult-treated mice. Given the huge increase in transgene output observed in young-treated mice, administration of LV in this phase of life can substantially reduce the dose of LV needed to reach a therapeutic level of transgene activity. Reduced effective doses would also mean reduced risks of possible acute toxicity, which represents a concern for *in vivo* gene therapy. We have previously shown that therapeutic levels of clotting factors activity can be reached with a lower dose of LV in NHP than in mice (3-fold lower), further reduced by exploiting CD47<sup>high</sup> LV (Milani *et al*, 2019). Thus, if our data are translatable also to NHP and to human, treatment at a young age would lead to a further decrease of the therapeutic LV dose, that constitutes an advantage also for manufacturing and cost of the final drug product. We show that one of the major causes of the higher efficiency of liver-directed gene therapy in young mice is the reduced uptake of LV particles by non-parenchymal cells, and in particular KC, that allow a higher transduction of transgene-expressing hepatocytes. Indeed, we have found a strong linear correlation between the percentage of transduced area and the output of hFIX in mice at all ages. A possible explanation for the differences observed in transgene output between newborn and 2- or 3-week-old treated mice could be attributed to the promoter used. By substituting the ET with the HCR/hAAT promoter we detected the highest FIX concentration in bloodstream in newborn treated mice. We hypothesized that targeting of different hepatocyte subpopulations occurs by administering LV to mice at post-natal day 1 or week 2, that might differently express the promoters. However, serial administration of different LV in the same mouse at D1 and W2 did not result in reduction of double-positive hepatocytes compared to co-administration at D1. Thus, the cause(s) of the differences in transgene output within young mice of different ages still remain to be elucidated. They may be related to differential pattern of LV genomic integration sites, chromatin states and secretory activity of different hepatocyte subsets transduced at the different ages, overall suggesting a high degree of hepatocyte heterogeneity and dynamic changes during liver growth. We also hypothesized that polyploidization of transduced hepatocytes in mice treated at 2

weeks contribute to the higher transgene output by amplifying transgene content. However, our preliminary experimental evidence does not support this hypothesis, because we could not observe any difference in percentage of mono- and bi-nucleated transduced hepatocytes in mice treated at different ages.

Interestingly, we have also described a pattern of transgene output in newborn-treated mice that is not present in older-treated mice, with an increase between W2 and W4 and a stabilization from W6 at an intermediate level. As anticipated above, these variations have been observed also for endogenous proteins expressed by hepatocytes and are probably not specific of the transgene and may be related to general metabolic changes occurring in hepatocytes during liver growth.

#### **4.5. Role of KC on gene therapy efficiency**

Phagocytosis of LV particles from tissue resident macrophages represent a major obstacle to transduction of liver parenchyma. To circumvent this obstacle, our lab developed phagocytosis-shielded LV by increasing display of CD47 molecules on vector surface and reported a reduced uptake of LV by KC and 3-fold increase in hFIX output in NHP (Milani *et al*, 2019). Here, we confirm that phagocytosis of LV particles represents a major limitation for liver-directed gene therapy in adult mice, however we show that it is less impactful in young-treated mice. Indeed, by administering LV in adult mice, we observed high VCN in nPC and in particular in KC (VCN=49), while in mice treated at D1 or W2 there is an almost 6-fold reduction in VCN in nPC, and KC have a VNC of 1.8 in newborn mice and 5 in 2-week-old mice. This reduction is paralleled by an increased transduction of liver parenchyma, that is observed both in terms of VCN in sorted hepatocytes 3 days after treatment and percentage of transgene positive area. Thus, we propose that the higher efficiency of liver-directed LV-based gene therapy in young compared to adult mice is determined at least in part by the lower uptake of LV particles by non-parenchymal cells. The reason underlying this outcome remains to be elucidated. Considering the impact of phagocytosis on hepatocyte transduction, we also investigated the role of KC in the determination of transduction bias, in particular in portal area in adult-treated mice. It has been recently shown that KC are homogeneously distributed in the liver lobule before weaning, but they move towards the peri-portal area in adult mice, increasing their overall capacity to phagocyte pathogens (Gola *et al*, 2021). We thus wondered if this zonation of KC increases the uptake of LV particle in adult mice, determining a lower availability for hepatocytes, and also reduce the probability for them to reach the central area, thus also explaining the peri-portal transduction bias. Unexpectedly, we observed an increased peri-portal transduction bias in KC depleted mice.

Conversely to Gola et al., we observed higher concentration of KC in central area of newborn mice and a more homogenous distribution in adult mice, however we observed the same shift towards portal area during growth. Our results show that LV phagocytosis by KC does not determine the peri-portal transduction bias observed in adult mice, indicating the existence of other factors that control LV transduction, such as size and distribution of LSEC fenestrae dimension or receptors availability. Nonetheless, it emerged that zonation of KC correlate with distribution of transduced hepatocytes in the liver lobule, and the switch in transduction bias from peri-central in young mice to peri-portal in adult mice seems to coincide with the shift of KC from central to portal area, and the drop in overall gene therapy efficiency.

#### **4.6. Limitations of the work**

Our study presents some limitations. In IF cluster analysis, the number of cells present in each cluster is calculated based on the average size of hepatocytes at each age. To reduce the error on this calculation we decided not to distinguish between clusters made of one or two cells. Therefore, we are considering as quiescent also those hepatocytes that might have done a single replication step. Second, in this model we have not taken into accounts death of hepatocytes, which could contribute to reduce the dimension of some clusters. Moreover, the use of the Confetti mouse strain limits clonal analysis of hepatocytes to only 3 markers, thus retaining the possibility to mark two or more hepatocytes independently with the same color and wrongly consider them belonging to the same cluster. To strengthen our clonal analysis, we are planning to use a barcoded LV to increase the number of unique markers for hepatocytes and then monitor their proliferation by evaluating the abundance of each barcode after liver growth and measuring the enrichment of a fraction of barcodes.

To confirm local proliferation of transduced hepatocytes, we also performed 3D analysis to evaluate percentage and dimension of expanding clusters. However, the data that we obtain from 2D and 3D imaging analysis are partially inconsistent. In 3D imaging analysis we measured a majority of expanding clusters, with the increase of the percentage of middle and high-volume clusters over time, while from 2D imaging we concluded that around 75% of clusters are quiescent or slowly proliferating. It is worth noting, however, that in the two sets of experiments, we used different criteria to identify proliferating and quiescent clusters. In 3D imaging small-volume clusters are defined on the basis of the dimension of the majority of clusters at the first time point of analysis (1 week of age), that are single-cell clusters, and is maintained fixed for all the other ages. Therefore, it does not consider the

increase in the size of hepatocytes during growth. Moreover, it is based on the dimension of one hepatocyte, thus also a single cycle of proliferation would classify the cluster as middle-volume, while in 2D imaging analysis we defined as quiescent clusters composed of 1 or 2 cells.

Moreover, it is not clear why we observed a linear correlation between transgene output and percentage of transduced area by administering LV.FIX.IRES.GFP in mice at different ages, while in multiple previous experiments we could measure higher transgene output in mice treated at W2 compared to newborn-treated mice, despite the percentage of transduced area was always similar among these groups. Further analyses are needed to better understand the correlation between percentage of transduced hepatocytes and transgene output.

Most of the experiments described in this work have been performed using a dose of LV of  $2.5 \times 10^{10}$  TU/Kg, that we showed in the past to guarantee a therapeutic level of FIX expression in hemophilia mouse model. We did not perform yet a dose-response study to identify the lowest amount of LV that is necessary to administer in newborn mice to correct a pathologic phenotype, in particular in the context of hemophilia. This analysis will inform about the doses to be tested in future pre-clinical and potentially clinical work.

Lastly, our candidate LV to be eventually carried into clinical trials is shielded from phagocytosis by high human CD47 surface content, however our studies of hepatocytes transduction have been performed in wild-type immunocompetent C57 mice, which do not sense the human CD47 signaling. Despite these mice have been shown to be a reliable model for liver gene therapy studies, and we have investigated the role of KC in hepatocyte transduction, it might be relevant to evaluate also whether the presence of anti-phagocytic signals can influence zonation or efficiency of hepatocytes transduction.

#### **4.7. Future directions**

Our observation of a reduced clonality in the adult liver caused by proliferation of 25-30% of hepatocytes in the newborn liver suggests that it may be possible to reach a high degree of genetic correction also by targeting a small fraction of hepatocytes, if we are able to target specifically those that proliferate. Specific targeting of proliferating hepatocytes may also be relevant for the application of those techniques that so far showed a low efficiency of correction, such as genome editing or GeneRide (see 1.4.5), which exploit HDR, that is known to preferentially occur in cycling cells (Scully *et al*, 2019). We will attempt to characterize this subpopulation of proliferating

hepatocytes exploiting spatial transcriptomic analysis (Ståhl *et al*, 2016), and then we could explore strategies to specifically target them in the future.

The age-related differences in liver transduction have been observed also for IDLV. This non-integrating platform may be exploited for genome editing strategies (Lombardo *et al*, 2007b), and since HDR is more efficient in cycling cells, the higher transduction efficiency of hepatocytes in newborn mice, in which hepatocytes are actively proliferating, may give a rationale to implement this therapeutic strategy in young mice.

Furthermore, the evidence of a reduced proliferation rate of hepatocytes already at the 2<sup>nd</sup> week of age might be helpful also for the application of non-integrating vectors, such as AAV vectors, in which dilution of the transgene caused by proliferation of targeted cells over time is of concern. Considering the low proliferation of hepatocytes in the liver of mice that are still very young (before weaning), we might expect that transduction with AAV vector would lead to a reduced dilution of the vector genome from this age. Direct conversion of ages in mice and humans is challenging. The life-span of mice is much shorter than human life, thus the low hepatocytes proliferation rate observed in juvenile and adult mice might still be converted in a relevant number of cell divisions in the human liver. It may be difficult to extrapolate our findings in mice to larger species or humans, however we may attempt to assess proliferation of hepatocytes from liver sections collected from NHP or humans at different ages, if available.

Further investigation is needed to establish the cause(s) of LV transduction bias and to predict on the possible outcome in human patients. We are exploiting spatial transcriptomic analysis of liver of transduced and non-transduced mice of different ages to investigate differential expression of genes involved in LV transduction. The identification of different transduction bias in mice treated at different ages is particularly relevant to choose the right promoter for gene therapy, to avoid those that are not expressed in the transduced zone, but also to target cell-autonomous metabolic diseases, that might involve a specific lobule zone.

#### **4.8. Conclusions**

Overall, we show here that the age of LV administration strongly influences the outcome of liver-directed gene therapy. We found that administration of LV in young mice results in higher transduction of hepatocytes and higher transgene output, likely caused by reduced uptake of vector particles by non-parenchymal cells. Moreover, the age of treatment also impacts on the distribution of LV in the liver lobule, switching from peri-central in young-treated mice to peri-portal in adult-treated mice,



independently by KC phagocytosis. These results suggest that major changes occur in the liver upon weaning that impact on LV-mediated gene therapy. We also showed that LV-transduced hepatocytes propagate the transgene upon cell proliferation, and that transduction does not induce major alterations in hepatocyte proliferation. We propose here a model of post-natal liver growth, in which only a fraction of hepatocytes proliferates, originating the vast majority of the adult liver tissue. Our results may strengthen the rationale for application of *in vivo* liver-directed LV gene therapy to pediatric patients, but have implications also for other strategies based on integrating technologies.

## **5. Material and methods**

### **5.1. Plasmid construction**

Plasmid containing transfer construct were generated by standard cloning techniques starting from already available plasmids, by substituting the transgene between the ET promoter sequence and WPRE sequence. LV.ET.mCherry was generated starting from LV.ET.GFP plasmid (Brown *et al*, 2007a), digesting it with NheI-HF and BamHI-HF restriction enzymes (New England Biolabs) and inserting mCherry sequence obtained from a previously described plasmid (Zonari *et al*, 2017). Similarly, LV.ET.BFP was cloned by digesting LV.ET.GFP with SalI-HF and PmeI enzymes (New England Biolabs) and inserting BFP sequence obtained from a previously described plasmid (Zonari *et al*, 2017). LV.ET.CreERT2 was cloned by digestion of LV.ET.GFP plasmid using SalI-HF and NheI-HF enzymes and inserting CreERT2 sequences obtained by digestion of pMuLE ENTR SV40 CreERT2 L3-L2 plasmid (Addgene #62174) with SpeI and PspXI enzymes (New England Biolabs). LV.ET.FIX.IRES.GFP was generated starting from LV.ET.FIXR338L (Cantore *et al*, 2012) by digesting it with SalI-HF enzyme and inserting IRES.GFP sequence obtained by gene synthesis.

### **5.2. Plasmid DNA preparation**

Large-scale quantity of plasmid DNA was prepared using Macherey-Nagel endotoxin-free high purity plasmid maxi prep system according to manufacturer's protocol. Plasmid DNA is resuspended in TE (10 mM TrisHcl pH 8.0, 1 mM EDTA).

Large-scale packaging and envelope plasmids were produced by Nature Technology Corp.

For small-scale preparation, following cloning, Wizard® Plus SV Minipreps DNA Purification System (Promega) was used. Colonies were screened by enzymatic digestion and sequencing.

### **5.3. Cell culture**

Human embryonic kidney (HEK) 293T cells were used for vector production and titration, and for analysis of LV mix composition of the experiment in figure 13 A. Cells were maintained in culture with Iscove's modified Dulbecco's medium (IMDM,

Corning) supplemented with 10% fetal bovine serum (FBS, Euroclone) and penicillin/streptomycin 100 international units (IU)/ml (Lonza). Adherent cells were detached using PBS 0.05% trypsin 4mM EDTA solution. Cells were kept in a humidified incubator at 37°C 5% CO<sub>2</sub>.

#### **5.4. LV production**

Third-generation SIN LV were produced by transient transfection of HEK 293T cells. 8-10x10<sup>6</sup> 293T cells were plated 24 hours before transfection in a 15cm dish, and medium was changed 2 hours before transfection with 22.5 ml of fresh medium per plate. Transfection mix is prepared with the packaging plasmids pMDLg/pRRE (12.5 µg/dish) and pCMV.REV (6.25 µg/dish), envelope plasmids PMD2-VSV.G (9 µg/dish) or pBA-AcMNPV-gp64 (Schauber *et al*, 2004) (9 µg/dish), transfer plasmid (35 µg/dish) and pAdvantage plasmids (15 µg/dish) in 0.1X TE-supplemented cell-culture grade water (Sigma) to a final volume of 1.25 ml per plate. Plasmid mix was aliquoted in 15ml tube (one for each plate) and 125 µl of CaCl<sub>2</sub> 2.5 M were added to each tube. Finally, 1.25ml of 2X HBS (281 mM NaCl, 100 mM HEPES, 1.5 mM Na<sub>2</sub>HPO<sub>4</sub>, pH 7.12, prepared in house) were added dropwise to the mix in each tube while kept in agitation, and the mix is transferred into the culture medium. Culture medium was changed 14-16 hours after transfection and then collected after additional 30 hours. Supernatant was filtered with a 0.22 µm filter (Millipore) and ultracentrifuged in polyallomer tubes (Beckman) at 20.000 g for 120 min at 20°C (Beckman Optima XL-100K Ultracentrifuge). LV-containing pellet was resuspended in the appropriate amount of phosphate saline buffer (PBS, Corning) to reach a 500X concentration, aliquoted and stored at -80°C.

For IDLV production the same procedure was followed, but pMDLg/pRRE plasmid is substitute with pMDLg/p.RRE.D64Vint plasmid (Lombardo *et al*, 2007a).

#### **5.5. LV titration**

LV titer was calculated by in vitro transduction of 293T cells and quantitative polymerase chain reaction (qPCR). 75.000 293T cells were plated in each well of a 6-well plate the day before the titration (or in alternative 100.000 the same day) to reach 100.000 cells at the moment of transduction. Cells are transduced with 10-fold serial dilutions (from 10<sup>-3</sup> to 10<sup>-7</sup>) of LV prepared in fresh medium in presence of polybrene (final concentration 8 µg/ml). 10 days after transduction cells were collected for VCN determination.

## 5.6. ddPCR for LV titration and VCN determination

Genomic DNA (gDNA) was extracted from transduced cells or organ sample using Maxwell 16 DNA purification Kit (Promega) following manufacturer's instructions. gDNA from primary sorted cells was extracted using QIAamp DNA mini kit or QIAamp DNA micro kit (Qiagen), following manufacturer's protocol.

VCN per diploid genome was determined by analyzing 15-20 ng of gDNA through digital droplet PCR (ddPCR) with QX200 Droplet Digital PCR System (Biorad), according to manufacturer's recommendations (each primer 900nM, probe 250nM). For quantification of LV genome copies the following primers and a probe were used:

- HIV Fw: 5'-TACTGACGCTCTCGCACC-3'
- HIV Rv: 5'- TCTCGACGCAGGACTCG-3'
- HIV Pr 5'-(FAM)-ATCTCTCTCCTTCTAGCCTC-(MGBNFQ)-3').

For quantification of human gDNA were used primers and probe designed on GAPDH gene (Applied Biosystems Hs00483111\_cn). For quantification of mouse gDNA were used primers and probe designed on Sema3a gene:

- Sema Fw: 5'- ACCGATTCCAGATGATTGGC-3'
- Sema Rv: 5'- TCCATATTAATGCAGTGCTTGC-3'
- Sema Pr: 5'-(HEX)-AGAGGCCTGTCCTGCAGCTCATGG-(BHQ1)-3').

To calculate VCN, was used the formula  $VCN = \frac{ng\ LV}{ng\ gDNA} \times 2$ . Infectious titer is calculated with the formula  $TU/ml = \frac{VCN \times 100.000}{1/dilution\ factor}$ . LV physical particles were measured by p24 ELISA assay (Perkin Elmer). Infectivity was calculated as the ratio between infectious titer and physical particles.

## 5.7. Flow cytometry

Flow cytometry analysis was performed using CytoFLEX S analyzer (Beckman Coulter) equipped with 405, 488, 561 and 638 lasers. Approximately 500.000 cells were harvested in MACS buffer (PBS pH 7.2 0.5% bovine serum albumin, 2Mm EDTA, Miltenyi Biotec) and analyzed without antibody staining, because cells expressed endogenous fluorescent proteins. Data analysis was performed with FCS Express 6 software.

## 5.8. Mice experiments

Mice were housed in specific pathogen-free conditions. C57BL/6 mice were purchased from Charles River. Rosa26-Confetti and AlbCreERT2 mice were kindly

provided by Dr. Iannacone's lab and bred in house. For experiments in Confetti mice or AlbCreERT2-Confetti mice, male and female were both used randomly, according to availability. For experiments in newborns and 2-weeks old C56BL/6 wild-type mice, male and female were used according to availability at birth, while for adult C57BL/6 mice only females were used. Blood samples were collected with capillary tubes from the retro-orbital plexus and supplemented with 0.38% sodium citrate buffer pH7.4 to avoid coagulation. LV administration in adult mice (8-10 weeks old) was carried out by tail-vein injection, in 2-weeks old mice by tail-vein or retro-orbital injection, in newborn mice (1-2 days old) by temporal vein injection. Tamoxifen was dissolved in corn oil 10 mg/ml, stored at -20°C and administered subcutaneously in newborn mice and intraperitoneally in older mice at the dose of 0.1 mg/g. Clodronate liposomes or PBS liposomes were administered by tail-vein injection 10 µl/g as recommended by manufacturers. EdU was suspended in PBS at the final concentration of 10mM, stored at -20°C and administered intraperitoneally. Mice were euthanized by cervical dislocation or CO<sub>2</sub> inhalation. All protocols were approved by the Institutional Animal Care and Use Committee.

### 5.9. Sorting of liver cell subpopulations

Fractionation of liver cell subpopulation was performed as previously described (Milani *et al*, 2019). Liver was digested by perfusion via the inferior vena cava first with PBS 0.5 mM EDTA (~10 ml), then HBSS (Hank's balanced salt solution, Gibco) 1% HEPES ((4-(2-hydroxyethyl)-1-piperazineethanesulfonic acid) (~10 ml) and finally HBSS 1% HEPES 0.03% collagenase IV (Sigma) (~16.5 ml). Liver was then collected and passed through a 100 µm cell strainer (BD Biosciences). Cell suspension was centrifuged three times at 30, 25 and 20 g for 3 minutes to separate non-parenchymal cells (in the supernatant) from hepatocytes (in the pellet). Supernatant was centrifuged 7 min 650g and cells were loaded onto a 30%-60% Percoll (Sigma) gradient and centrifuged 1800g for 15 min. nPC interface was collected and washed twice with HBSS 1% HEPES. Hepatocyte fraction was stained with the following mix of antibodies, in 200 µl of volume:

<i>Antigen</i>	<i>Fluorochrome</i>	<i>Clone</i>	<i>Company (code)</i>	<i>Volume</i>
CD31	APC	MEC 13.3	BD Biosciences (551262)	3 µl
CD45	APC	30-F11	BD Biosciences (559864)	3 µl
FC Block		2.4G2	BD Biosciences (553142)	5 µl

Hepatocyte fraction was sorted to remove contaminants using FACSria Fusion (BD Biosciences). nPC fraction was first incubated with FC Block and then stained with the following mix of antibodies in 200 µl of volume:

<i>Antigen</i>	<i>Fluorochrome</i>	<i>Clone</i>	<i>Company (code)</i>	<i>Volume</i>
CD31	FITC	MEC 13.3	BD Biosciences (551262)	7 µl
CD45	e-fluor 450	30-F11	Invitrogen (48-0451-82)	7 µl
F4/80	PE	CI:A3-1	BD Biosciences (553142)	7 µl
CD45R/B220	PE-Cy5	RA3-6B2	BD Biosciences (553091)	7 µl
CD11c	PE-Cy7	N418	Invitrogen (25-0114-82)	7 µl

### **5.10. Gene expression analysis**

Organ samples and primary sorted cells were stored at -80°C in RLT plus buffer (Qiagen) solution for RNA extraction. Organs were mechanically homogenized using gentleMACS™ Octo Dissociator (Miltenyi Biotec) in 700 µl of RLT plus buffer. RNA from homogenized organs and cells was extracted using RNeasy Plus mini kit (Qiagen) following manufacturer's protocol. DNA was digested on columns using RNase-Free DNase Set (Qiagen), according to manufacturer's recommendations. RNA was retrotranscribed using SuperScript IV VILO Master Mix with exDNase Enzyme (Thermo Fisher) according to manufacturer's protocol. cDNA was analyzed by ddPCR as described above using probe systems. For albumin (Mm00802090, Applied Biosystems) and LDLR (dMmu CPE5122114, Biorad) were used commercially available primers and probes, while for WPRE custom primers and probe (WPRE Fw: 5'-GGCTGTTGGGCACTGACAAT-3'; WPRE Rv: 5'- ACGTCCCGCGCAGAATC-3'; WPRE Pr: 5'- (FAM)-TTTCCATGGCTGCTCGCCTGTGT-(MGB)-3') were used. As normalizer commercial Hprt primers and probe (dMmu CPE5095493, Biorad) were used. Gene expression levels were calculated with the formula  $ng\ cDNA\ gene/ng\ cDNA\ normalizer$

### **5.11. ELISA assays**

Mouse blood was centrifuged 6500 rpm for 6 min 30 sec to collect plasma, which was stored at -80°C. Samples were diluted according to necessity. ELISA assay specific for human FIX antigen was used to determine its concentration in mouse plasma samples (Asserachrom IX:Ag, Stago), following manufacturer's protocol. Mouse PCSK9 plasma concentration was determined by ELISA assay (Mouse

Proprotein Convertase 9/PCSK9 Quantikine ELISA Kit, R&D Systems), according to manufacturer's protocol. Mouse albumin concentration was determined by ELISA assay (Mouse Albumin Matched Antibody Pair Kit, Abcam) according to manufacturer's protocol.

For IgG and IgM ELISA assay, plates were coated with 100ng of VSV.G (Vinci-Biochem V3-VSIG15-R-10) protein and of IgG and IgM antibodies for the standard curve and incubated 16 hours at 4°C. Plates were washed 3 times with PBS 0.05% Tween 20 and incubated for 2 hours at room temperature with 200µl of blocking solution (PBS 0.05% Tween-20 1% Chicken Ova). Plates were washed again 3 times and incubated with 100 µl of diluted samples and incubated 2 hours at 37°C. Plates were washed 4 times and anti-IgG (1:10000; Sigma A2554-1ML) or anti-IgM (1:5000, Southern Biotech 1140-05), HRP conjugated detection antibodies were added and incubated 1 hour at 37°C. Plates were washed 4 times and incubated with 100 µl of TMB for 10 minutes and stopped with 50 µl of HCl. Plates were read at 450nm using a Multiskan GO microplate reader (Thermo Fisher Scientific).

### **5.12. Immunofluorescence imaging**

Livers were harvested from mice, washed briefly in PBS and fixed 4 hours in PBS 4% paraformaldehyde (PFA), then washed again briefly in PBS before being stored at least 24 hours in 30% sucrose 0.02% sodium azide in H<sub>2</sub>O. Livers were frozen in OCT (optimal cutting temperature) compound (Killik, Bio Optica) and slices 5 to 20 µm thick were cut at cryostat (Histo-line MC5050), placed on Superfrost® Plus microscope slides (Thermo Scientific) and stored at -80°C. All the staining steps were performed protected from lights to preserve endogenous fluorescence. Slides were thawed at room temperature for at least 2 hours, then washed 3 times 5 minutes in PBS 0.1% X-Triton. Edges were drawn around the tissue using immunostaining paper pen (Sigma-Aldrich) to contain staining solutions. Blocking step was performed using PBS 0.1% X-Triton 1% bovine serum albumin (BSA) 5% FBS for 1 hour at room temperature in a humid chamber. Blocking solution was substituted with mix containing primary antibodies in blocking solution and incubation was carried on for 12-16 hours at 4°C in a humid chamber. Primary antibodies mix solution was removed and slides were washed 3 times 5 minutes in PBS 0.1% X-Triton. Secondary antibodies were diluted in blocking solution together with Hoechst and incubated for 1 hour at room temperature in a humid chamber. Slides were then washed in PBS and coverslip was added using Fluoromount-G (Invitrogen) as mounting medium. Slides were dried for 16 hours at room temperature or for longer at 4°C, and stored

at 4°C before acquisition. EdU staining was performed using Click-iT™ EdU Cell Proliferation Kit with AlexaFluor 488 dye (Invitrogen C10337) according to manufacturer's protocol. Antigen unmasking was performed by incubating slides 20 min in citrate buffer (10mM Citric Acid, pH 6.0) at 98°C. For nuclear staining concentration of X-Triton has been raised to 0.5% for blocking buffer and washing solution. The following antibodies were used for immunofluorescence staining:

<i>Antigen</i>	<i>Species</i>	<i>Fluorochrome</i>	<i>Clone</i>	<i>Company (code)</i>	<i>Dilution</i>
GFP	Rabbit	-	Polyclonal	Invitrogen (A11122)	1:1000
GFP	Chicken	-	Polyclonal	Invitrogen (A10262)	1:250
GFP	Chicken	-	Polyclonal	Abcam (ab13970)	1:500
mCherry	Rabbit	-	Polyclonal	Abcam (ab167453)	1:200
mCherry	Chicken	-	Polyclonal	Abcam (ab205402)	1:1000
CK7	Rabbit	-	EPR17078	Abcam (ab181598)	1:250
GS	Rabbit	-	Polyclonal	Novus Bio. (NB110-4104)	1:5000
F4/80	Rat	-	CI:A3-1	Abcam (ab6640)	1:200
HNF4a	Rabbit	-	C11F12	Cell Sig. (3113S)	1:50
Rabbit IgG	Goat	AF488	Polyclonal	Invitrogen (A11034)	1:1000
Rabbit IgG	Goat	AF546	Polyclonal	Invitrogen (A11010)	1:1000
Rabbit IgG	Donkey	AF647	Polyclonal	Invitrogen (A31573)	1:1000
Chicken IgY	Goat	AF488	Polyclonal	Invitrogen (A11039)	1:1000
Chicken IgY	Goat	AF561	Polyclonal	Invitrogen (A11040)	1:1000
Rat IgG	Goat	AF561	Polyclonal	Invitrogen (A11081)	1:1000
Rat IgG	Goat	AF647	Polyclonal	Invitrogen (A21247)	1:1000
Hoechst	-	-	-	Invitrogen (H3570)	1:20000

Images were acquired using confocal microscope Leica TCS SP5, Leica TCS SP8 or Mavig Rs-G4 at 20X or 40X magnification. Images were analyzed using Image J or MATLAB software. Identification of stained cells was performed by manually selecting a threshold and counting objects bigger than 10  $\mu\text{m}^2$  for nuclei, 20  $\mu\text{m}^2$  for KC and 100  $\mu\text{m}^2$  for hepatocytes. Total liver area was measured by saturating signal from the whole tissue. Cells positive for two or more colors were identified by calculating pixels positive in two or more channels using Image J. Cluster dimension was measured using Image J, number of cells per cluster was calculated by dividing dimension of each cluster by the average size of a hepatocyte at each age, that was calculated by segmenting clusters in representative images and measuring average



cell dimension. Peri-portal and peri-central areas were identified by marking tissue area within a fixed distance from CK7<sup>+</sup> or GS<sup>+</sup> area using MATLAB. Mono- and bi-nucleated cells in figure 9B were measured by performing segmentation and then counting Hoechst<sup>+</sup> objects with dimension between 100 and 700 pixels and sphericity higher than 0.8. Nuclei closer than 6 pixels were considered belonging to the same cell.

### **5.13. Immunohistochemistry imaging**

Livers were perfused from the inferior vena cava with PBS EDTA 5mM to remove blood, then harvested and fixed at least 24h in zinc-formalin. Embedding and cutting of livers and slides preparation, staining and acquisition were performed by Centro di Imaging Sperimentale facility in San Raffaele hospital. Images were acquired using Aperio Image Scope software.

### **5.14. Liver clearing and 3D imaging**

Livers were perfused with PBS 5mM EDTA (~10 ml) and PBS 4% PFA (150 ml), were then harvested and incubate in PBS 4% PFA for 30 min and then moved in PBS and stored at room temperature protected from light. X-CLARITY™ system (Logos Biosystems) was used for liver clarification (Chung *et al*, 2013). Liver lobes were separated and incubated in X-CLARITY™ Hydrogel Solution supplemented with X-CLARITY™ Polymerization Initiator for 24 hours at 4°C protected from light in a 6-weel plate. The plate was then moved into the X-CLARITY™ Polymerization System and incubated for 3 hours at 37°C in vacuum conditions (-90kPa). Liver lobes were stored into Electrophoretic Tissue Clearing Solution until the next step was performed. Liver lobes were then cut into smaller pieces, placed in holder chamber and moved into X-CLARITY™ Tissue Clearing System II for electrophoresis (4.5h, 1.4 A, 37°C). Samples were stored in PBS at room temperature protected from light. 2 hours before acquisition samples were moved into X-CLARITY™ Mounting Solution. Acquisition was performed using Nikon A1 MP 2-photon microscope or Zeiss Lightsheet Z.1.

### **5.15. Western blot**

For protein extraction, liver samples were lysed using RIPA lysis buffer (Millipore) supplemented with one tablet of cOmplete™, mini, EDTA-free Protease Inhibitor Cocktail (Sigma). Ice cold lysis buffer was added to the tissue 1:5 weight/volume, tissue was homogenized with an electric homogenizer and stored 30 min at 4°C, then centrifuged 20 min 4°C 12000rpm and supernatant was collected. Protein concentration in the lysate was quantified using DC Protein Assay (Biorad, 5000111) according to manufacturer's protocol.

For western blot, 40 µg of total proteins were denatured with NuPAGE™ LDS Sample Loading Buffer (Invitrogen) and NuPAGE™ Sample Reducing Agent (Invitrogen) in 15 µl of final volume 70°C 10 minutes. Samples were run on a NuPAGE™ 4-12% Bis-Tris Midi Gel (Invitrogen) in NuPAGE™ MOPS (Invitrogen) for 1.5 hours at 150V. Transfer to the membrane has been performed using iBlot™ 2 Gel Transfer Device (Invitrogen). Membrane was stained with Ponceau (Biorad) to check presence of proteins and then washed in H<sub>2</sub>O. Staining was performed with iBind™ Flex Solution Kit (Invitrogen) according to manufacturer's protocol, using Goat anti-LDLR (1:2000, R&D AF2255) and Mouse anti-βactin (1:5000, Sigma A2228) primary antibodies and anti-goat (1:200, Jackson ImmunoResearch Laboratories 111-035-144) and anti-mouse (1:4000, Jackson ImmunoResearch Laboratories 115-035-003) HRP-conjugated secondary antibodies.

Images were acquired at Chemidoc and analyzed using Image J.

## 6. References

- Aiuti A, Ficara F, Cattaneo F, Bordignon C & Roncarolo MG (2003) Gene therapy for adenosine deaminase deficiency. *Current Opinion in Allergy and Clinical Immunology* 3: 461–466
- Akkina RK, Walton RM, Chen ML, Li QX, Planelles V & Chen IS (1996) High-efficiency gene transfer into CD34+ cells with a human immunodeficiency virus type 1-based retroviral vector pseudotyped with vesicular stomatitis virus envelope glycoprotein G. *Journal of Virology* 70: 2581–2585
- Alemanly R, Suzuki K & Curiel DT (2000) Blood clearance rates of adenovirus type 5 in mice. *Journal of General Virology* 81: 2605–2609
- Alves-Bezerra M & Cohen DE (2017) Triglyceride Metabolism in the Liver. In *Comprehensive Physiology* pp 1–22. Wiley
- Annoni A, Goudy K, Akbarpour M, Naldini L & Roncarolo MG (2013) Immune responses in liver-directed lentiviral gene therapy. *Translational Research* 161: 230–240
- Antoniou A, Raynaud P, Cordi S, Zong Y, Tronche F, Stanger BZ, Jacquemin P, Pierreux CE, Clotman F & Lemaigre FP (2009) Intrahepatic Bile Ducts Develop According to a New Mode of Tubulogenesis Regulated by the Transcription Factor SOX9. *Gastroenterology* 136: 2325–2333
- Anundi I, Lähteenmäki T, Rundgren M, Moldeus P & Lindros KO (1993) Zonation of acetaminophen metabolism and cytochrome P450 2E1-mediated toxicity studied in isolated periportal and perivenous hepatocytes. *Biochemical Pharmacology* 45: 1251–1259
- Aponte-Ubillus JJ, Barajas D, Peltier J, Bardliving C, Shamlou P & Gold D (2018) Molecular design for recombinant adeno-associated virus (rAAV) vector production. *Applied Microbiology and Biotechnology* 102: 1045–1054
- Banugaria SG, Prater SN, Ng Y-K, Kobori JA, Finkel RS, Ladda RL, Chen Y-T, Rosenberg AS & Kishnani PS (2011) The impact of antibodies on clinical outcomes in diseases treated with therapeutic protein: Lessons learned from infantile Pompe disease. *Genetics in Medicine* 13: 729–736
- Barberá-Guillem E, Arrue JM, Ballesteros J & Vidal-Vanaclocha F (1986) Structural changes in endothelial cells of developing rat liver in the transition from fetal to postnatal life. *Journal of Ultrastructure and Molecular Structure Research* 97: 197–206
- Barzel A, Paulk NK, Shi Y, Huang Y, Chu K, Zhang F, Valdmanis PN, Spector LP, Porteus MH, Gaensler KM, *et al* (2014) Promoterless gene targeting without

- nucleases ameliorates haemophilia B in mice. *Nature* 2014 517:7534 517: 360–364
- Bell P, Wang L, Gao G, Haskins ME, Tarantal AF, McCarter RJ, Zhu Y, Yu H & Wilson JM (2011) Inverse zonation of hepatocyte transduction with AAV vectors between mice and non-human primates. *Molecular Genetics and Metabolism* 104: 395–403
- Benhamouche S, Decaens T, Godard C, Chambrey R, Rickman DS, Moinard C, Vasseur-Cognet M, Kuo CJ, Kahn A, Perret C, *et al* (2006) Apc Tumor Suppressor Gene Is the “Zonation-Keeper” of Mouse Liver. *Developmental Cell* 10: 759–770
- Ben-Moshe S & Itzkovitz S (2019) Spatial heterogeneity in the mammalian liver. *Nature Reviews Gastroenterology and Hepatology* 16: 395–410  
doi:10.1038/s41575-019-0134-x [PREPRINT]
- Bennett J, Ashtari M, Wellman J, Marshall KA, Cyckowski LL, Chung DC, McCague S, Pierce EA, Chen Y, Bennicelli JL, *et al* (2012) AAV2 Gene Therapy Readministration in Three Adults with Congenital Blindness. *Science Translational Medicine* 4
- Bennett J, Wellman J, Marshall KA, McCague S, Ashtari M, DiStefano-Pappas J, Elci OU, Chung DC, Sun J, Wright JF, *et al* (2016) Safety and durability of effect of contralateral-eye administration of AAV2 gene therapy in patients with childhood-onset blindness caused by RPE65 mutations: a follow-on phase 1 trial. *The Lancet* 388: 661–672
- Biffi A, Montini E, Lorioli L, Cesani M, Fumagalli F, Plati T, Baldoli C, Martino S, Calabria A, Canale S, *et al* (2013) Lentiviral Hematopoietic Stem Cell Gene Therapy Benefits Metachromatic Leukodystrophy. *Science* 341
- Blaese RM, Culver KW, Miller AD, Carter CS, Fleisher T, Clerici M, Shearer G, Chang L, Chiang Y, Tolstoshev P, *et al* (1995) T lymphocyte-directed gene therapy for ADA-SCID: Initial trial results after 4 years. *Science* 270: 475–480
- Bordignon C, Notarangelo LD, Nobili N, Ferrari G, Casorati G, Panina P, Mazzolari E, Maggioni D, Rossi C, Servida P, *et al* (1995) Gene therapy in peripheral blood lymphocytes and bone marrow for ADA- immunodeficient patients. *Science* 270: 470–475
- Bou-Nader M, Caruso S, Donne R, Celton-Morizur S, Calderaro J, Gentric G, Cadoux M, L’Hermitte A, Klein C, Guilbert T, *et al* (2020) Polyploidy spectrum: a new marker in HCC classification. *Gut* 69: 355–364

- Bouwens L, Baekeland M, de Zanger R & Wisse E (1986) Quantitation, tissue distribution and proliferation kinetics of kupffer cells in normal rat liver. *Hepatology* 6: 718–722
- Bradford KL, Moretti FA, Carbonaro-Sarracino DA, Gaspar HB & Kohn DB (2017) Adenosine Deaminase (ADA)-Deficient Severe Combined Immune Deficiency (SCID): Molecular Pathogenesis and Clinical Manifestations. *Journal of Clinical Immunology* 2017 37:7 37: 626–637
- Bramson JL, Graham FL & Gauldie J (1995) The use of adenoviral vectors for gene therapy and gene transfer in vivo. *Current Opinion in Biotechnology* 6: 590–595
- Braun CJ, Boztug K, Paruzynski A, Witzel M, Schwarzer A, Rothe M, Modlich U, Beier R, Göhring G, Steinemann D, *et al* (2014) Gene Therapy for Wiskott-Aldrich Syndrome—Long-Term Efficacy and Genotoxicity. *Science Translational Medicine* 6
- Brown BD, Cantore A, Annoni A, Sergi LS, Lombardo A, della Valle P, D’Angelo A & Naldini L (2007a) A microRNA-regulated lentiviral vector mediates stable correction of hemophilia B mice. *Blood* 110: 4144–4152
- Brown BD, Cantore A, Annoni A, Sergi LS, Lombardo A, Valle P della, D’angelo A, Naldini L, San C, Del R, *et al* (2007b) A microRNA-regulated lentiviral vector mediates stable correction of hemophilia B mice.
- Brown BD, Venneri MA, Zingale A, Sergi LS & Naldini L (2006) Endogenous microRNA regulation suppresses transgene expression in hematopoietic lineages and enables stable gene transfer. *Nature Medicine* 12: 585–591
- Brunner KT, Hurez D, McCluskey RT & Benacerraf B (1960) Blood clearance of P32-labeled vesicular stomatitis and Newcastle disease viruses by the reticuloendothelial system in mice. *Journal of immunology (Baltimore, Md : 1950)* 85: 99–105
- Bulbake U, Doppalapudi S, Kommineni N & Khan W (2017) Liposomal Formulations in Clinical Use: An Updated Review. *Pharmaceutics* 2017, Vol 9, Page 12 9: 12
- Bulcha JT, Wang Y, Ma H, Tai PWL & Gao G (2021) Viral vector platforms within the gene therapy landscape. *Signal Transduction and Targeted Therapy* 6 doi:10.1038/s41392-021-00487-6 [PREPRINT]
- Buonaguro L, Buonaguro FM, Tornesello ML, Beth-Giraldo E, Gaudio E del, Ensoli B & Giraldo G (1994) Role of HIV-1 Tat in the Pathogenesis of AIDS-Associated Kaposi’s Sarcoma. *Antibiotics and chemotherapy* 46: 62–72
- Burns JC, Friedmann T, Driever W, Burrascano M & Yee JK (1993) Vesicular stomatitis virus G glycoprotein pseudotyped retroviral vectors: concentration

- to very high titer and efficient gene transfer into mammalian and nonmammalian cells. *Proceedings of the National Academy of Sciences* 90: 8033–8037
- Bushman FD (2020) Retroviral Insertional Mutagenesis in Humans: Evidence for Four Genetic Mechanisms Promoting Expansion of Cell Clones. *Molecular Therapy* 28: 352–356
- Calcedo R, Somanathan S, Qin Q, Betts MR, Rech AJ, Vonderheide RH, Mueller C, Flotte TR & Wilson JM (2017) Class I-restricted T-cell responses to a polymorphic peptide in a gene therapy clinical trial for  $\alpha$ -1-antitrypsin deficiency. *Proceedings of the National Academy of Sciences* 114: 1655–1659
- Caldovic L, Abdikarim I, Narain S, Tuchman M & Morizono H (2015) Genotype–Phenotype Correlations in Ornithine Transcarbamylase Deficiency: A Mutation Update. *Journal of Genetics and Genomics* 42
- Calne RY, Sells RA, Pena JR, Davis DR, Millard PR, Herbertson BM, Binns RM & Davies DAL (1969) Induction of Immunological Tolerance by Porcine Liver Allografts. *Nature* 223
- De Caneva A, Porro F, Bortolussi G, Sola R, Lisjak M, Barzel A, Giacca M, Kay MA, Vlahoviček K, Zentilin L, *et al* (2019) Coupling AAV-mediated promoterless gene targeting to SaCas9 nuclease to efficiently correct liver metabolic diseases. *JCI Insight* 4
- Cantore A, Nair N, della Valle P, di Matteo M, Màtrai J, Sanvito F, Brombin C, di Serio C, D’Angelo A, Chuah M, *et al* (2012) Hyperfunctional coagulation factor IX improves the efficacy of gene therapy in hemophilic mice. *Blood* 120: 4517–4520
- Cantore A, Ranzani M, Bartholomae CC, Volpin M, Valle P della, Sanvito F, Sergi LS, Gallina P, Benedicenti F, Bellinger D, *et al* (2015) Liver-directed lentiviral gene therapy in a dog model of hemophilia B. *Science translational medicine* 7: 277ra28
- Cartier N, Hacein-Bey-Abina S, Bartholomae CC, Veres G, Schmidt M, Kutschera I, Vidaud M, Abel U, Dal-Cortivo L, Caccavelli L, *et al* (2009) Hematopoietic Stem Cell Gene Therapy with a Lentiviral Vector in X-Linked Adrenoleukodystrophy. *Science* 326: 818–823
- Cavazzana M & Mavilio F (2018) Gene Therapy for Hemoglobinopathies. *Human Gene Therapy* 29: 1106–1113
- Chan CC (2012) Portal-systemic collaterals and hepatic encephalopathy. *Journal of the Chinese Medical Association* 75: 1–2

- Chandler RJ & Venditti CP (2019) Gene Therapy for Methylmalonic Acidemia: Past, Present, and Future. *Human Gene Therapy* 30: 1236–1244
- Chang M, Parker EA, Muller TJM, Haenen C, Mistry M, Finkielstain GP, Murphy-Ryan M, Barnes KM, Sundaram R & Baron J (2008) Changes in Cell-Cycle Kinetics Responsible for Limiting Somatic Growth in Mice. *Pediatric Research* 2008 64:3 64: 240–245
- Chen F, Jimenez RJ, Sharma K, Luu HY, Hsu BY, Ravindranathan A, Stohr BA & Willenbring H (2020) Broad Distribution of Hepatocyte Proliferation in Liver Homeostasis and Regeneration. *Cell Stem Cell* 26: 27-33.e4
- Chen ST, Iida A, Guo L, Friedmann T & Yee JK (1996) Generation of packaging cell lines for pseudotyped retroviral vectors of the G protein of vesicular stomatitis virus by using a modified tetracycline inducible system. *Proceedings of the National Academy of Sciences* 93: 10057–10062
- Choi TY, Ninov N, Stainier DYR & Shin D (2014) Extensive Conversion of Hepatic Biliary Epithelial Cells to Hepatocytes After Near Total Loss of Hepatocytes in Zebrafish. *Gastroenterology* 146: 776–788
- Chung K, Wallace J, Kim S-Y, Kalyanasundaram S, Andalman AS, Davidson TJ, Mirzabekov JJ, Zalocusky KA, Mattis J, Denisin AK, *et al* (2013) Structural and molecular interrogation of intact biological systems. *Nature* 2013 497:7449 497: 332–337
- Cicalese MP, Ferrua F, Castagnaro L, Pajno R, Barzaghi F, Giannelli S, Dionisio F, Brigida I, Bonopane M, Casiraghi M, *et al* (2016) Update on the safety and efficacy of retroviral gene therapy for immunodeficiency due to adenosine deaminase deficiency. *Blood* 128: 45–54
- Corbic M, Lebrec D, Dafniet M le & Erlinger S (1984) A New Method to Measure Portal and Hepatic Blood Flow Using Taurocholate in the Rat. *Hepatology* 4: 112–115
- Cronin J, Zhang X-Y & Reiser J (2005) Altering the Tropism of Lentiviral Vectors through Pseudotyping. *Current Gene Therapy* 5: 387–398
- Crudele JM, Finn JD, Siner JI, Martin NB, Niemeyer GP, Zhou S, Mingozzi F, Lothrop CD & Arruda VR (2015) AAV liver expression of FIX-Padua prevents and eradicates FIX inhibitor without increasing thrombogenicity in hemophilia B dogs and mice. *Blood* 125: 1553–1561
- Cullis PR & Hope MJ (2017) Lipid Nanoparticle Systems for Enabling Gene Therapies. *Molecular Therapy* 25: 1467–1475
- Dalkara D, Byrne LC, Klimczak RR, Visel M, Yin L, Merigan WH, Flannery JG & Schaffer D v. (2013) In Vivo-Directed Evolution of a New Adeno-Associated

- Virus for Therapeutic Outer Retinal Gene Delivery from the Vitreous. *Science Translational Medicine* 5
- DePolo NJ, Reed JD, Sheridan PL, Townsend K, Sauter SL, Jolly DJ & Dubensky TW (2000) VSV-G Pseudotyped Lentiviral Vector Particles Produced in Human Cells Are Inactivated by Human Serum. *Molecular Therapy* 2: 218–222
- Dietzen DJ, Rinaldo P, Whitley RJ, Rhead WJ, Hannon WH, Garg UC, Lo SF & Bennett MJ (2009) National Academy of Clinical Biochemistry Laboratory Medicine Practice Guidelines: Follow-Up Testing for Metabolic Disease Identified by Expanded Newborn Screening Using Tandem Mass Spectrometry; Executive Summary. *Clinical Chemistry* 55: 1615–1626
- Donne R, Saroul-Aïnama M, Cordier P, Celton-Morizur S & Desdouets C (2020) Polyploidy in liver development, homeostasis and disease. *Nature Reviews Gastroenterology and Hepatology* 17: 391–405 doi:10.1038/s41575-020-0284-x [PREPRINT]
- Doudna JA (2020) The promise and challenge of therapeutic genome editing. *Nature* 2020 578:7794 578: 229–236
- Duan D, Sharma P, Yang J, Yue Y, Dudus L, Zhang Y, Fisher KJ & Engelhardt JF (1998) Circular Intermediates of Recombinant Adeno-Associated Virus Have Defined Structural Characteristics Responsible for Long-Term Episomal Persistence in Muscle Tissue. *Journal of Virology* 72: 8568–8577
- Dull T, Zufferey R, Kelly M, Mandel RJ, Nguyen M, Trono D & Naldini L (1998) A Third-Generation Lentivirus Vector with a Conditional Packaging System. *Journal of Virology* 72: 8463–8471
- Duncan AW, Taylor MH, Hickey RD, Hanlon Newell AE, Lenzi ML, Olson SB, Finegold MJ & Grompe M (2010) The ploidy conveyor of mature hepatocytes as a source of genetic variation. *Nature* 467: 707–710
- Eichler F, Duncan C, Musolino PL, Orchard PJ, de Oliveira S, Thrasher AJ, Armant M, Dansereau C, Lund TC, Miller WP, *et al* (2017) Hematopoietic Stem-Cell Gene Therapy for Cerebral Adrenoleukodystrophy. *New England Journal of Medicine* 377: 1630–1638
- Eloy JO, Petrilli R, Trevizan LNF & Chorilli M (2017) Immunoliposomes: A review on functionalization strategies and targets for drug delivery. *Colloids and Surfaces B: Biointerfaces* 159: 454–467
- Escobar G, Barbarossa L, Barbiera G, Norelli M, Genua M, Ranghetti A, Plati T, Camisa B, Brombin C, Cittaro D, *et al* (2018) Interferon gene therapy reprograms the leukemia microenvironment inducing protective immunity to multiple tumor antigens. *Nature Communications* 2018 9:1 9: 1–16



- Escobar G, Gentner B, Naldini L & Mazziere R (2016) Engineered tumor-infiltrating macrophages as gene delivery vehicles for interferon- $\alpha$  activates immunity and inhibits breast cancer progression.
- Farber E (1956) Similarities in the sequence of early histological changes induced in the liver of the rat by ethionine, 2-acetylaminofluorene, and 3'-methyl-4-dimethylaminoazobenzene. *Cancer research* 16: 142–8
- Ferla R, O'Malley T, Calcedo R, O'Donnell P, Wang P, Cotugno G, Claudiani P, Wilson JM, Haskins M & Auricchio A (2013) Gene Therapy for Mucopolysaccharidosis Type VI Is Effective in Cats Without Pre-Existing Immunity to AAV8. *Human Gene Therapy* 24: 163–169
- Ferreira CR, van Karnebeek CDM, Vockley J & Blau N (2018) A proposed nosology of inborn errors of metabolism. *Genetics in Medicine* 21:1 21: 102–106
- Ferrua F & Aiuti A (2017) Twenty-Five Years of Gene Therapy for ADA-SCID: From *Bubble Babies* to an Approved Drug. *Human Gene Therapy* 28: 972–981
- Finkelshtein D, Werman A, Novick D, Barak S & Rubinstein M (2013) LDL receptor and its family members serve as the cellular receptors for vesicular stomatitis virus. *Proceedings of the National Academy of Sciences* 110: 7306–7311
- Finn JD, Smith AR, Patel MC, Shaw L, Youniss MR, Heteren J van, Dirstine T, Ciullo C, Lescarbeau R, Seitzer J, et al (2018) A Single Administration of CRISPR/Cas9 Lipid Nanoparticles Achieves Robust and Persistent In Vivo Genome Editing. *Cell Reports* 22: 2227–2235
- Follenzi A, Ailles LE, Bakovic S, Geuna M & Naldini L (2000) Gene transfer by lentiviral vectors is limited by nuclear translocation and rescued by HIV-1 pol sequences. *Nature Genetics* 25:2 25: 217–222
- Follenzi A, Sabatino G, Lombardo A, Boccaccio C & Naldini L (2002) Efficient Gene Delivery and Targeted Expression to Hepatocytes *In Vivo* by Improved Lentiviral Vectors. *Human Gene Therapy* 13: 243–260
- Font-Burgada J, Shalapour S, Ramaswamy S, Hsueh B, Rossell D, Umemura A, Taniguchi K, Nakagawa H, Valasek MA, Ye L, et al (2015) Hybrid Periportal Hepatocytes Regenerate the Injured Liver without Giving Rise to Cancer. *Cell* 162: 766–779
- Foust KD, Nurre E, Montgomery CL, Hernandez A, Chan CM & Kaspar BK (2008) Intravascular AAV9 preferentially targets neonatal neurons and adult astrocytes. *Nature Biotechnology* 27:1 27: 59–65
- Fumagalli F, Calbi V, Sessa M, Zambon A, Baldoli C, Rancoita PMV, Acquati S, de Mattia F, Tucci F, Gallo V, et al (2020) Lentiviral hematopoietic stem and progenitor cell gene therapy (HSPC-GT) for metachromatic leukodystrophy

- (MLD): Clinical outcomes from 33 patients. *Molecular Genetics and Metabolism* 129: S59
- Gambello MJ & Li H (2018) Current strategies for the treatment of inborn errors of metabolism. *Journal of Genetics and Genomics* 45: 61–70
- Gao B, Jeong W-I & Tian Z (2008) Liver: An organ with predominant innate immunity. *Hepatology* 47: 729–736
- Gao C & Peng J (2021) All routes lead to Rome: multifaceted origin of hepatocytes during liver regeneration. *Cell Regeneration* 10: 2
- Garrison LP, Jiao B & Dabbous O (2021) Gene therapy may not be as expensive as people think: challenges in assessing the value of single and short-term therapies. *Journal of Managed Care & Specialty Pharmacy* 27: 674–681
- Gebhardt R (1992) Metabolic zonation of the liver: Regulation and implications for liver function. *Pharmacology & Therapeutics* 53: 275–354
- George LA, Sullivan SK, Giermasz A, Rasko JEJ, Samelson-Jones BJ, Ducore J, Cuker A, Sullivan LM, Majumdar S, Teitel J, *et al* (2017) Hemophilia B Gene Therapy with a High-Specific-Activity Factor IX Variant. *New England Journal of Medicine* 377: 2215–2227
- Gillmore JD, Gane E, Taubel J, Kao J, Fontana M, Maitland ML, Seitzer J, O’Connell D, Walsh KR, Wood K, *et al* (2021) CRISPR-Cas9 In Vivo Gene Editing for Transthyretin Amyloidosis. *New England Journal of Medicine* 385: 493–502
- Gola A, Dorrington MG, Speranza E, Sala C, Shih RM, Radtke AJ, Wong HS, Baptista AP, Hernandez JM, Castellani G, *et al* (2021) Commensal-driven immune zonation of the liver promotes host defence. *Nature* 589: 131–136
- Greig JA, Nordin JML, Draper C, Bell P & Wilson JM (2018) AAV8 Gene Therapy Rescues the Newborn Phenotype of a Mouse Model of Crigler–Najjar. *Human Gene Therapy* 29: 763–770
- Groux H, Bigler M, de Vries JE & Roncarolo MG (1996) Interleukin-10 induces a long-term antigen-specific anergic state in human CD4+ T cells. *Journal of Experimental Medicine* 184: 19–29
- Guidotti JE, Br erie O, Robert A, Debey P, Brechot C & Desdouets C (2003) Liver Cell Polyploidization: A Pivotal Role for Binuclear Hepatocytes. *Journal of Biological Chemistry* 278: 19095–19101
- Hacein-Bey-Abina S, Garrigue A, Wang GP, Soulier J, Lim A, Morillon E, Clappier E, Caccavelli L, Delabesse E, Beldjord K, *et al* (2008) Insertional oncogenesis in 4 patients after retrovirus-mediated gene therapy of SCID-X1. *The Journal of Clinical Investigation* 118: 3132–3142

- Hacein-Bey-Abina S, Kalle C von, Schmidt M, McCormack MP, Wulffraat N, Leboulch P, Lim A, Osborne CS, Pawliuk R, Morillon E, *et al* (2003) LMO2-Associated Clonal T Cell Proliferation in Two Patients after Gene Therapy for SCID-X1. *Science* 302: 415–419
- Halpern KB, Shenhav R, Matcovitch-Natan O, Tóth B, Lemze D, Golan M, Massasa EE, Baydatch S, Landen S, Moor AE, *et al* (2017) Single-cell spatial reconstruction reveals global division of labour in the mammalian liver. *Nature* 542: 352–356
- Han S oh, Ronzitti G, Arnson B, Leborgne C, Li S, Mingozi F & Koeberl D (2017) Low-Dose Liver-Targeted Gene Therapy for Pompe Disease Enhances Therapeutic Efficacy of ERT via Immune Tolerance Induction. *Molecular Therapy - Methods & Clinical Development* 4: 126–136
- Harmatz P (2017) Mucopolysaccharidosis VI pathophysiology diagnosis and treatment. *Frontiers in Bioscience* 22: 4490
- Hassan S, Monahan RC, Mauser-Bunschoten EP, Vulpen LFD van, Eikenboom J, Beckers EAM, Hooimeijer L, Ypma PF, Nieuwenhuizen L, Coppens M, *et al* (2021) Mortality, life expectancy, and causes of death of persons with hemophilia in the Netherlands 2001–2018. *Journal of Thrombosis and Haemostasis* 19: 645–653
- He J, Lu H, Zou Q & Luo L (2014) Regeneration of Liver After Extreme Hepatocyte Loss Occurs Mainly via Biliary Transdifferentiation in Zebrafish. *Gastroenterology* 146: 789-800.e8
- He L, Pu W, Liu X, Zhang Z, Han M, Li Y, Huang X, Han X, Li Y, Liu K, *et al* (2021) Proliferation tracing reveals regional hepatocyte generation in liver homeostasis and repair. *Science* 371
- Herkel J (2003) MHC class II-expressing hepatocytes function as antigen-presenting cells and activate specific CD4 T lymphocytes. *Hepatology* 37
- Hordeaux J, Buza EL, Dyer C, Goode T, Mitchell TW, Richman L, Denton N, Hinderer C, Katz N, Schmid R, *et al* (2020) Adeno-Associated Virus-Induced Dorsal Root Ganglion Pathology. <https://home-liebertpub-com.sanraffaele.idm.oclc.org/hum> 31: 808–818
- Howe SJ, Mansour MR, Schwarzwaelder K, Bartholomae C, Hubank M, Kempinski H, Brugman MH, Pike-Overzet K, Chatters SJ, Ridder D de, *et al* (2008) Insertional mutagenesis combined with acquired somatic mutations causes leukemogenesis following gene therapy of SCID-X1 patients. *The Journal of Clinical Investigation* 118: 3143

- Huang Q, Zeng J & Yan J (2021a) COVID-19 mRNA vaccines. *Journal of Genetics and Genomics* 48: 107–114
- Huang TP, Newby GA & Liu DR (2021b) Precision genome editing using cytosine and adenine base editors in mammalian cells. *Nature Protocols* 2021 16:2 16: 1089–1128
- Huch M, Dorrell C, Boj SF, van Es JH, Li VSW, van de Wetering M, Sato T, Hamer K, Sasaki N, Finegold MJ, *et al* (2013) In vitro expansion of single Lgr5 + liver stem cells induced by Wnt-driven regeneration. *Nature* 494: 247–250
- Ilyinskii PO, Michaud AM, Rizzo GL, Roy CJ, Leung SS, Elkins SL, Capela T, Chowdhury A, Li L, Chandler RJ, *et al* (2021) ImmTOR nanoparticles enhance AAV transgene expression after initial and repeat dosing in a mouse model of methylmalonic acidemia. *Molecular Therapy - Methods & Clinical Development* 22: 279–292
- Iorio A, Stonebraker JS, Chambost H, Makris M, Coffin D, Herr C & Germini F (2019) Establishing the Prevalence and Prevalence at Birth of Hemophilia in Males. *Annals of Internal Medicine* 171: 540
- Jensen TL, Gøtzsche CR & Woldbye DPD (2021) Current and Future Prospects for Gene Therapy for Rare Genetic Diseases Affecting the Brain and Spinal Cord. *Frontiers in molecular neuroscience* 14: 695937
- Jeune VL, Joergensen JA, Hajjar RJ & Weber T (2013) Pre-existing Anti-Adeno-Associated Virus Antibodies as a Challenge in AAV Gene Therapy. <https://home.liebertpub.com/hgtb> 24: 59–67
- Jinek M, Chylinski K, Fonfara I, Hauer M, Doudna JA & Charpentier E (2012) A programmable dual-RNA-guided DNA endonuclease in adaptive bacterial immunity. *Science* 337: 816–821
- June CH, O'Connor RS, Kawalekar OU, Ghassemi S & Milone MC (2018) CAR T cell immunotherapy for human cancer. *Science* 359: 1361–1365
- Kamiya A, Kinoshita T, Ito Y, Matsui T, Morikawa Y, Senba E, Nakashima K, Taga T, Yoshida K, Kishimoto T, *et al* (1999) Fetal liver development requires a paracrine action of oncostatin M through the gp130 signal transducer. *The EMBO Journal* 18: 2127–2136
- Kamran F, Andrade AC, Nella AA, Clokie SJ, Rezvani G, Nilsson O, Baron J & Lui JC (2015) Evidence That Up-Regulation of MicroRNA-29 Contributes to Postnatal Body Growth Deceleration. *Molecular Endocrinology* 29: 921–932
- Keam SJ (2021) Elivaldogene Autotemcel: First Approval. *Molecular Diagnosis & Therapy* 25: 803–809

- Kietzmann T (2017) Metabolic zonation of the liver: The oxygen gradient revisited. *Redox Biology* 11: 622–630
- Kietzmann T, Cornesse Y, Brechtel K, Modaresi S & Jungermann K (2001) Perivenous expression of the mRNA of the three hypoxia-inducible factor alpha-subunits, HIF1alpha, HIF2alpha and HIF3alpha, in rat liver. *Biochemical Journal* 354: 531
- Kim SH, Kim S & Robbins PD (2000) Retroviral vectors. In *Advances in Virus Research* pp 545–563.
- Kingsman SM, Mitrophanous K & Olsen JC (2004) Potential oncogene activity of the woodchuck hepatitis post-transcriptional regulatory element (WPRE). *Gene Therapy* 2005 12:1 12: 3–4
- Knoll P, Schlaak J, Uhrig A, Kempf P, zum Büschenfelde KHM & Gerken G (1995) Human Kupffer cells secrete IL-10 in response to lipopolysaccharide (LPS) challenge. *Journal of Hepatology* 22: 226–229
- Knolle, Uhrig, Hegenbarth, Löser, Schmitt, Gerken & Lohse (1998) IL-10 down-regulates T cell activation by antigen-presenting liver sinusoidal endothelial cells through decreased antigen uptake via the mannose receptor and lowered surface expression of accessory molecules. *Clinical & Experimental Immunology* 114: 427–433
- Kojima T, Yamamoto T, Murata M, Chiba H, Kokai Y & Sawada N (2003) Regulation of the blood?biliary barrier: interaction between gap and tight junctions in hepatocytes. *Medical Electron Microscopy* 36: 157–164
- Kotin RM, Menninger JC, Ward DC & Berns KI (1991) Mapping and direct visualization of a region-specific viral DNA integration site on chromosome 19q13-qter. *Genomics* 10: 831–834
- Lai Y, Yue Y, Liu M, Ghosh A, Engelhardt JF, Chamberlain JS & Duan D (2005) Efficient in vivo gene expression by trans-splicing adeno-associated viral vectors. *Nature Biotechnology* 2005 23:11 23: 1435–1439
- Leborgne C, Barbon E, Alexander JM, Hanby H, Delignat S, Cohen DM, Collaud F, Muraleetharan S, Lupo D, Silverberg J, et al (2020) IgG-cleaving endopeptidase enables in vivo gene therapy in the presence of anti-AAV neutralizing antibodies. *Nature Medicine* 2020 26:7 26: 1096–1101
- Leebeek F, Miesbach W, Recht M, Sey N, Lattimore S, Castman G, Sawyer E, Cooper D, Ferriera V, Pipe S, et al (2021) Clinical Outcomes in Adults with Hemophilia B with and without Pre-existing Neutralizing Antibodies to AAV5: 6 Month Data from the Phase 3 etranacogene Dezaparvovec HOPE-B Gene Therapy Trial. *Research and Practice in Thrombosis and Haemostasis* 5

- Leebeek FWG & Miesbach W (2021) Gene therapy for hemophilia: a review on clinical benefit, limitations, and remaining issues. *Blood* 138: 923–931
- Levrero M & Zucman-Rossi J (2016) Mechanisms of HBV-induced hepatocellular carcinoma. *Journal of Hepatology* 64: S84–S101
- Li J, Sun W, Wang B, Xiao X & Liu X-Q (2008) Protein Trans-Splicing as a Means for Viral Vector-Mediated In Vivo Gene Therapy. <https://home.liebertpub.com/hum> 19: 958–964
- Li M (2018) Enzyme replacement therapy: A review and its role in treating lysosomal storage diseases. *Pediatric Annals* 47: e191–e197
- Lieber A, He CY, Meuse L, Schowalter D, Kirillova I, Winther B & Kay MA (1997) The role of Kupffer cell activation and viral gene expression in early liver toxicity after infusion of recombinant adenovirus vectors. *Journal of Virology* 71: 8798–8807
- Lin S, Nascimento EM, Gajera CR, Chen L, Neuhöfer P, Garbuzov A, Wang S & Artandi SE (2018) Distributed hepatocytes expressing telomerase repopulate the liver in homeostasis and injury. *Nature* 556: 244–248
- Locke FL, Ghobadi A, Jacobson CA, Miklos DB, Lekakis LJ, Oluwole OO, Lin Y, Braunschweig I, Hill BT, Timmerman JM, *et al* (2019) Long-term safety and activity of axicabtagene ciloleucel in refractory large B-cell lymphoma (ZUMA-1): a single-arm, multicentre, phase 1–2 trial. *The Lancet Oncology* 20: 31–42
- Lombardo A, Genovese P, Beausejour CM, Colleoni S, Lee Y-L, Kim KA, Ando D, Urnov FD, Galli C, Gregory PD, *et al* (2007a) Gene editing in human stem cells using zinc finger nucleases and integrase-defective lentiviral vector delivery. *Nature Biotechnology* 25:11 25: 1298–1306
- Lombardo A, Genovese P, Beausejour CM, Colleoni S, Lee YL, Kim KA, Ando D, Urnov FD, Galli C, Gregory PD, *et al* (2007b) Gene editing in human stem cells using zinc finger nucleases and integrase-defective lentiviral vector delivery. *Nature Biotechnology* 25: 1298–1306
- Lu P, Prost S, Caldwell H, Tugwood JD, Betton GR & Harrison DJ (2007) Microarray analysis of gene expression of mouse hepatocytes of different ploidy. *Mammalian Genome* 18: 617–626
- Lui JC, Chen W, Cheung CSF & Baron J (2014) Broad Shifts in Gene Expression during Early Postnatal Life Are Associated with Shifts in Histone Methylation Patterns. *PLOS ONE* 9: e86957
- Lui JC, Forcinito P, Chang M, Chen W, Barnes KM & Baron AJ (2010) Coordinated postnatal down-regulation of multiple growth-promoting genes: evidence for a genetic program limiting organ growth. *The FASEB Journal* 24: 3083–3092

- Lüth S, Huber S, Schramm C, Buch T, Zander S, Stadelmann C, Brück W, Wraith DC, Herkel J & Lohse AW (2008) Ectopic expression of neural autoantigen in mouse liver suppresses experimental autoimmune neuroinflammation by inducing antigen-specific Tregs. *The Journal of Clinical Investigation* 118: 3403–3410
- MacDonald BT, Tamai K & He X (2009) Wnt/ $\beta$ -Catenin Signaling: Components, Mechanisms, and Diseases. *Developmental Cell* 17: 9–26
- MacParland SA, Liu JC, Ma X-Z, Innes BT, Bartczak AM, Gage BK, Manuel J, Khuu N, Echeverri J, Linares I, *et al* (2018) Single cell RNA sequencing of human liver reveals distinct intrahepatic macrophage populations. *Nature Communications* 9: 4383
- Malato Y, Naqvi S, Schürmann N, Ng R, Wang B, Zape J, Kay MA, Grimm D & Willenbring H (2011) Fate tracing of mature hepatocytes in mouse liver homeostasis and regeneration. *The Journal of Clinical Investigation* 121: 4850–4860
- Maldarelli F, Wu X, Su L, Simonetti FR, Shao W, Hill S, Spindler J, Ferris AL, Mellors JW, Kearney MF, *et al* (2014) Specific HIV integration sites are linked to clonal expansion and persistence of infected cells. *Science* 345: 179–183
- Manno CS, Pierce GF, Arruda VR, Glader B, Ragni M, Rasko JJE, Ozelo MC, Hoots K, Blatt P, Konkle B, *et al* (2006) Successful transduction of liver in hemophilia by AAV-Factor IX and limitations imposed by the host immune response. *Nature Medicine* 2006 12:3 12: 342–347
- Mannucci PM (2020) Hemophilia therapy: the future has begun. *Haematologica* 105: 545–553
- Mannucci PM & Tuddenham EGD (2001) The Hemophilias — From Royal Genes to Gene Therapy. *New England Journal of Medicine* 344: 1773–1779
- Margall-Ducos G, Celton-Morizur S, Couton D, Brégerie O & Desdouets C (2007) Liver tetraploidization is controlled by a new process of incomplete cytokinesis. *Journal of Cell Science* 120: 3633–3639
- Martin NC, McCullough CT, Bush PG, Sharp L, Hall AC & Harrison DJ (2002) Functional analysis of mouse hepatocytes differing in DNA content: Volume, receptor expression, and effect of IFN $\gamma$ . *Journal of Cellular Physiology* 191: 138–144
- Martino AT, Suzuki M, Markusic DM, Zolotukhin I, Ryals RC, Moghimi B, Ertl HCJ, Muruve DA, Lee B & Herzog RW (2011) The genome of self-complementary adeno-associated viral vectors increases Toll-like receptor 9-dependent innate immune responses in the liver. *Blood* 117: 6459–6468

- Mátrai J, Cantore A, Bartholomae CC, Annoni A, Wang W, Acosta-Sanchez A, Samara-Kuko E, de Waele L, Ma L, Genovese P, *et al* (2011) Hepatocyte-targeted expression by integrase-defective lentiviral vectors induces antigen-specific tolerance in mice with low genotoxic risk. *Hepatology* 53: 1696–1707
- Matsumoto T, Wakefield L, Tarlow BD & Grompe M (2020) In Vivo Lineage Tracing of Polyploid Hepatocytes Reveals Extensive Proliferation during Liver Regeneration. *Cell Stem Cell* 26: 34-47.e3
- Maude SL, Laetsch TW, Buechner J, Rives S, Boyer M, Bittencourt H, Bader P, Verneris MR, Stefanski HE, Myers GD, *et al* (2018) Tisagenlecleucel in Children and Young Adults with B-Cell Lymphoblastic Leukemia. *The New England journal of medicine* 378: 439–448
- McCarty DM, Fu H, Monahan PE, Toulson CE, Naik P & Samulski RJ (2003) Adeno-associated virus terminal repeat (TR) mutant generates self-complementary vectors to overcome the rate-limiting step to transduction in vivo. *Gene Therapy* 2003 10:26 10: 2112–2118
- Meliani A, Boisgerault F, Hardet R, Marmier S, Collaud F, Ronzitti G, Leborgne C, Costa Verdera H, Simon Sola M, Charles S, *et al* (2018) Antigen-selective modulation of AAV immunogenicity with tolerogenic rapamycin nanoparticles enables successful vector re-administration. *Nature Communications* 9: 4098
- Mendell JR, Al-Zaidy S, Shell R, Arnold WD, Rodino-Klapac LR, Prior TW, Lowes L, Alfano L, Berry K, Church K, *et al* (2017) Single-Dose Gene-Replacement Therapy for Spinal Muscular Atrophy. *New England Journal of Medicine* 377: 1713–1722
- Mendonça SA, Lorincz R, Boucher P & Curiel DT (2021) Adenoviral vector vaccine platforms in the SARS-CoV-2 pandemic. *npj Vaccines* 2021 6:1 6: 1–14
- Mennechet FJD, Paris O, Ouoba AR, Salazar Arenas S, Sirima SB, Takoudjou Dzomo GR, Diarra A, Traore IT, Kania D, Eichholz K, *et al* (2019) A review of 65 years of human adenovirus seroprevalence. *Expert Review of Vaccines* 18: 597–613
- Michalopoulos GK & Bhushan B (2020) Liver regeneration: biological and pathological mechanisms and implications. *Nature Reviews Gastroenterology & Hepatology* 2020 18:1 18: 40–55
- Miettinen TP, Pessa HKJ, Caldez MJ, Fuhrer T, Diril MK, Sauer U, Kaldis P & Björklund M (2014) Identification of Transcriptional and Metabolic Programs Related to Mammalian Cell Size. *Current Biology* 24: 598–608
- Milani M, Annoni A, Bartolaccini S, Biffi M, Russo F, di Tomaso T, Raimondi A, Lengler J, Holmes MC, Scheiflinger F, *et al* (2017) Genome editing for scalable



- production of alloantigen-free lentiviral vectors for in vivo gene therapy . *EMBO Molecular Medicine* 9: 1558–1573
- Milani M, Annoni A, Moalli F, Liu T, Cesana D, Calabria A, Bartolaccini S, Biffi M, Russo F, Visigalli I, *et al* (2019) Phagocytosis-shielded lentiviral vectors improve liver gene therapy in nonhuman primates. *Science Translational Medicine* 11: 7325
- Milligan ID, Gibani MM, Sewell R, Clutterbuck EA, Campbell D, Plested E, Nuthall E, Voysey M, Silva-Reyes L, McElrath MJ, *et al* (2016) Safety and Immunogenicity of Novel Adenovirus Type 26- and Modified Vaccinia Ankara-Vectored Ebola Vaccines. *JAMA* 315: 1610
- Mingozi F & High KA (2011) Therapeutic in vivo gene transfer for genetic disease using AAV: progress and challenges. *Nature Reviews Genetics* 12: 341–355
- Mingozi F, Liu Y-L, Dobrzynski E, Kaufhold A, Liu JH, Wang Y, Arruda VR, High KA & Herzog RW (2003a) Induction of immune tolerance to coagulation factor IX antigen by in vivo hepatic gene transfer. *The Journal of Clinical Investigation* 111: 1347–1356
- Mingozi F, Liu Y-L, Dobrzynski E, Kaufhold A, Liu JH, Wang Y, Arruda VR, High KA & Herzog RW (2003b) Induction of immune tolerance to coagulation factor IX antigen by in vivo hepatic gene transfer. *The Journal of Clinical Investigation* 111: 1347–1356
- Mingozi F, Maus M v, Hui DJ, Sabatino DE, Murphy SL, Rasko JEJ, Ragni M v, Manno CS, Sommer J, Jiang H, *et al* (2007) CD8+ T-cell responses to adeno-associated virus capsid in humans. *Nature Medicine* 2007 13:4 13: 419–422
- Miyajima A, Tanaka M & Itoh T (2014) Stem/Progenitor Cells in Liver Development, Homeostasis, Regeneration, and Reprogramming. *Cell Stem Cell* 14: 561–574
- Miyaoka Y, Ebato K, Kato H, Arakawa S, Shimizu S & Miyajima A (2012) Hypertrophy and Unconventional Cell Division of Hepatocytes Underlie Liver Regeneration. *Current Biology* 22: 1166–1175
- Monteilhet V, Saheb S, Boutin S, Leborgne C, Veron P, Montus MF, Moullier P, Benveniste O & Masurier C (2011) A 10 Patient Case Report on the Impact of Plasmapheresis Upon Neutralizing Factors Against Adeno-associated Virus (AAV) Types 1, 2, 6, and 8. *Molecular Therapy* 19: 2084–2091
- Montini E, Cesana D, Schmidt M, Sanvito F, Bartholomae CC, Ranzani M, Benedicenti F, Sergi LS, Ambrosi A, Ponzoni M, *et al* (2009) The genotoxic potential of retroviral vectors is strongly modulated by vector design and integration site selection in a mouse model of HSC gene therapy. *The Journal of Clinical Investigation* 119: 964–975

- Mount JD, Herzog RW, Tillson DM, Goodman SA, Robinson N, McClelland ML, Bellingier D, Nichols TC, Arruda VR, Lothrop CD, *et al* (2002) Sustained phenotypic correction of hemophilia B dogs with a factor IX null mutation by liver-directed gene therapy. *Blood* 99: 2670–2676
- Muhuri M, Zhan W, Maeda Y, Li J, Lotun A, Chen J, Sylvia K, Dasgupta I, Arjomandnejad M, Nixon T, *et al* (2021) Novel Combinatorial MicroRNA-Binding Sites in AAV Vectors Synergistically Diminish Antigen Presentation and Transgene Immunity for Efficient and Stable Transduction. *Frontiers in Immunology* 12
- Musunuru K, Chadwick AC, Mizoguchi T, Garcia SP, DeNizio JE, Reiss CW, Wang K, Iyer S, Dutta C, Clendaniel V, *et al* (2021) In vivo CRISPR base editing of PCSK9 durably lowers cholesterol in primates. *Nature* 2021 593:7859 593: 429–434
- Nakai H, Storm TA & Kay MA (2000) Increasing the size of rAAV-mediated expression cassettes in vivo by intermolecular joining of two complementary vectors. *Nature Biotechnology* 2000 18:5 18: 527–532
- Naldini L (2011) Ex vivo gene transfer and correction for cell-based therapies. *Nature Reviews Genetics* 12: 301–315
- Naldini L, Blömer U, Gallay P, Ory D, Mulligan R, Gage FH, Verma IM & Trono D (1996) In vivo gene delivery and stable transduction of nondividing cells by a lentiviral vector. *Science* 272: 263–267
- Naldini L & Verma IM (2000) Lentiviral vectors. In *Advances in Virus Research* pp 599–609.
- Nathwani AC, Reiss UM, Tuddenham EGD, Rosales C, Chowdhary P, McIntosh J, della Peruta M, Lheriteau E, Patel N, Raj D, *et al* (2014) Long-Term Safety and Efficacy of Factor IX Gene Therapy in Hemophilia B. *New England Journal of Medicine* 371: 1994–2004
- Nathwani AC, Tuddenham EGD, Rangarajan S, Rosales C, McIntosh J, Linch DC, Chowdhary P, Riddell A, Pie AJ, Harrington C, *et al* (2011) Adenovirus-Associated Virus Vector-Mediated Gene Transfer in Hemophilia B. *New England Journal of Medicine* 365: 2357–2365
- Nault J-C, Datta S, Imbeaud S, Franconi A, Mallet M, Couchy G, Letouzé E, Pilati C, Verret B, Blanc J-F, *et al* (2015) Recurrent AAV2-related insertional mutagenesis in human hepatocellular carcinomas. *Nature Genetics* 2015 47:10 47: 1187–1193
- Nguyen GN, Everett JK, Kafle S, Roche AM, Raymond HE, Leiby J, Wood C, Assenmacher CA, Merricks EP, Long CT, *et al* (2021) A long-term study of AAV

- gene therapy in dogs with hemophilia A identifies clonal expansions of transduced liver cells. *Nature Biotechnology* 39: 47–55
- Nguyen TH, Bellodi-Privato M, Aubert D, Pichard V, Myara A, Trono D & Ferry N (2005) Therapeutic Lentivirus-Mediated Neonatal in Vivo Gene Therapy in Hyperbilirubinemic Gunn Rats. *Molecular Therapy* 12: 852–859
- Ober EA & Lemaigre FP (2018) Development of the liver: Insights into organ and tissue morphogenesis. *Journal of Hepatology* 68: 1049–1062
- O’Driscoll M & Jeggo PA (2006) The role of double-strand break repair — insights from human genetics. *Nature Reviews Genetics* 2006 7:1 7: 45–54
- Ohmori T, Nagao Y, Mizukami H, Sakata A, Muramatsu S, Ozawa K, Tominaga S, Hanazono Y, Nishimura S, Nureki O, *et al* (2017) CRISPR/Cas9-mediated genome editing via postnatal administration of AAV vector cures haemophilia B mice. *Scientific Reports* 7: 4159
- Oldenborg P-A, Gresham HD & Lindberg FP (2001) Cd47-Signal Regulatory Protein  $\alpha$  (Sirp $\alpha$ ) Regulates Fc $\gamma$  and Complement Receptor-Mediated Phagocytosis. *Journal of Experimental Medicine* 193: 855–862
- Oldenborg P-A, Zheleznyak A, Fang Y-F, Lagenaur CF, Gresham HD & Lindberg FP (2000) Role of CD47 as a Marker of Self on Red Blood Cells. *Science* 288: 2051–2054
- Oldfield EH, Ram Z, Culver KW, Blaese RM, DeVroom HL & Anderson WF (1993) Gene Therapy for the Treatment of Brain Tumors Using Intra-Tumoral Transduction with the Thymidine Kinase Gene and Intravenous Ganciclovir. National Institutes of Health. *Human Gene Therapy* 4: 39–69
- Orkin SH, Motulsky AG & Varmus H (1995) Report And Recommendations Of The Panel To Assess The Nih Investment In Research On Gene Therapy Executive Summary of Findings and Recommendations
- Orlova NA, Kovnir S v., Vorobiev II & Gabibov AG (2012) Coagulation Factor IX for Hemophilia B Therapy. *Acta Naturae* 4: 62
- De Palma M, Mazziere R, Politi LS, Pucci F, Zonari E, Sitia G, Mazzoleni S, Moi D, Venneri MA, Indraccolo S, *et al* (2008) Tumor-Targeted Interferon- $\alpha$  Delivery by Tie2-Expressing Monocytes Inhibits Tumor Growth and Metastasis. *Cancer Cell* 14: 299–311
- Park F, Ohashi K, Chiu W, Naldini L & Kay MA (2000) Efficient lentiviral transduction of liver requires cell cycling in vivo. *Nature Genetics* 24: 49–52
- Pasi KJ, Rangarajan S, Mitchell N, Lester W, Symington E, Madan B, Laffan M, Russell CB, Li M, Pierce GF, *et al* (2020) Multiyear Follow-up of AAV5-hFVIII-

- SQ Gene Therapy for Hemophilia A. *New England Journal of Medicine* 382: 29–40
- Patel SR, Lundgren TS, Spencer HT & Doering CB (2020) The Immune Response to the fVIII Gene Therapy in Preclinical Models. *Frontiers in Immunology* 11
- Pei X, Shao W, Xing A, Askew C, Chen X, Cui C, Abajas YL, Gerber DA, Merricks EP, Nichols TC, *et al* (2020) Development of AAV Variants with Human Hepatocyte Tropism and Neutralizing Antibody Escape Capacity. *Molecular Therapy - Methods & Clinical Development* 18: 259–268
- Pien GC, Basner-Tschakarjan E, Hui DJ, Mentlik AN, Finn JD, Hasbrouck NC, Zhou S, Murphy SL, Maus M v., Mingozzi F, *et al* (2009) Capsid antigen presentation flags human hepatocytes for destruction after transduction by adeno-associated viral vectors. *Journal of Clinical Investigation* 119: 1688–1695
- Pittman D, Alderman E, Tomkinson K, Wang J, Giles A & Kaufman R (1993) Biochemical, Immunological, and In Vivo Functional Characterization of B-Domain-Deleted Factor VIII. *Blood* 81: 2925–2935
- Planas-Paz L, Orsini V, Boulter L, Calabrese D, Pikiólek M, Nigsch F, Xie Y, Roma G, Donovan A, Mart P, *et al* (2016) The RSPO-LGR4/5-ZNRF3/RNF43 module controls liver zonation and size. *Nature Cell Biology* 18: 467–479
- Post J & Hoffman J (1964) Changes in the replication times and patterns of the liver cell during the life of the rat. *Experimental Cell Research* 36: 111–123
- Rangarajan S, Walsh L, Lester W, Perry D, Madan B, Laffan M, Yu H, Vettermann C, Pierce GF, Wong WY, *et al* (2017) AAV5–Factor VIII Gene Transfer in Severe Hemophilia A. *New England Journal of Medicine* 377: 2519–2530
- Raper SE, Chirmule N, Lee FS, Wivel NA, Bagg A, Gao GP, Wilson JM & Batshaw ML (2003) Fatal systemic inflammatory response syndrome in a ornithine transcarbamylase deficient patient following adenoviral gene transfer. *Molecular Genetics and Metabolism* 80: 148–158
- Reiser J, Harmison G, Kluepfel-Stahl S, Brady RO, Karlsson S & Schubert M (1996) Transduction of nondividing cells using pseudotyped defective high-titer HIV type 1 particles. *Proceedings of the National Academy of Sciences* 93: 15266–15271
- Ren S, Wang M, Wang C, Wang Y, Sun C, Zeng Z, Cui H & Zhao X (2021) Application of Non-Viral Vectors in Drug Delivery and Gene Therapy. *Polymers* 13: 3307
- Richards DY, Winn SR, Dudley S, Nygaard S, Mighell TL, Grompe M & Harding CO (2020) AAV-Mediated CRISPR/Cas9 Gene Editing in Murine Phenylketonuria. *Molecular Therapy - Methods & Clinical Development* 17: 234–245

- Rishi G & Subramaniam VN (2017) The liver in regulation of iron homeostasis. *American Journal of Physiology-Gastrointestinal and Liver Physiology* 313: G157–G165
- Robinson MW, Harmon C & O’Farrelly C (2016) Liver immunology and its role in inflammation and homeostasis. *Cellular & Molecular Immunology* 13: 267–276
- Sakoda T, Kasahara N, Hamamori Y & Kedes L (1999) A High-Titer Lentiviral Production System Mediates Efficient Transduction of Differentiated Cells Including Beating Cardiac Myocytes. *Journal of Molecular and Cellular Cardiology* 31: 2037–2047
- Sambrook J, Westphal H, Srinivasan PR & Dulbecco R (1968) The integrated state of viral DNA in SV40-transformed cells. *Proceedings of the National Academy of Sciences* 60: 1288–1295
- Samelson-Jones BJ & Arruda VR (2020) Translational Potential of Immune Tolerance Induction by AAV Liver-Directed Factor VIII Gene Therapy for Hemophilia A. *Frontiers in Immunology* 11: 618
- Sands MS & Davidson BL (2006) Gene therapy for lysosomal storage diseases. *Molecular Therapy* 13: 839–849
- Sanjeev Gupta (2000) Hepatic polyploidy and liver growth control. *Seminars in Cancer Biology* 10: 161–171
- Schaub JR, Huppert KA, Kurial SNT, Hsu BY, Cast AE, Donnelly B, Karns RA, Chen F, Rezvani M, Luu HY, *et al* (2018) De novo formation of the biliary system by TGF $\beta$ -mediated hepatocyte transdifferentiation. *Nature* 2018 557:7704 557: 247–251
- Schauber C, Tuerk M, Pacheco C, Escarpe P & Veres G (2004) Lentiviral vectors pseudotyped with baculovirus gp64 efficiently transduce mouse cells in vivo and show tropism restriction against hematopoietic cell types in vitro. *Gene Therapy* 2004 11:3 11: 266–275
- Schioli G, Conti A, Ferrari S, Volpe L della, Jacob A, Albano L, Beretta S, Calabria A, Vavassori V, Gasparini P, *et al* (2019) Precise Gene Editing Preserves Hematopoietic Stem Cell Function following Transient p53-Mediated DNA Damage Response. *Cell Stem Cell* 24: 551-565.e8
- Scholz SJ, Fronza R, Bartholomä CC, Cesana D, Montini E, von Kalle C, Gil-Farina I & Schmidt M (2017) Lentiviral Vector Promoter is Decisive for Aberrant Transcript Formation. *Human Gene Therapy* 28: 875–885
- Schröder ARW, Shinn P, Chen H, Berry C, Ecker JR & Bushman F (2002) HIV-1 Integration in the Human Genome Favors Active Genes and Local Hotspots. *Cell* 110: 521–529

- Schulze RJ, Schott MB, Casey CA, Tuma PL & McNiven MA (2019) The cell biology of the hepatocyte: A membrane trafficking machine. *Journal of Cell Biology* 218: 2096–2112
- Schuster SJ, Bishop MR, Tam CS, Waller EK, Borchmann P, McGuirk JP, Jäger U, Jaglowski S, Andreadis C, Westin JR, *et al* (2019) Tisagenlecleucel in Adult Relapsed or Refractory Diffuse Large B-Cell Lymphoma. *The New England journal of medicine* 380: 45–56
- Scott LJ (2015) Alipogene Tiparovec: A Review of Its Use in Adults with Familial Lipoprotein Lipase Deficiency. *Drugs* 75: 175–182
- Scully R, Panday A, Elango R & Willis NA (2019) DNA double-strand break repair-pathway choice in somatic mammalian cells. *Nature Reviews Molecular Cell Biology* 20:11 20: 698–714
- Sebastian S & Lambe T (2018) Clinical Advances in Viral-Vectored Influenza Vaccines. *Vaccines* 2018, Vol 6, Page 29 6: 29
- Shaw AR & Suzuki M (2019) Immunology of Adenoviral Vectors in Cancer Therapy. *Molecular Therapy - Methods & Clinical Development* 15: 418–429
- Shi B, Keough E, Matter A, Leander K, Young S, Carlini E, Sachs AB, Tao W, Abrams M, Howell B, *et al* (2011) Biodistribution of Small Interfering RNA at the Organ and Cellular Levels after Lipid Nanoparticle-mediated Delivery. *Journal of Histochemistry & Cytochemistry* 59: 727–740
- Shukla V, Seoane-Vazquez E, Fawaz S, Brown L & Rodriguez-Monguio R (2019) The Landscape of Cellular and Gene Therapy Products: Authorization, Discontinuations, and Cost. *Human Gene Therapy Clinical Development* 30: 102–113
- Sikka R (2005) Bench to Bedside: Pharmacogenomics, Adverse Drug Interactions, and the Cytochrome P450 System. *Academic Emergency Medicine* 12: 1227–1235
- Silva G, Poirot L, Galetto R, Smith J, Montoya G, Duchateau P & Paques F (2011) Meganucleases and Other Tools for Targeted Genome Engineering: Perspectives and Challenges for Gene Therapy. *Current Gene Therapy* 11: 11–27
- Simioni P, Tormene D, Tognin G, Gavasso S, Bulato C, Iacobelli NP, Finn JD, Spiezia L, Radu C & Arruda VR (2009) X-Linked Thrombophilia with a Mutant Factor IX (Factor IX Padua). *New England Journal of Medicine* 361: 1671–1675
- Sladky VC, Eichin F, Reiberger T & Villunger A (2021) Polyploidy control in hepatic health and disease. *Journal of Hepatology* 75: 1177–1191

- Sleyster EC & Knook DL (1982) Relation between localization and function of rat liver Kupffer cells. *Laboratory investigation; a journal of technical methods and pathology* 47: 484–90
- Smith RH (2008) Adeno-associated virus integration: virus versus vector. *Gene Therapy* 15: 817–822
- Snippert HJ, van der Flier LG, Sato T, van Es JH, van den Born M, Kroon-Veenboer C, Barker N, Klein AM, van Rheenen J, Simons BD, *et al* (2010) Intestinal crypt homeostasis results from neutral competition between symmetrically dividing Lgr5 stem cells. *Cell* 143: 134–144
- Snyder RO, Miao C, Meuse L, Tubb J, Donahue BA, Lin H-F, Stafford DW, Patel S, Thompson AR, Nichols T, *et al* (1999) Correction of hemophilia B in canine and murine models using recombinant adeno-associated viral vectors. *Nature Medicine* 1999 5:1 5: 64–70
- Squeri G, Passerini L, Ferro F, Laudisa C, Tomasoni D, Deodato F, Donati MA, Gasperini S, Aiuti A, Bernardo ME, *et al* (2019) Targeting a Pre-existing Anti-transgene T Cell Response for Effective Gene Therapy of MPS-I in the Mouse Model of the Disease. *Molecular Therapy* 27: 1215–1227
- Ståhl PL, Salmén F, Vickovic S, Lundmark A, Navarro JF, Magnusson J, Giacomello S, Asp M, Westholm JO, Huss M, *et al* (2016) Visualization and analysis of gene expression in tissue sections by spatial transcriptomics. *Science* 353: 78–82
- Stein S, Ott MG, Schultze-Strasser S, Jauch A, Burwinkel B, Kinner A, Schmidt M, Krämer A, Schwäble J, Glimm H, *et al* (2010) Genomic instability and myelodysplasia with monosomy 7 consequent to EVI1 activation after gene therapy for chronic granulomatous disease. *Nature Medicine* 2010 16:2 16: 198–204
- Stone D, Kenkel EJ, Loprieno MA, Tanaka M, de Silva Felixge HS, Kumar AJ, Stensland L, Obenza WM, Wangari S, Ahrens CY, *et al* (2021) Gene Transfer in Adeno-Associated Virus Seropositive Rhesus Macaques Following Rapamycin Treatment and Subcutaneous Delivery of AAV6, but Not Retargeted AAV6 Vectors. *Human Gene Therapy* 32: 96–112
- Strauss O, Phillips A, Ruggiero K, Bartlett A & Dunbar PR (2017) Immunofluorescence identifies distinct subsets of endothelial cells in the human liver. *Scientific Reports* 7: 44356
- Suksaweang S, Lin C-M, Jiang T-X, Hughes MW, Widelitz RB & Chuong C-M (2004) Morphogenesis of chicken liver: identification of localized growth zones and the role of  $\beta$ -catenin/Wnt in size regulation. *Developmental Biology* 266: 109–122

- Sun T, Pikiólek M, Orsini V, Bergling S, Holwerda S, Morelli L, Hoppe PS, Planas-Paz L, Yang Y, Ruffner H, *et al* (2020) AXIN2+ Pericentral Hepatocytes Have Limited Contributions to Liver Homeostasis and Regeneration. *Cell Stem Cell* 26: 97-107.e6
- Tanami S, Ben-Moshe S, Elkayam A, Mayo A, Bahar Halpern K & Itzkovitz S (2017) Dynamic zonation of liver ploidy. *Cell and Tissue Research* 368: 405–410
- Tatum EL (1966) Molecular Biology, Nucleic Acids, and the Future of Medicine. *Perspectives in Biology and Medicine* 10: 19–32
- Temin HM (1961) Mixed infection with two types of Rous sarcoma virus. *Virology* 13: 158–163
- Terheggen HG, Lowenthal A, Lavinha F, Colombo JP & Rogers S (1975) Unsuccessful trial of gene replacement in arginase deficiency. *European Journal of Pediatrics* 119: 1–3
- Thompson AA, Walters MC, Kwiatkowski J, Rasko JEJ, Ribeil J-A, Hongeng S, Magrin E, Schiller GJ, Payen E, Semeraro M, *et al* (2018) Gene Therapy in Patients with Transfusion-Dependent  $\beta$ -Thalassemia. *New England Journal of Medicine* 378: 1479–1493
- Thorat T, Neumann PJ & Chambers JD (2018) Hemophilia Burden of Disease: A Systematic Review of the Cost-Utility Literature for Hemophilia. *Journal of Managed Care & Specialty Pharmacy* 24: 632–642
- Van Til NP, Markusic DM, van der Rijt R, Kunne C, Hiralall JK, Vreeling H, Frederiks WM, Oude-Elferink RPJ & Seppen J (2005) Kupffer Cells and Not Liver Sinusoidal Endothelial Cells Prevent Lentiviral Transduction of Hepatocytes. *Molecular Therapy* 11: 26–34
- Tsui L v., Kelly M, Zayek N, Rojas V, Ho K, Ge Y, Moskalenko M, Mondesire J, Davis J, Roey M van, *et al* (2002) Production of human clotting Factor IX without toxicity in mice after vascular delivery of a lentiviral vector. *Nature Biotechnology* 20: 53–57
- VandenDriessche T, Thorrez L, Naldini L, Follenzi A, Moons L, Berneman Z, Collen D & Chuah MKL (2002) Lentiviral vectors containing the human immunodeficiency virus type-1 central polypurine tract can efficiently transduce nondividing hepatocytes and antigen-presenting cells in vivo. *Blood* 100: 813–822
- Vekemans K & Braet F (2005) Structural and functional aspects of the liver and liver sinusoidal cells in relation to colon carcinoma metastasis. *World J Gastroenterol* 11: 5095–5102



- Viola-Magni MP (1972) Synthesis and turnover of DNA in hepatocytes of neonatal rats. *Journal of Microscopy* 96: 191–203
- WALSH M, MACGREGOR D, STUCKLESS S, BARRETT B, KAWAJA M & SCULLY M-F (2008) Health-related quality of life in a cohort of adult patients with mild hemophilia A. *Journal of Thrombosis and Haemostasis* 6: 755–761
- Wang B, Zhao L, Fish M, Logan CY & Nusse R (2015) Self-renewing diploid Axin2 + cells fuel homeostatic renewal of the liver. *Nature* 524: 180–185
- Wang D, Zhang F & Gao G (2020) CRISPR-Based Therapeutic Genome Editing: Strategies and In Vivo Delivery by AAV Vectors. *Cell* 181: 136–150
- Wang L, Bell P, Lin J, Calcedo R, Tarantal AF & Wilson JM (2011) AAV8-mediated Hepatic Gene Transfer in Infant Rhesus Monkeys (*Macaca mulatta*). *Molecular Therapy* 19: 2012–2020
- Ward P & Walsh CE (2012) Targeted integration of a rAAV vector into the AAVS1 region. *Virology* 433: 356–366
- Wasserman DH (2009) Four grams of glucose. *American Journal of Physiology-Endocrinology and Metabolism* 296: E11–E21
- Waters D, Adeloje D, Woolham D, Wastnedge E, Patel S & Rudan I (2018) Global birth prevalence and mortality from inborn errors of metabolism: a systematic analysis of the evidence. *Journal of Global Health* 8
- Wei Y, Wang YG, Jia Y, Li L, Yoon J, Zhang S, Wang Z, Zhang Y, Zhu M, Sharma T, et al (2021) Liver homeostasis is maintained by midlobular zone 2 hepatocytes. *Science* 371
- Willebrords J, Crespo Yanguas S, Maes M, Decrock E, Wang N, Leybaert L, da Silva TC, Veloso Alves Pereira I, Jaeschke H, Cogliati B, et al (2015) Structure, Regulation and Function of Gap Junctions in Liver. *Cell Communication & Adhesion* 22: 29–37
- Wilson JM & Flotte TR (2020) Moving Forward After Two Deaths in a Gene Therapy Trial of Myotubular Myopathy. *Human Gene Therapy* 31: 695–696
- Wisse E, de Zanger RB, Jacobs R & McCuskey RS (1983) Scanning electron microscope observations on the structure of portal veins, sinusoids and central veins in rat liver. *Scanning electron microscopy*: 1441–52
- Wu X, Li Y, Crise B & Burgess SM (2003) Transcription Start Regions in the Human Genome Are Favored Targets for MLV Integration. *Science* 300: 1749–1751
- Wu Z, Asokan A & Samulski RJ (2006) Adeno-associated Virus Serotypes: Vector Toolkit for Human Gene Therapy. *Molecular Therapy* 14: 316–327

- Yang Y-S, Xie J, Wang D, Kim J-M, Tai PWL, Gravallesse E, Gao G & Shim J-H (2019) Bone-targeting AAV-mediated silencing of Schnurri-3 prevents bone loss in osteoporosis. *Nature Communications* 2019 10:1 10: 1–13
- Yin C, Evason KJ, Asahina K & Stainier DYR (2013) Hepatic stellate cells in liver development, regeneration, and cancer. *Journal of Clinical Investigation* 123: 1902–1910
- Yin H, Kanasty RL, Eltoukhy AA, Vegas AJ, Dorkin JR & Anderson DG (2014) Non-viral vectors for gene-based therapy. *Nature Reviews Genetics* 15: 541–555
- Yin H, Song C-Q, Dorkin JR, Zhu LJ, Li Y, Wu Q, Park A, Yang J, Suresh S, Bizhanova A, *et al* (2016) Therapeutic genome editing by combined viral and non-viral delivery of CRISPR system components in vivo. *Nature Biotechnology* 34: 328–333
- Yoshimitsu M, Sato T, Tao K, Walia JS, Rasaiah VI, Sleep GT, Murray GJ, Poepl AG, Underwood J, West L, *et al* (2004) Bioluminescent imaging of a marking transgene and correction of Fabry mice by neonatal injection of recombinant lentiviral vectors. *Proceedings of the National Academy of Sciences* 101: 16909–16914
- Zanger UM & Schwab M (2013) Cytochrome P450 enzymes in drug metabolism: Regulation of gene expression, enzyme activities, and impact of genetic variation. *Pharmacology & Therapeutics* 138: 103–141
- Zanta-Boussif MA, Charrier S, Brice-Ouzet A, Martin S, Opolon P, Thrasher AJ, Hope TJ & Galy A (2009) Validation of a mutated PRE sequence allowing high and sustained transgene expression while abrogating WHV-X protein synthesis: application to the gene therapy of WAS. *Gene Therapy* 2009 16:5 16: 605–619
- Zhang L, Dailey PJ, Gettie A, Blanchard J & Ho DD (2002) The Liver Is a Major Organ for Clearing Simian Immunodeficiency Virus in Rhesus Monkeys. *Journal of Virology* 76: 5271–5273
- Zhang S, Lin Y-H, Tarlow B & Zhu H (2019) The origins and functions of hepatic polyploidy. *Cell Cycle* 18: 1302–1315
- Zhen S & Li X (2019) Liposomal delivery of CRISPR/Cas9. *Cancer Gene Therapy* 2019 27:7 27: 515–527
- Zincarelli C, Soltys S, Rengo G & Rabinowitz JE (2008) Analysis of AAV Serotypes 1–9 Mediated Gene Expression and Tropism in Mice After Systemic Injection. *Molecular Therapy* 16: 1073–1080
- Zonari E, Desantis G, Petrillo C, Boccalatte FE, Lidonnici MR, Kajaste-Rudnitski A, Aiuti A, Ferrari G, Naldini L & Gentner B (2017) Efficient Ex Vivo Engineering

and Expansion of Highly Purified Human Hematopoietic Stem and Progenitor Cell Populations for Gene Therapy. *Stem Cell Reports* 8: 977–990

Zufferey R, Donello JE, Trono D & Hope TJ (1999) Woodchuck Hepatitis Virus Posttranscriptional Regulatory Element Enhances Expression of Transgenes Delivered by Retroviral Vectors. *Journal of Virology* 73: 2886–2892

Zufferey R, Dull T, Mandel RJ, Bukovsky A, Quiroz D, Naldini L & Trono D (1998) Self-Inactivating Lentivirus Vector for Safe and Efficient In Vivo Gene Delivery. *Journal of Virology* 72: 9873–9880

A handwritten signature in black ink, appearing to read "Francesco Geronzi". The signature is written in a cursive, flowing style with some capital letters.